PB84-223064

Analysis of Particulate Matter Concentrations and Visibility in the Eastern United States

Santa Fe Research Corp., NM

Prepared for

Environmental Protection Agency
Research Triangle Park, NC

Aug 84

U.S. Department of Commerce
National Technical Information Service
NTIS

PB84-223064

United States
Environmental Protection
Agency

Office of Air Quality
Planning and Standards
Research Triangle Park NC 27711

EPA-450/4-84-008
August 1983

Air

EPA

Analysis Of Particulate Matter Concentrations And Visibility In The Eastern United States

REPRODUCED BY
NATIONAL TECHNICAL
INFORMATION SERVICE
U.S. DEPARTMENT OF COMMERCE
SPRINGFIELD, VA. 22161

TECHNICAL REPORT DATA

(Please read Instructions on the reverse before completing)

1. REPORT NO. EPA-450/4-84-008	2.	3. RECIPIENT'S ACCESSION NO. PB84 223064
4. TITLE AND SUBTITLE Analysis Of Particulate Matter Concentrations And Visibility In The Eastern U. S.		5. REPORT DATE August 1984
		6. PERFORMING ORGANIZATION CODE
7. AUTHOR(S) John Trijonis		8. PERFORMING ORGANIZATION REPORT NO.
9. PERFORMING ORGANIZATION NAME AND ADDRESS Santa Fe Research Corporation Santa Fe, NM 87501		10. PROGRAM ELEMENT NO.
		11. CONTRACT/GRANT NO. 68-02-3578
12. SPONSORING AGENCY NAME AND ADDRESS U. S. Environmental Protection Agency Office Of Air Quality Planning And Standards Monitoring And Data Analysis Division Research Triangle, NC 27711		13. TYPE OF REPORT AND PERIOD COVERED
		14. SPONSORING AGENCY CODE

15. SUPPLEMENTARY NOTES

EPA Project Officer: Thompson G. Pace

16. ABSTRACT

An analysis is conducted of EPA IP Network data for the eastern U.S. of particulate concentrations and airport data for visibility and relative humidity. Physically meaningful regression equations are used to determine light extinction (visibility degradation) as a function of aerosol concentrations and relative humidity. As expected from optical theory, the results indicate that fine particles (FP) are much more closely tied to visibility than inhalable particles (IP) or total suspended particles (TSP). Sulfate particles have a much greater extinction efficiency (per unit mass) than nonsulfate TSP and nonsulfate IP; fine sulfate particles also appear to have a somewhat greater extinction efficiency than fine nonsulfate particles. The results suggest that sulfates and associated water account for approximately 45% of total light extinction in the East. Dichotomous FP and IP concentrations can be predicted fairly well from airport visibility data in conjunction with Hi-Vol TSP data, with standard errors of prediction about 30-40% on a daily basis and 16-17% on an annual basis. It is shown that airport visibility data are of good quality for analyzing the spatial/temporal extent of fine particle episodes in the East. Visibility maps provide important qualitative insights regarding the spatial extent, transport patterns, and origins of fine particle episodes.

17. KEY WORDS AND DOCUMENT ANALYSIS

a. DESCRIPTORS	b. IDENTIFIERS/OPEN ENDED TERMS	c. COSATI Field/Group

18. DISTRIBUTION STATEMENT	19. SECURITY CLASS *(This Report)*	21. NO. OF PAGES 137
	20. SECURITY CLASS *(This page)*	22. PRICE

EPA-450/4-84-008

Analysis Of Particulate Matter Concentrations And Visibility In The Eastern United States

By
John Trijonis
Santa Fe Research Corp.

EPA Contract No. 68-02-3578

Thompson Pace, Project Officer

Office Of Air And Radiation
Office Of Air Quality Planning And Standards
U.S. Environmental Protection Agency
Research Triangle Park, North Carolina 27711

August 1983

This report has been reviewed by the Office Of Air Quality Planning And Standards, U. S. Environmental Protection Agency, and approved for publication as received from Santa Fe Research Corporation. Approval does not signify that the contents necessarily reflect the views and policies of the Agency, neither does mention of trade names or commercial products constitute endorsement or recommendation for use.

ABSTRACT

For the eastern half of the U.S., an analysis is conducted of EPA IP Network data for particulate concentrations combined with airport data for visibility and relative humidity. Physically meaningful and statistically well-fitting regression equations are used to determine light extinction (visibility degradation) as a function of aerosol concentrations and relative humidity. As expected from optical theory, the results indicate that fine particles (FP) are much more closely tied to visibility than inhalable particles (IP) or total suspended particles (TSP). It is found that sulfate particles have a much greater extinction efficiency (per unit mass) than nonsulfate TSP and nonsulfate IP; fine sulfate particles also appear to have a somewhat greater extinction efficiency than fine nonsulfate particles. The results suggest that sulfates and associated water account for approximately 45% of total light extinction in the East. It is found that dichotomous FP and IP concentrations can be predicted fairly well from airport visibility data in conjunction with Hi-Vol TSP data, with standard errors of prediction about 30-40% on a daily basis and 16-17% on an annual basis. Many of the above statistical studies would benefit greatly by the inclusion of more data when available. It is shown that airport visibility data are of good quality for analyzing the spatial/temporal extent of fine particle episodes in the East. Visibility maps provide important qualitative insights regarding the spatial extent, transport patterns, and origins of fine particle episodes.

TABLE OF CONTENTS

ABSTRACT iii

EXECUTIVE SUMMARY 1

1. INTRODUCTION 9
   1.1 Basic Concepts and Definitions 10
   1.2 Organization of the Report 14

2. DESCRIPTION OF DATA BASES 15
   2.1 Types of Data 15
   2.2 Data Quality Assurance 17
   2.3 Data Base for Development Phase 19
   2.4 Data Base for Application Phase 23

3. RELATIONSHIPS BETWEEN PARTICULATE CONCENTRATIONS AND VISIBILITY . 27
   3.1 Elimination of Variables and Functional Forms 27
      3.1.1. Motor Vehicle Particles 27
      3.1.2 Fine Versus Coarse Fractions from Dichotomous Samplers 29
      3.1.3 Relative Humidity and the Role of Aerosol Water . . . 31
   3.2 Light Extinction from Aerosol Concentrations 35
      3.2.1 Variable Definition and Regression Methodology . . . 35
      3.2.2 Overall Correlation Levels 37
      3.2.3 Regression Results 41
      3.2.4 Conclusions Regarding Issues of Concern 43
      3.2.5 Geographical Variations 46
      3.2.6 Limitations of the Analysis 49
   3.3 Prediction of Dichotomous FP and IP from Airport Data and Hi-Vol Data 50
      3.3.1 Prediction of FP 52
      3.3.2 Prediction of IP 56

4. CHARACTERIZATION OF PARTICULATE EPISODES USING AIRPORT DATA . . . 59
   4.1 Information Base 59
   4.2 Episode Case Studies 61
      4.2.1 30 June 1980 to 6 July 1980 61
      4.2.2 11 July 1980 to 18 July 1980 72
      4.2.3 24 July 1980 to 3 August 1980 82
      4.2.4 20 January to 22 January 1981 96

Preceding page blank

4.3 Potential Uses for the Methodology. 98

5.0 REFERENCES. 101

APPENDIX A A-1

EXECUTIVE SUMMARY

In accordance with the provisions of the 1977 Clean Air Act Amendments, EPA is presently reviewing the National Ambient Air Quality Standard for suspended particulate matter. Based on this review, the present standards for total suspended particles (TSP $\leq$ 50 μm) may be supplemented or replaced with standards for inhalable particles (IP < 15 μm), 10 micron particles (PM10 < 10 μm), and/or fine particles (FP < 2.5 μm). In order to assist in the standards review and to provide information on current particulate concentrations, EPA has established a major monitoring system, the EPA IP Network, throughout the United States.

The EPA IP Network is providing Hi-Vol sampler data for TSP and dichotomous sampler data for IP and FP at nearly 200 locations on a six-day sampling schedule. As part of a program to start making use of this large data set, EPA contracted with Santa Fe Research Corporation to analyze the currently available particulate data for the Eastern U. S. in conjunction with airport data for visibility and relative humidity. The purpose of this study is to improve the understanding of visibility/aerosol relationships and long range particle transport in the East.

The man-made haze that covers the East may be an important welfare effect to be considered in setting Secondary National Ambient Air Quality Standards for particulate matter. The first major objective of this study is to improve our technical knowledge of the Eastern haze, specifically with respect to the relationships among visibility, particle size distribution, and particle chemical composition. Major questions to be addressed are as follows: How much better does FP relate to visibility than IP or TSP? How does the chemical composition of fine particles (in particular the sulfate fraction) affect visibility? Are the Eastern IP Network data consistent with other studies showing that sulfate aerosols dominate visibility reduction in the East?

As an auxiliary to the first objective, we also address the problem of predicting FP and IP concentrations from airport visibility data and Hi-Vol TSP data. Such predictions would be very useful in expanding the historical record for FP and IP to cover more regions and more years.

The second major goal of this study is to show how airport visibility data can be used to supplement the EPA IP Network data in short-term episode studies. Because EPA IP Network data are rather sparse geographically, and because the frequency of collection is only every 6th day, considerable gaps exist in the particulate data. These data gaps hinder a full understanding of fine particle transport and of the spatial/temporal extent of fine particle concentrations. In this study, we show that routine airport data can be used qualitatively to fill in the spatial/temporal gaps in the EPA IP Network data and thereby provide a better understanding of fine particulate concentrations and large scale transport.

Before we present our results, it is worthwhile to discuss some basic definitions and concepts for those readers who are not well versed in visibility studies. In this report, we define "visibility" as "visual range," the farthest distance that an observer could distinguish a large dark object against the horizon sky. We also use a more technically precise term, "extinction coefficient," the fraction of light that is attenuated per unit distance as a light beam traverses the atmosphere. In a uniform atmosphere, it can be shown that visual range is inversely proportional to the extinction coefficient, with a constant of proportionality depending on the contrast detection threshold of the observer. Also, it is known from basic principles that the extinction coefficient is a simple linear sum of four components: light scattering by air molecules (blue-sky scatter), light absorption by gases (essentially all from NO_2), light scattering by particles (usually dominated by sulfates and other fine particles), and light absorption by particles (basically all from elemental carbon). In the Eastern U.S., the particulate contribution to the extinction coefficient, in particular light scattering by particles, generally far exceeds the gaseous contribution to the extinction coefficient.

Description of Data Bases

Three types of data are used in this report: visibility observations from airports, relative humidity readings from airports, and particulate measurements from the EPA IP Network. The latter include all Hi-Vol and dichotomous sampler measurements of particulate mass, sulfate, and lead that were recorded by the EPA IP Network through the middle of 1981. The quality of the airport data for visibility and relative humidity is assured in four ways: (1) restricting the visibility data to daylight readings each day, (2) limiting the airports to

Class-1 weather stations, (3) conducting a telephone survey to make sure that all airports used have adequate visibility marker systems, and (4) identifying possibly erroneous data using histograms of single variables and scatterplots of correlated variables. We also formulate and apply data quality screens that eliminate highly dubious values from the EPA IP Network data. The particulate data quality screens are based on both physical and statistical considerations.

The data base for the first part of this study -- development of relationships between particulate concentrations and visibility -- consists of daily particulate measurements from 14 EPA IP Network sites combined with corresponding visibility and relative humidity observations from nearby airports. The 14 EPA IP Network sites are located in 6 metropolitan areas: Birmingham (5 sites), Washington, D.C. (1 site), Boston (2 sites), Minneapolis (2 sites), Buffalo (2 sites), and Philadelphia (2 sites). Using data from 8 of these sites, we assemble a "development" data set to analyze the relationship between particulate concentrations and visibility. This development data set contains 254 daily values, approximately one-third of which include chemical composition measurements for the particulate samples ($SO_4^=$ and Pb). Considering that the data cover nearly one and one-half years (beginning of 1980 to the middle of 1981), the sample size is not extremely large; there are four reasons for this: (1) some sites were not operational for the full one and one-half years, (2) the particulate data were taken only every sixth day (every 12th or 24th day for chemical constituents), (3) there were missing values within the routine particulate sampling schedule, and (4) certain days were eliminated based on weather considerations. Using data for the other six sites, we create an "independent test" data base of 197 daily values to be used for checking the conclusions based on the development data set. Furthermore, with data from all 14 locations, an "annual mean" data base is formulated to test predictive formulas for FP and IP on a yearly average basis.

In the second part of this study -- characterization of particulate episodes -- the particulate data and airport data are used separately. First, maps are prepared listing particulate concentrations at EPA IP Network sites in the Eastern U.S. during the period April 1980 to March 1981. These maps allow us to identify particulate episodes. Then, visibility data from 70 carefully selected airports in the East are used to investigate the particulate episodes. The airport data provide greater resolution than the EPA IP Network data both spatially and temporally.

Relationships Between Particulate Concentrations and Visibility

We find that it is possible to formulate physically meaningful and statistically well-fitting regression equations that predict light extinction levels as a function of aerosol concentrations and relative humidity. In these equations, it is important to include relative humidity as a multiplicative factor of the form $(1\text{-}RH)^{-1}$ on the aerosol concentrations. Such an approach correctly includes water as an integral part of the particulate concentrations and correctly approximates the hyperbolic dependence of aerosol water on relative humidity.

As expected from theoretical principles, we find that fine particles correlate much better with extinction than inhalable particles, which in turn correlate much better with extinction than total suspended particles. The best statistical fits are achieved with regression models that include nonlinear relative humidity effects and that distinguish sulfate particles from nonsulfate particles. Our results imply that, if welfare standards are to be established to protect visibility, such standards should be set for FP and/or sulfates, not TSP, IP, or PM10.

The extinction efficiency (per unit mass) for sulfate aerosols is much greater than the extinction efficiency for the nonsulfate portion of TSP and IP. The extinction efficiency for fine sulfate particles also appears to be somewhat greater than the extinction efficiency for fine nonsulfate particles (an obvious exception, on theoretical grounds, being fine elemental carbon). Our results suggest that, on the average, sulfates and associated water account for about 45% of total light extinction in the East. This estimate is subject to uncertainties and is somewhat lower than other estimates of 50 to 75% published in the literature.

The small contribution to extinction from coarse particles cannot be precisely quantified with the limited data currently available from the EPA IP Network. The same conclusion holds for the small contribution from fine primary vehicular particles (estimated using Pb as a tracer element). The extinction properties of primary vehicular particles should be given emphasis in future studies because elemental carbon particles from increased diesel use may cause a national deterioration in visibility over the next twenty years.

The inverse process of predicting fine particle concentrations as a function of visibility and relative humidity is less physically straightforward and less statistically well-fitting than the direct process discussed above. Although visibility is a good qualitative indicator of fine particle and sulfate concentrations, we find that airport data alone cannot be used as a precise, quantitative substitute for fine particle monitors, especially on a daily basis. Fine particle concentrations can be predicted from airport visibility data with a standard error of 45-60% on a daily basis and 25% on an annual mean basis. Although TSP alone also is a poor predictor of FP, TSP in conjunction with airport visibility yields more reasonable estimates of FP, with errors potentially as low as 40% on a daily basis and 16% on an annual basis. Adding relative humidity data does not significantly improve predictive accuracy. We further find that airport data is a poor predictor of IP, but that TSP alone is a fairly good predictor of IP (30-35% daily errors and about 17% annual errors).

Many of our conclusions can be made more certain and more precise when more data become available from the EPA IP Network. Specific issues that can be quantified more accurately are as follows: (1) the extinction efficiency of coarse particles, (2) the extinction efficiency of primary vehicular particles, (3) the relative extinction efficiencies of fine sulfates and fine nonsulfates, (4) geographical variations in aerosol extinction efficiencies, and (5) the coefficients and errors for equations predicting FP and IP from airport data and TSP data.

Characterization of Particulate Episodes Using Airport Data

Airport visibility data are of fairly good quality and utility for studying the spatial/temporal extent of fine particle episodes in the East. For several case studies in the summer of 1980, we find that the geographical distribution of haziness (based on airport data) generally agrees with the geographical distribution of fine particle concentrations. For example, Figure 1 shows a visibility map on a day when extremely high fine particle concentrations were recorded in the Ohio Valley. Furthermore, the day-to-day movement of the haziness generally appears to agree with large scale wind patterns.

Studies with large scale visibility maps can be useful, in an overall sense, by establishing the general need for interstate considerations in control policies for fine particles and sulfates. Also, whenever a specific fine particle episode is analyzed with respect to control requirements for short-term standards, visibility maps can provide important qualitative insights regarding the spatial extent, transport patterns, and origins of the episode. Because visibility data are routinely available, such data can be incorporated in episode studies at very little cost.

The main drawback of the visibility mapping technique is that it is not quantitative. Visibility maps do not serve as an accurate substitute for fine particle monitors, nor do they provide a quantitative estimate of ambient contributions from local sources versus ambient contributions from large scale transport.

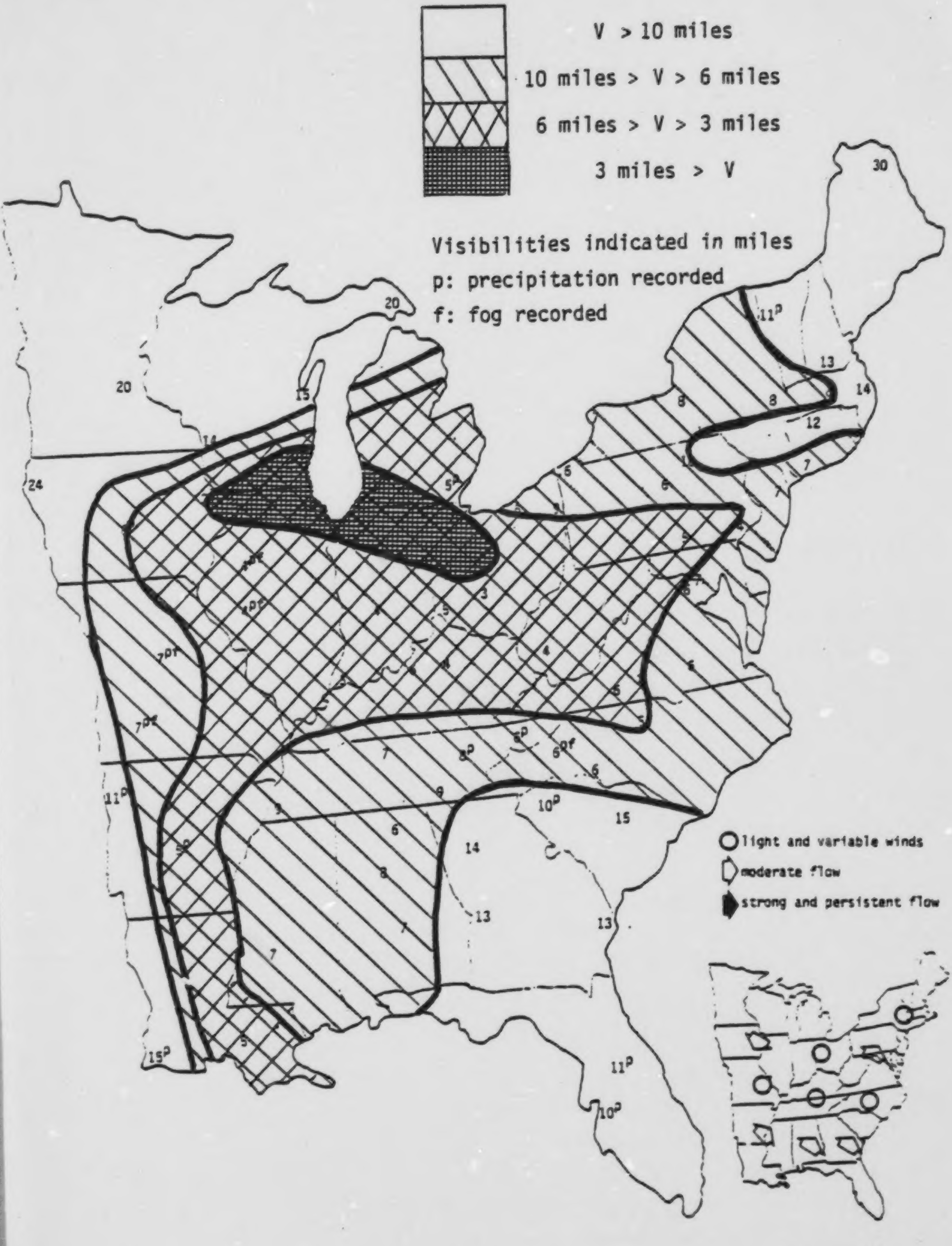
V > 10 miles
10 miles > V > 6 miles
6 miles > V > 3 miles
3 miles > V
Visibilities indicated in miles
p: precipitation recorded
f: fog recorded
light and variable winds
moderate flow
strong and persistent flow
30
20
20
15
14
24
11p
13
14
8
8
12
7
6
6
5p
3
4
5
6
7pf
7pf
11p
5p
7
8p
5p
6pf
6
9
10p
15
14
6
8
13
13
7
7
5
15p
11p
10p

Figure 1 Visibility map for 26 July 1980.

Reproduced from best available copy.

1. INTRODUCTION

In accordance with the provisions of the 1977 Clean Air Act Amendments, EPA is presently reviewing the National Ambient Air Quality Standards for suspended particulate matter. It is anticipated that this review may result in new standards for specific size fractions of particulate matter. That is, the present standards for total suspended particles (TSP $\leq 50\mu m$) may be supplemented or replaced with standards for inhalable particles (IP $< 15\ \mu m$), ten-micron particles (PM10 $< 10\ \mu m$), and/or fine particles (FP $< 2.5\ \mu m$). In order to assist in the standards review, to provide information on current particulate concentrations, and to facilitate future implementation planning, EPA has established a major monitoring system, the EPA IP Network, throughout the United States.

The EPA IP Network is providing Hi-Vol sampler data for TSP and dichotomous sampler data for IP and FP at nearly two hundred locations. The particulate samples are being collected every sixth day, with chemical analyses performed every twenty-fourth day. As part of a program to start making use of this large data set, EPA has contracted with Santa Fe Research Corporation to study the currently available particulate data for the Eastern U.S. in conjunction with airport data for visibility and relative humidity. The purpose of the study, for which this document is the final report, is to improve the understanding of visibility/aerosol relationships and long-range particle transport in the East.

Visibility degradation is an important welfare effect that must be considered in setting Secondary National Ambient Air Quality Standards for particulate matter (EPA 1982). The issue of particulate standards and visibility has special importance in the East, where a rather dense man-made haze occurs (Trijonis 1982a). The first major goal of this study is to improve our knowledge of the relationships among visibility, particle size distribution, and particle chemical composition in the East. Specific questions to be addressed are as follows: How much better does FP relate

Preceding page blank

to visibility than IP or TSP? How does the chemical composition of fine particles (in particular the sulfate fraction) affect visibility? Are the Eastern IP Network data consistent with other studies showing that sulfate aerosols dominate visibility reduction in the East?

There is another statistical problem that is closely related to the first objective. This problem concerns quantitative predictions of FP and IP from airport visibility data and Hi-Vol TSP data. Such predictions would be useful in expanding the historical record for FP and IP to include many more regions and years. This problem is addressed as an auxiliary to the first objective.

The second major goal of this study is to show how airport visibility data can be used as a qualitative supplement to the EPA IP Network data in short-term studies (e.g. episode analyses). Because EPA IP Network data are rather sparse geographically, and because the frequency of collection is only every sixth day, considerable gaps exist in the particulate data. These data gaps hinder a full understanding of fine particle transport and of the spatial/temporal extent of fine particle concentrations. It is important to try to improve this understanding because attainment of particulate standards could be significantly affected by the long-range transport of fine particles, especially in the Eastern United States. In this study, we show that routine airport data can be used qualitatively to fill in the spatial/temporal gaps in the EPA IP Network data and thereby provide a better understanding of fine particle patterns and large-scale transport.

1.1 BASIC CONCEPTS AND DEFINITIONS

The definitions for the particulate (aerosol) parameters used in this study are fairly straightforward. The term total suspended particles (TSP) refers to the mass of particles measured by a Hi-Vol sampler (those particles less than approximately 50 μm in aerodynamic diameter). Inhalable particles (IP) and fine particles (FP) refer to dichotomous sampler measurements with size ranges < 15 μm and < 2.5 μm, respectively. Coarse particles (CP) denotes IP minus FP, particle mass in the range 2.5 to 15 μm. In this study, we also use chemical composition data for particulate sulfate ion ($SO_4^=$) and particulate lead (Pb).

The basic concepts of visibility deserve a more extended introductory discussion because they are not as straightforward and because they may not be familiar to the reader. Generally, visibility refers to the clarity of the atmosphere. Visibility can be defined quantitatively in terms of discoloration (wavelength shifts produced by the atmosphere), contrast (the relative brightness of visible objects), and/or visual range (the farthest distance that one would be able to distinguish a large black object against the horizon sky). Because this study is based on weather-station measurements of visual range, we will define visibility as visual range and will use the two terms interchangeably. It should be noted that the concept of visual range makes most sense in situations of large-scale homogeneous haze, which is the type of visibility phenomenon addressed in this report.

Visibility through the atmosphere is restricted by the absorption and scattering of light by both gases and particles. The sum of absorption and scattering is called total extinction which is measured by the extinction coefficient "B". The extinction coefficient represents the fraction of light that is attenuated per unit distance as a light beam traverses the atmosphere. In a homogeneous atmosphere, visibility is inversely proportional to extinction; the Koschmeider formula expressing this relationship is:

$$B = \frac{k}{V} . \qquad (1\text{-}1)$$

The constant in Equation (1-1) is usually chosen to be k = 3.9 or k = 3.0, depending on whether one assumes a 2% or 5% contrast detection threshold for the observer. As explained later in Section 3.2.1, a Koschmeider constant of 3.0 is most appropriate when using airport visibility data.

Figure 1.1 presents a map of annual median visual range for nonurban areas of the United States. It is obvious that the eastern one-half of the U.S., the study area for this project, has much lower visibility than most of the West. Although some parts of the study area (e.g., northern New England or northern Minnesota) experience moderate visibility levels ($\sim$25 miles), median visual range is generally 10-15 miles in areas east of the Mississippi and south of the Great Lakes. For a Koschmeider constant of 3.0, this range corresponds to a median extinction coefficient of 1.2 - 1.9 $10^{-4} m^{-1}$ (the conventional units for extinction).

Reproduced from best available copy.

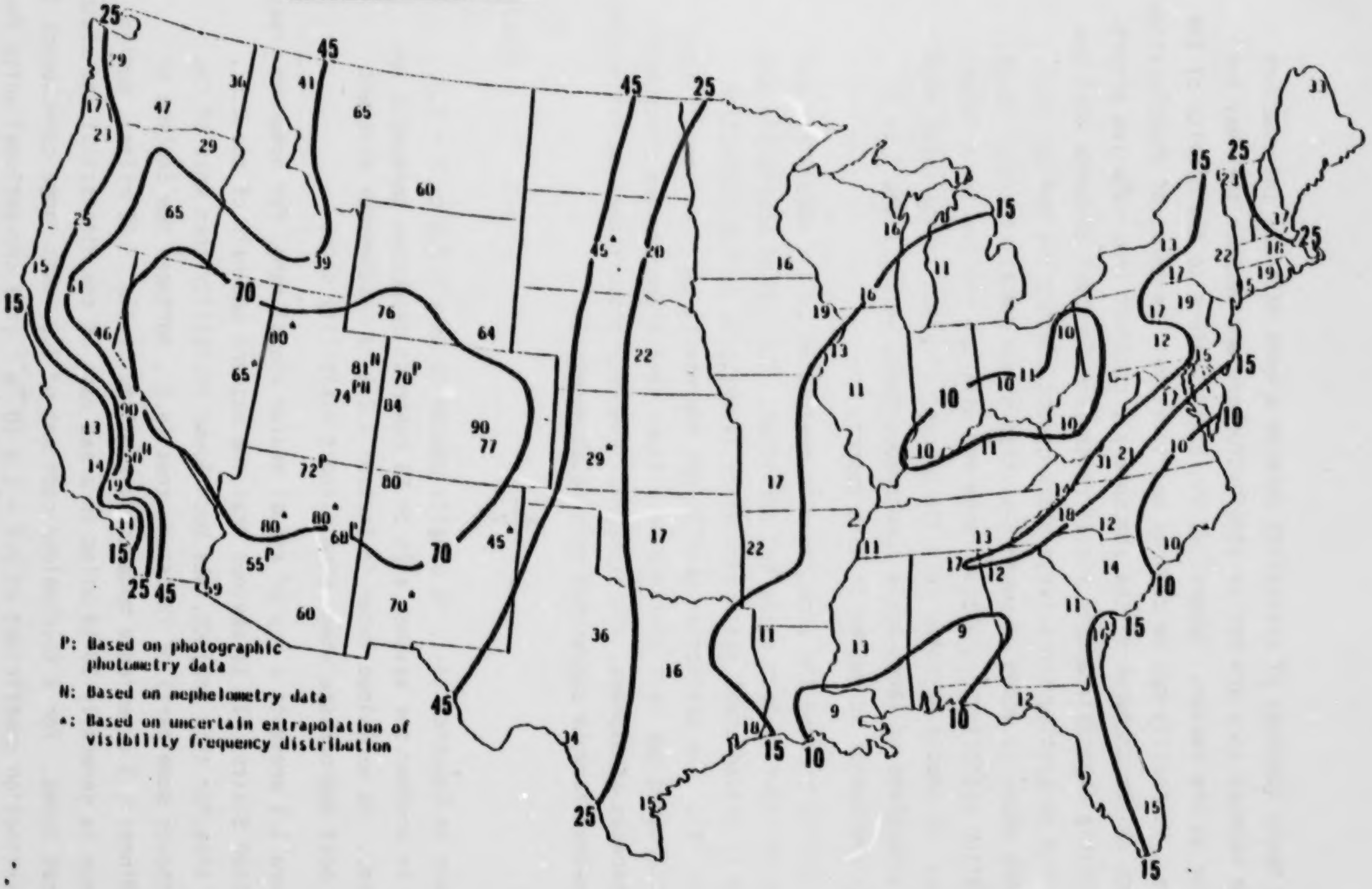
25
45
45
25
15
25
15
15
10
10
10
15
70
70
45
25
15
10
10
15
15
45
25
15
25
45
29
17
21
47
36
41
65
29
65
25
15
61
46
60
39
76
64
80
65
81
70
74
84
90
77
29
45
20
22
17
22
16
19
13
11
16
11
10
11
10
10
11
10
13
14
19
11
72
80
80
80
68
55
59
60
70
45
17
36
16
34
15
11
13
9
9
12
12
14
11
10
15
31
21
18
14
17
12
13
12
17
19
22
23
17
18
19
15
17
11
31
10
10
11

P: Based on photographic photometry data

N: Based on nephelometry data

*: Based on uncertain extrapolation of visibility frequency distribution

Figure 1.1 Median mid-day visibilities (in miles) and visibility isopleths for suburban/nonurban areas in the United States (Trijonis 1982a; Trijonis and Shapland 1979).

It is often preferable to discuss visibility in terms of extinction coefficient rather than visual range because the extinction coefficient can be linearly subdivided into contributions from various atmospheric components. In general, total extinction is a linear sum of four terms:

$$B = B_{\text{Rayleigh}} + B_{\text{Ab-Gas}} + B_{\text{Scat-Part}} + B_{\text{Ab-Part}} \, . \qquad (1\text{-}2)$$

An explanation of each of these terms is as follows:

B_{Rayleigh} = light scattering by air molecules (Rayleigh or blue-sky scatter). This term is on the order of .10 to .12 $(10^4 m)^{-1}$ depending on altitude (i.e. depending on the density of air); it would restrict visibility to approximately 155-190 miles (for a 5% contrast) if all particles and pollutant gases were absent.

$B_{\text{Ab-Gas}}$ = light absorption by gases. Nitrogen dioxide (NO_2) is the only prevalent gaseous pollutant that is a significant light absorber. Although concentrations of NO_2 are usually not large enough to produce significant reductions in overall visual range, NO_2 can produce significant brownish discoloration because it preferentially absorbs blue light.

$B_{\text{Scat-Part}}$ = light scattering by particles (aerosols). In most cases, this is the dominant part of total extinction. As shown later in Figure 3.1, light scattering per unit mass of particle depends strongly on particle size; particles in the 0.1 to 1.0 micron size range are much more efficient light scatterers than particles outside that size range. Significant contributions to light scattering can be made by many types of particle: particles emitted from fuel combustion, particles emitted from vegetative burning, fine dust particles, and secondary aerosols (aerosols formed from gas-to particle conversion in the atmosphere). Secondary aerosols, especially sulfates, are often major contributors to light scattering because they tend to form in the 0.1 to 1 micron size range. Hygroscopic particles -- again sulfates are the obvious example -- often attract a substantial volume of water into the particle phase, thereby further increasing aerosol light-scattering.

$B_{Ab\text{-}Part}$ = light absorption by particles. The most important light absorping aerosol is usually graphitic carbon. Light absorption by aerosols can be substantial in those urban areas where soot contributes a significant fraction of the aerosol.

1.2 ORGANIZATION OF THE REPORT

This report is organized into four chapters. This chapter has provided a statement of objectives and an introduction to the basic technical concepts of visibility. Chapter 2 describes the data bases used in the project. Chapter 3 deals with the first major objective of the study -- exploring the statistical relationships between particulate concentrations and visibility. The second major objective -- using airport visibility data to investigate the spatial extent and transport patterns of fine particle episodes -- is addressed in Chapter 4.

2. DESCRIPTION OF DATA BASES

This chapter discusses the data sets that serve as the basis for this report. Section 2.1 reviews the various types of measurements included in the data sets. Section 2.2 discusses data quality considerations. The specific data bases for the development and application phases of this project are summarized in Sections 2.3 and 2.4, respectively.

2.1 TYPES OF DATA

Three types of data are used in this report -- visibility observations from airports, relative humidity readings from airports, and particulate measurements from the EPA IP Network. Table 2.1 lists the specific parameters included, as well as their averaging times and units.

The visibility data consist of "prevailing visibility" readings made by human observers at weather stations (airports). According to National Weather Service procedures, prevailing visibility is defined as the greatest visual range that is attained or surpassed around at least half of the horizon circle, but not necessarily in continuous sectors (Williamson 1973). Daytime visibility is measured by observing markers (e.g. buildings, mountains, towers, etc.) against the horizon sky; nighttime visibility measurements are based on unfocused, moderately intense light sources. Because our experience indicates that daytime and nighttime observations are often incompatible, and that daytime data are usually of higher quality (Trijonis and Yuan 1978; Trijonis 1979), only daytime observations are employed in this study.

Weather observers usually perform visibility measurements each hour, but only the readings from every third hour are contained in the formal data reports published by the National Climatic Center. The visibility readings that we used were the observations for 7:00 AM, 10:00 AM, 1:00 PM, and 4:00 PM Standard Time in the Eastern Time Zone, and 6:00 AM, 9:00 AM, noon, and 3:00 PM Standard Time in the Central Time Zone.

The relative humidity readings were obtained for the same airports and for the same four daytime hours as the visibility observations. All the airport data were acquired from the National Climatic Center in hard-copy form, monthly summaries of Local Climatological Data (monthly LCD's). The daily visibility and relative humidity recordings were averaged manually, with the 4-hour means then transcribed into computerized form.

TABLE 2.1 PARAMETERS INCLUDED IN THE DATA BASE

PARAMETER (SYMBOL)	UNITS	AVERAGING TIME
Airport Weather Data		
Visual Range (V)	miles	4 daylight hours*
Relative Humidity (RH)	none(fraction)	" " "
EPA IP Network Particulate Data		
Hi-Vol mass (TSP)	$\mu g/m^3$	24 hours
Hi-Vol sulfate ($TSPSO_4^=$)	"	"
Hi-Vol lead (TSPPb)	"	"
Dichotomous inhalable mass (IP)**	"	"
Dichotomous inhalable sulfate ($IPSO_4^=$)	"	"
Dichotomous inhalable lead (IPPb)	"	"
Dichotomous fine mass (FP)***	"	"
Dichotomous fine sulfate ($FPSO_4^=$)	"	"
Dichotomous fine lead (FPPb)	"	"

* 7:00 AM/10:00 AM/1:00 PM/4:00 PM EST and 6:00 AM/9:00 AM/noon/3:00 PM CST

** Inhalable measured as ≤ 15 μm.

*** Fine measured as ≤ 2.5 μm.

The particulate data were acquired from EPA in computerized form (magnetic tape). These data consisted of all Hi-Vol and dichotomous sampler measurements of particulate mass, sulfate, and lead that had been processed for the EPA IP Network as of February 1982. The available particulate data covered the approximate time period of the middle of 1979 to the middle of 1981, although the specific start and end dates of the data varied greatly (by many months) from site to site.

It should be noted that the EPA IP Network basically involves sampling every sixth day, simultaneouly over the entire network. Chemical analyses for sulfate, lead, and other species are conducted on every fourth sample (e.g. every 24th day), although chemical analyses have been performed on every other sample (every 12th day) at most sites during the first six months of station operation.

Because the Hi-Vol data prior to 1980 were taken using quartz fiber filters, and because such data are not necessarily equivalent to the subsequent Hi-Vol measurements on glass fiber filters, we restricted our analyses to the years 1980 and 1981. To insure consistent periods for our analyses with and without chemical composition data, we decided to limit the data at each site to the period for which chemical composition measurements had been processed (often deleting a slightly extended period containing data on particulate mass but not on particulate chemical composition). Furthermore, because our data quality screens for the particulate data are based on comparisons of the Hi-Vol and dichotomous sampler measurements, we restricted our data sets at each site only to days reporting Hi-Vol TSP as well as dichotomous IP and FP.

2.2 DATA QUALITY ASSURANCE

Several previous studies (Trijonis and Yuan 1978; Trijonis 1979, 1980, 1982c; Trijonis et al. 1982; Cass 1979; Leaderer and Stolwijk 1979) have shown that airport data are of good quality for use in characterizing visibility/aerosol relationships. The quality of the data are indicated by the high correlations (typically 0.7 to 0.9) obtained in relating airport visibility data to independent particulate and/or meteorological measurements. Some of the limitations of airport visibility data and the resulting implications for our statistical analyses are discussed later in Section 3.2.6.

To help assure the quality of the airport visibility and relative humidity data used in this study, three steps were taken. First, the airports considered were restricted to Class-1 weather stations operated by National Weather Service personnel; because of the functional priorities, such stations likely have higher quality weather data than lesser class stations or stations operated by FAA and military personnel. Second, a telephone survey was conducted to insure that all airports used had adequate visibility marker systems. Third, outlier or unusual values for visibility and relative humidity were identified using histograms of single variables and scatter plots of correlated variables. All unusual values and many normal values were checked against the original hard-copy NCC forms to eliminate manual transcription errors.

A statistical screening test of the particulate data has already been conducted by EPA. This test flags a significant number of data points (Rodes 1981). However, EPA only eliminates a data point when there is an obvious cause for a measurement error; as a result, most of the questionable points are left in the data base. For example, recordings remained for certain sites and days with IP values two to five times greater than TSP values. Because TSP essentially represents the mass of particles less than 50 μm in diameter while IP only represents the mass of particles less than 15 μm in diameter, and because TSP also tends to be inflated over IP due to "artifact" collection of gases on Hi-Vol filters, such recordings are obviously unreasonable. We decided to eliminate these and other highly unreasonable data points by formulating our own data quality screening procedure.

Our data quality screens (see Table 2.2) are based on ratios of simultaneous Hi-Vol and dichotomous sampler data. We selected cut-offs for these ratios using both physical and statistical considerations. The physical considerations involved what would be reasonable given the particle size ranges measured by the samplers and the possibility of artifacts with the Hi-Vol samplers. The statistical considerations were based on identification of outliers in simple histogram plots of the ratios. We chose the cut-offs so that only the most egregious outliers, at most a few percent of the data, would be eliminated. Table 2.2 indicates the percent of data deleted by the data quality screens. About 2% of the data were eliminated entirely; of the chemical data in the remainder, about 4% of the sulfate data and about 8% of the Pb data were eliminated by screens on the chemical constituents.

TABLE 2.2 DATA QUALITY SCREENS APPLIED TO THE EPA PARTICULATE DATA BASE

DATA QUALITY SCREEN	PERCENT DATA ELIMINATED
Screens on particulate mass measurements.	
1. IP/TSP > 1.5	1.4%
2. TSP/IP > 4 and FP/IP > 0.6	.3%
Percent total data points eliminated:	1.7%
Screens on chemical constituent measurements	
3. $IPSO_4^=/TSPSO_4^= < .25$ or > 1.5	4.4%
4. IPPb/TSPPb < .5 or > 2.5 when either IPPb or TSPPb > 0.2 $\mu g/m^3$	8.1%

2.3 DATA BASE FOR DEVELOPMENT PHASE

The development phase of this project (Chapter 3) will involve regression studies interrelating atmospheric extinction coefficient (determined from visibility data), relative humidity, and particulate concentrations. The relationship will be developed using simultaneous daily measurements of particulate parameters at EPA IP Network sites and weather parameters at nearby airports. Locations were selected for this analysis based on the following criteria:

- The locations are in the eastern U.S., up to one tier of states west of the Mississippi River.
- The EPA IP Network sites have a relatively large number of daily particulate measurements, including an adequate amount of chemical composition data.
- The period of the particulate data is not extremely biased seasonally, e.g. the available data are not for only one season.
- The EPA IP Network sites are located near an airport weather station, not more than 15 km away, preferably less than 10 km away.
- The airport weather data include relative humidity.
- The airports have adequate sets of visibility markers and are preferably Class-1 weather stations.

Based on the above criteria, we selected 14 locations in 6 air basins (see Table 2.3). The selection of these locations was a rather obvious choice. All of the sites in Table 2.3 measure up very well against the criteria, while all other potential sites seriously fail the criteria.

A decision was required concerning how to handle the situation of more than one site in a given air basin. The data bases for the sites in a given air basin are partly redundant in the sense that some of the sampling dates are duplicated and in the sense that the same airport weather data are used (except in Philadelphia, where two different airports are considered). The data bases are not fully redundant, however, because the particulate data are unique to each site and because some of the sampling days are independent (because one particulate site was operating while another was not). We decided to handle this situation by creating two data bases -- a data base to develop the relationships and a data base to test the relationships. In each air basin, we chose the site with the greater amount of data for development and the site with the lesser amount of data for testing. The Birmingham area created a special problem because of five particulate sites. We chose three of these sites (010380003, 010570001, and 012540001) for development data and two (010380026 and 013200001) for testing data. To eliminate redundancies within these two data sets, we averaged the particulate measurements whenever more than one of the sites was operating on a given date. Thus, the daily particulate data for Birmingham represent averages over one, two, or three sites in the development set and averages over one or two sites in the testing set.

Table 2.4 lists the number of daily samples in the entire development and testing data bases. Considering that the data cover nearly one and a half years (beginning of 1980 to nearly the middle of 1981), the sample size is not extremely large. There are four reasons for this: (1) some sites were not operational for the full one and one-half years, (2) the particulate data were taken only every sixth day (every 12th or 24th day for chemical constituents), (3) within the routine particulate sampling schedule there were missing values, and (4) certain days were eliminated based on weather considerations. The fourth reason needs further clarification. Because we are interested in the relationship between visibility and particulate concentrations, we decided to eliminate days when visibility reduction was likely dominated

TABLE 2.3 STUDY LOCATIONS FOR THE DEVELOPMENT PHASE OF THE PROJECT

AIRPORT (NCC code)	PARTICULATE SITE (EPA Code)	DISTANCE FROM AIRPORT TO PARTICULATE SITE(km)
Birmingham Mun. (13876)	Birmingham, AL (010380003)	8
"	Center Point, AL (010570001)	6
"	Mountain Brook, AL (012540001)	10
"	Birmingham, AL (010380026)	3
"	Tarrant City, AL (013200001)	6
National Airport (13743)	Washington, D.C. (090020017)	9
Logan International (14739)	Boston, MA (220240013)	2
"	Boston, MA (220240012)	6
Minneapolis/St. Paul Int'l	Minneapolis, MN (242260049)	7
"	Minneapolis, MN (242260051)	12
Buffalo International (14733)	Buffalo, NY (330660003)	11
"	Buffalo, NY (330660010)	11
Northeast Philadelphia Apt.	Philadelphia, PA (397140024)	1
Philadelphia International	Philadelphia, PA (397140036)	6

TABLE 2.4 SUMMARY OF DATA BASES FOR THE DEVELOPMENT PHASE OF THE PROJECT

Table 2.4a Development Data

LOCATION (EPA CODE)	SAMPLE SIZE	CHEMICAL COMPOSITION SAMPLE SIZE	
		Dichotomous $SO_4^=$	Complete Sets for Both Hi-Vol and Dichotomous $SO_4^=$ and Pb.
Birmingham, AL (010380003, 010570001, and 012540001)	61	28	26
Washington, D.C. (090020017)	32	11	11
Boston, MA (220240013)	40	14	11
Minneapolis, MN (242260049)	38	15	13
Buffalo, NY (330660003)	29	9	5
Philadelphia, PA (397140024)	54	16	8
Total	254	93	74

Table 2.4b Testing Data

LOCATION (EPA CODE)	SAMPLE SIZE	CHEMICAL COMPOSITION SAMPLE SIZE	
		Dichotomous $SO_4^=$	Complete Sets for Both Hi-Vol and Dichotomous $SO_4^=$ and Pb.
Birmingham, AL (010380026 and 013200001)	54	14	11
Boston, MA (220240012)	31	9	7
Minneapolis, MN (242260051)	34	10	6
Buffalo, NY (330660010)	30	6	5
Philadelphia, PA (397140036)	48	10	6
Total	197	49	35

by weather events rather than by ambient aerosol concentrations. Based on our previous experience (Trijonis and Yuan 1978; Trijonis 1979, 1980, 1982c; Trijonis et al. 1982), the specific elimination criteria we chose were as follows: (1) eliminate the day if there was any measurable precipitation during the 24-hour period, and (2) eliminate the day if fog was reported during the daylight hours of useful visibility data (with the sole exception that a single fog observation at the 6:00 AM or 7:00 AM hour is permissible).

The development phase of this project examines not only how visibility depends on relative humidity and particulate concentrations, but also how dichotomous FP and IP can be predicted from TSP, visibility, and relative humidity. In the latter analysis, we want to evaluate FP and IP predictive formulae on an annual basis as well as a daily basis. For this purpose, we created an "annual" test data set consisting of yearly mean values at the 14 study locations. The yearly means were taken over the period January 1980 to March 1981 (data were sparse in the first quarters of both 1980 and 1981, so two first quarters were used to compensate for this scarcity). The yearly means were typically composed of about 40 daily values and thus corresponded to an "every ninth day" particulate sampling schedule.

2.4 DATA BASE FOR APPLICATION PHASE

Unlike the development phase of this project, where particulate data and airport weather data are melded together to analyze the interrelationships, the application phase treats the particulate measurements and airport recordings separately. Data from the EPA IP network are first used to identify episodes of high particulate concentrations in the East. Then, the airport data are used to provide greater temporal and spatial resolution during those episodes.

In organizing the EPA IP network data to search for particulate episodes, we limited ourselves to one complete year of data. This year was chosen as the second calendar quarter of 1980 to the first calendar quarter of 1981 (April 1980 to March 1981), because, at the time of our study, that period provided the greatest quantity of data from the EPA IP Network. During the year of interest, 51 EPA IP Network sites in the eastern U.S. reported at least some Hi-Vol and dichotomous data. However, some of the sites reported very little data, and several cities had more than one monitoring site. In preparing maps of the particulate data, we used only those sites with at least 18 data points during the year, and we selected only one site per city.[*] This restricted the analysis to the 25 sites illustrated in Figure 2.1.

Using data for these 25 sites, we constructed maps which listed daily TSP, IP, FP, sulfate, and lead concentrations (see Chapter 4). Because such maps are not very useful on days with few sites reporting data, the maps were prepared only for days having data from at least 15 locations (although we also allowed days with as few as 13 reporting sites, if at least seven of these sites had chemical composition data for that day).

In the application phase, particulate patterns during various episodes are studied using visibility and relative humidity data at 70 airports. The airport data provide greater resolution than the EPA IP Network data both temporally and spatially -- temporally because the airport data are available daily (rather than every sixth day), and spatially because the airport data are from 70 locations (rather than 15 to 25 locations).

Figure 2.2 illustrates the 70 airports included in the application phase.[**] The criteria for selecting these airports are (1) that they are geographically scattered over the East, (2) that they report data for relative humidity, and (3) that they have an adequate set of visibility markers and are preferably Class-1 weather stations.

---

[*] The criteria for selecting one site in each city were (1) quantity of data during the year and (2) (for comparison purposes) proximity to the nearby airport being used.

[**] We used a slightly more refined site-type classification in Figure 2.2 (metropolitan versus urban/suburban versus nonurban) than in Figure 2.1 (metropolitan/urban versus suburban/nonurban) for two reasons. First, airports are generally sited somewhat differently than EPA IPA Network sites, on the fringes of cities/towns rather than in the center of cities/towns. Second, Figure 2.2 contains many more sites than Figure 2.1, making a finer resolution more meaningful.

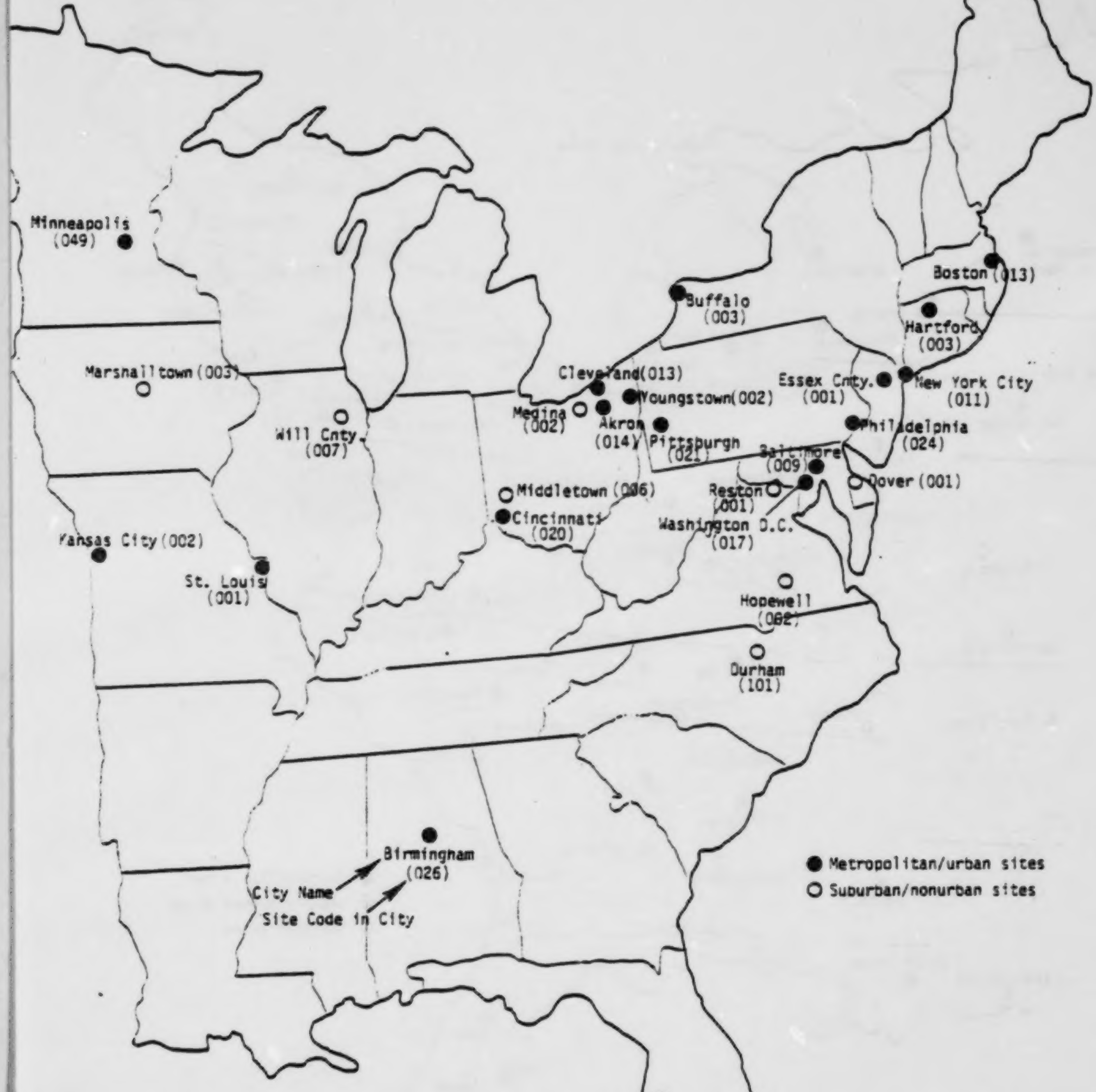
Minneapolis (049)
Marshalltown (003)
Will Cnty. (007)
Kansas City (002)
St. Louis (001)
Cleveland (013)
Medina (002)
Akron (014)
Youngstown (002)
Pittsburgh (021)
Middletown (006)
Cincinnati (020)
Buffalo (003)
Boston (013)
Hartford (003)
Essex Cnty. (001)
New York City (011)
Philadelphia (024)
Baltimore (009)
Reston (001)
Washington D.C. (017)
Dover (001)
Hopewell (002)
Durham (101)
Birmingham (026)
City Name
Site Code in City
● Metropolitan/urban sites
○ Suburban/nonurban sites

Figure 2.1 EPA IP network sites included in the application phase.

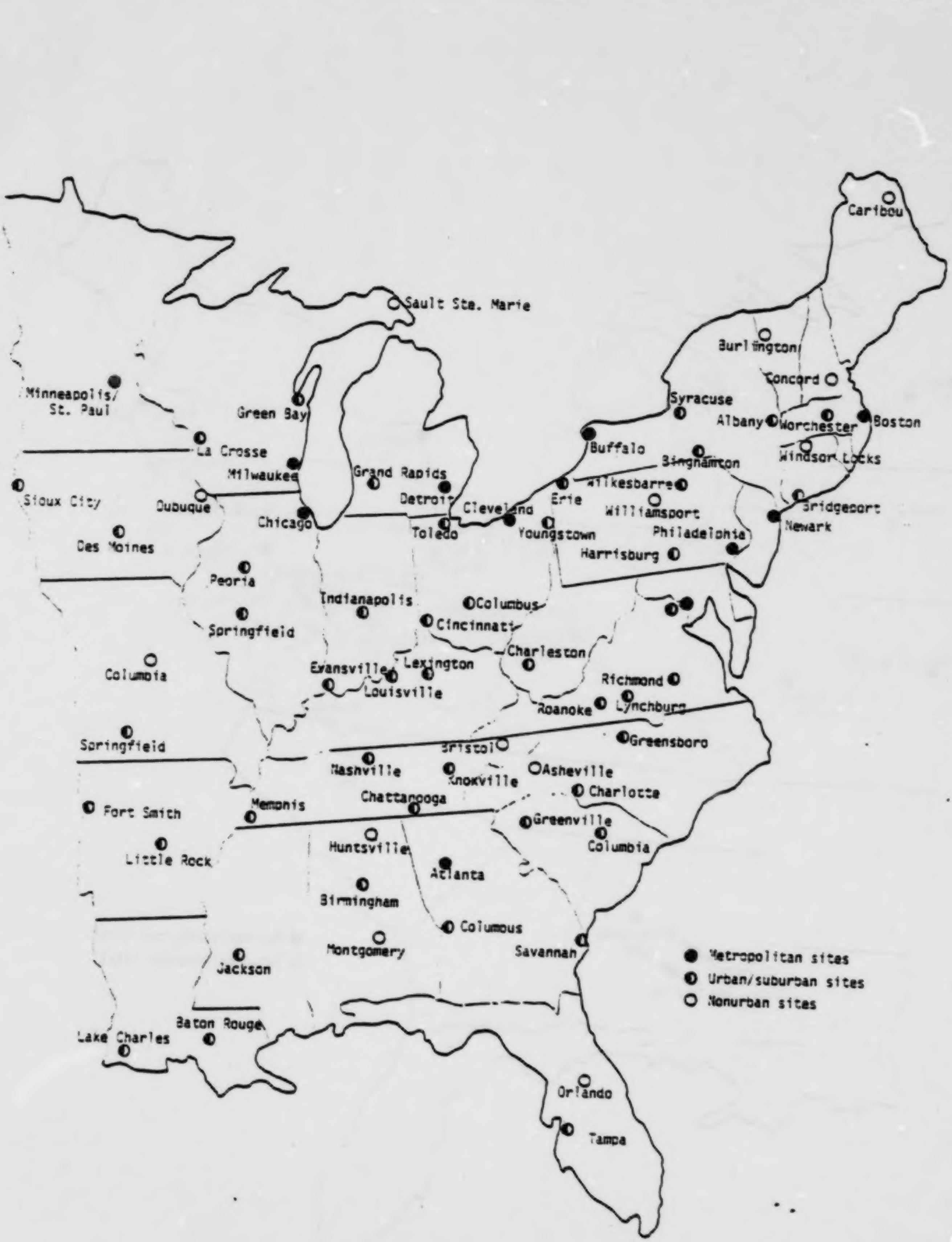
Caribou
Sault Ste. Marie
Burlington
Concord
Minneapolis/ St. Paul
Green Bay
Syracuse
Albany
Worchester
Boston
La Crosse
Buffalo
Binghamton
Windsor Locks
Milwaukee
Grand Rapids
Detroit
Wilkesbarre
Sioux City
Dubuque
Cleveland
Erie
Williamsport
Bridgeport
Chicago
Toledo
Youngstown
Philadelphia
Newark
Des Moines
Harrisburg
Peoria
Indianapolis
Columbus
Springfield
Cincinnati
Charleston
Columbia
Evansville
Lexington
Louisville
Richmond
Roanoke
Lynchburg
Springfield
Bristol
Greensboro
Nashville
Knoxville
Asheville
Charlotte
Fort Smith
Memphis
Chattanooga
Greenville
Little Rock
Huntsville
Columbia
Atlanta
Birmingham
Columbus
Savannah
Montgomery
Jackson
Baton Rouge
Lake Charles
Orlando
Tampa
● Metropolitan sites
◐ Urban/suburban sites
○ Nonurban sites

Figure 2.2 Airport weather stations included in the application phase.

3. RELATIONSHIPS BETWEEN PARTICULATE CONCENTRATIONS AND VISIBILITY

This chapter develops statistical relationships between the EPA IP Network data for particulate concentrations and the airport data for visibility and relative humidity. As discussed in the previous chapter (Section 2.3), the analysis is based on data from 14 sites in 6 air basins of the Eastern U.S. In the investigation, some data sets are used to develop the relationships, while other data sets are reserved to test the relationships.

In order to simplify later discussions, this chapter starts (Section 3.1) by eliminating those variables and formulations that were found to be insignificant in our analysis. Section 3.2 then presents regression studies relating atmospheric light extinction (determined from visibility data) to particulate concentrations and relative humidity. The regression models are formulated in a physically meaningful way, and they yield quantitative insights regarding the visibility reduction efficiencies of particles according to their size and chemical composition. Section 3.3 investigates the inverse type of problem -- statistical formulae for predicting dichotomous particulate concentrations (FP and IP) from airport data for visibility and relative humidity, as well as from Hi-Vol data for TSP.

3.1 ELIMINATION OF VARIABLES AND FUNCTIONAL FORMS

It is useful to begin describing our findings by addressing variables and formulations that were found to be of little significance or utility. By eliminating these variables and formulations, subsequent discussions of methodology and results can be simplified considerably.

3.1.1 Motor Vehicle Particles

Particulate matter from motor vehicles is one of the major aerosol fractions distinguished in our analysis. Total ambient particulate concentrations from auto exhaust, diesel exhaust, tire wear, and brake wear are estimated using lead (Pb) as a tracer for motor vehicle emissions. Specifically, the concentrations of suspendible, inhalable, or fine motor vehicle particles are determined by the equation:

$$\left[\text{Vehicular Particles}\right]_x = k_x \cdot \left[\text{Pb}\right]_x \quad . \qquad (3\text{-}1)$$

where $[\ ]$ denotes concentration and x signifies either TSP (suspendible), IP (inhalable), or FP (fine). The constant k_x is the ratio of (suspendible, inhalable, or fine) total vehicular particulate emissions to (suspendible, inhalable, or fine) noncatalyst exhaust Pb emissions. For the time period of our study, 1980 to mid 1981, the values of the constants are $k_{TSP} = 15$, $k_{IP} = 15$, and $k_{FP} = 14$ (Trijonis and Davis 1981).

In all of the various regression equations applied to the development data set, the vehicular particle term was found to be statistically insignificant. The regression coefficient (extinction efficiency per unit mass concentration) for vehicle particles was usually very small (e.g. compared to the sulfate coefficient) and sometimes even negative. This result is identical to our findings in a recent California study (Trijonis et al. 1982). It should be stressed, however, that the lack of statistically significant relationships does not imply that vehicular particles really have zero or negligible effect on visibility. Rather, our results indicate that the effect is not pronounced enough so that one can quantify it with the (admittedly limited) airport data sets. Actually, from the conclusions of other studies performed with more detailed aerosol and visibility data (Hidy et al. 1974; Groblicki et al. 1980; Wolff et al. 1980; Cass et al. 1981; Conklin et al. 1981), we know that vehicular particles (elemental carbon, organics, lead, etc,) do contribute significantly to visibility reduction. Unfortunately, we are unable to isolate and quantify this contribution with our current data set. The problem of isolating the vehicular contribution may be especially difficult in the East because of predominance by the sulfate/visibility relationship (see later discussions).

It is interesting to note that, in separate regressions run with the "test" data set, the vehicular particle term usually was statistically significant (at 95 to 99% confidence levels). Combining the development and test data sets together, we found the vehicular term to be sometimes significant, sometimes not, with vehicular particle extinction efficiencies ranging from 10 to 90% of sulfate extinction efficiencies. These results are encouraging because they suggest the possibility of quantifying the vehicular term better when more months or years of data become available from the EPA IP Network. It will be very important to analyze the vehicular term further in any subsequent studies because elemental carbon from diesels, the most critical visibility-related subcomponent of vehicular particles, is expected to cause a major deterioration in visibility over the next ten to twenty years (NRC 1981; Trijonis 1982b, Trijonis 1983a).

Having discussed our findings with respect to vehicular particles in this section, we will no longer distinguish vehicular particles as such. Rather, vehicular particles will be aggregated in the "nonsulfate particle" category for the purpose of subsequent discussions.

3.1.2 Fine Versus Coarse Fractions from Dichotomous Samplers

Several regression models were formulated with inhalable particles ($IP < 15\ \mu m$) separated into fine particles ($FP < 2.5\ \mu m$) and coarse particles ($2.5 < CP < 15\ \mu m$). In all such regressions conducted with the development data set, we found FP highly significant and CP statistically insignificant, suggesting that coarse particle contributions to visibility reduction in the East are minor if not negligible. This result is similar to the findings of Groblicki et al. (1980) in Denver and Ferman et al. (1981) in rural Virginia. This conclusion is also very consistent with the Mie theory of aerosol light scattering which indicates that coarse particles have very small scattering efficiencies per unit mass compared to particles in the 0.1 to 1.0 μm size range (see Figure 3.1).

It should be noted that a controversy may be brewing with respect to coarse particle contributions to visibility reduction. Recent work in the arid Southwest by Pitchford (1982) suggests that coarse particles account, on the average, for as much as one-third of aerosol light extinction. However, we would expect coarse particles to be relatively more important in the arid Southwest (where fugitive dust is relatively more significant and where fine particle extinction efficiencies are reduced due to lower relative humidity) than in the East. Although our current findings do not prove that coarse particle visibility effects are entirely negligible in the East, the results do indicate that coarse particle effects are minor.

It is interesting to note that, by combining the development and test data sets, we obtained a marginal statistical significance for CP in one case -- regression of extinction versus FP/(1-RH) and CP/(1-RH). The extinction efficiency for CP was small, about one-sixth that of FP. Because of the

Reproduced from best available copy.

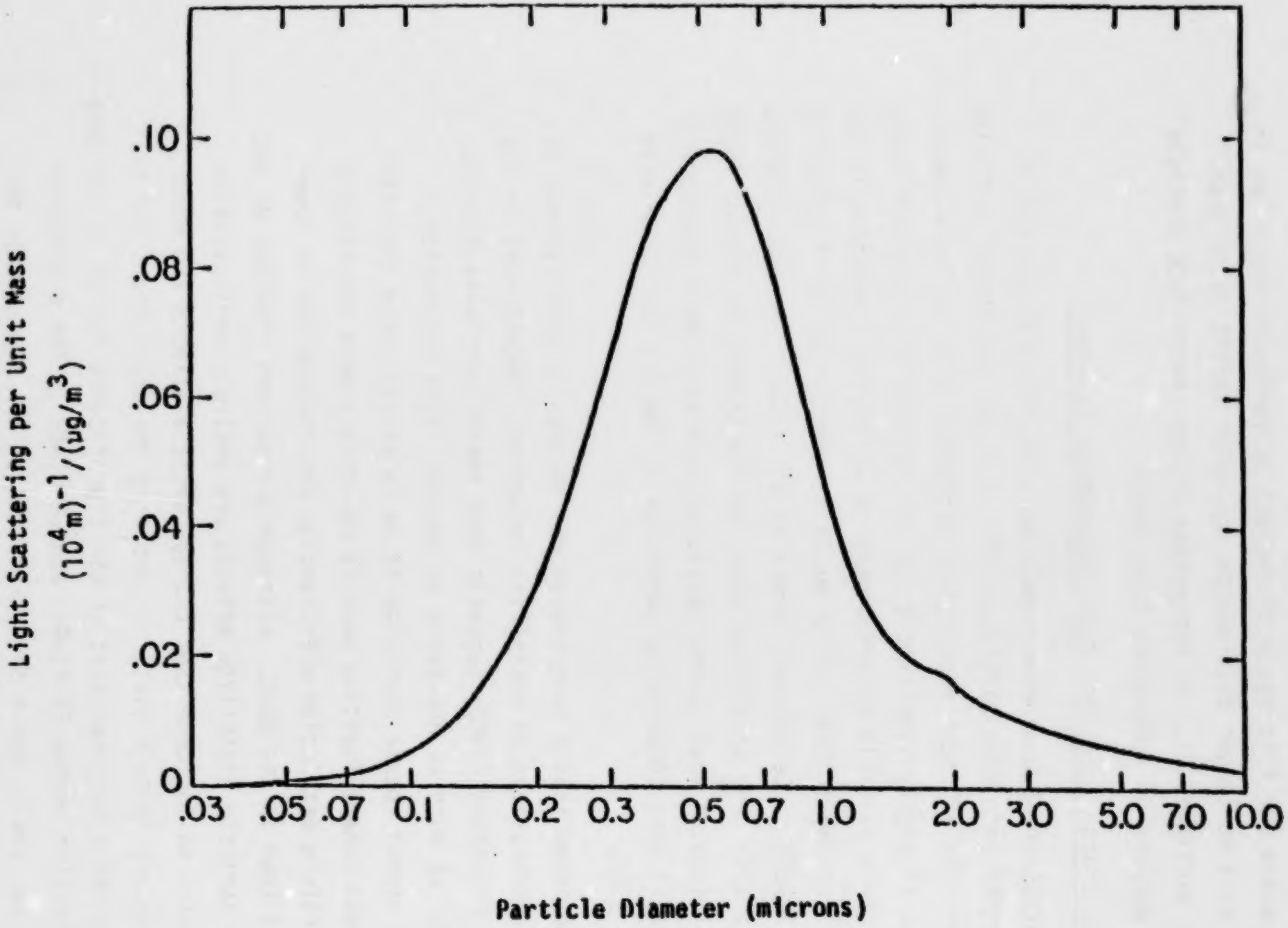

Figure 3.1 Light scattering by aerosols as a function of particle diameter. Computed for unit density spherical particles of refractive index 1.5 (White and Roberts 1977).

marginal statistical significance (just over 95%) and because of statistical colinearity problems in this regression form, the results can be viewed with very little confidence. However, these results suggest that it may be possible to quantify the (small) contribution from CP with larger amounts of data from the EPA IP Network.

3.1.3 Relative Humidity and the Role of Aerosol Water

The role of aerosol water is so important to visibility that it deserves an extensive preliminary discussion. Thermodynamic calculations (Tang 1981) as well as measurements made with microwave waterometers, nephelometers, and multi-stage cascade impactors (Covert et al. 1972; Hidy et al. 1974; Ho et al. 1974; Stelson and Seinfeld 1981; Ferman et al. 1981; Countess et al. 1981) suggest that, at relative humidities of 65-75%, the mass of water associated with fine ambient* aerosols is approximately equal to or slightly greater than the mass of aerosol electrolytes (e.g. sulfates and nitrates). As relative humidity increases toward 100%, the mass of aerosol water rises hyperbollically.

Figure 3.2 demonstrates that the dependence of aerosol water content on relative humidity varies significantly with the specific chemical form of the aerosol electrolyte (in this case, sulfates). For example, pure sulfuric acid aerosol retains water even at very low relative humidities. Pure ammonium sulfate aerosol, on the other hand, does not hydrate until the deliquescent point at 80% relative humidity. Under real atmospheric conditions, several chemical forms of sulfate are probably present, so that the aerosol water/ relative humidity dependence would be intermediate to the various curves shown in Figure 3.2. Also, under real atmospheric conditions, the deliquescent points might be smoothed out by hysteresis effects.

The role of water becomes all the more critical to visibility when one realizes that, because of density differences, water should scatter more light per unit mass than the aerosol electrolytes. For example, White (1981) has suggested that, because water is 1.7 times less dense than sulfate, it should

---

*In discussing aerosol water, it is imperative to distinguish between ambient particles and measured (filter-collected) particles. Filter-collected particles are typically equilibrated at about 40-50% relative humidity, and much, if not most, of the ambient water is lost in the measurement.

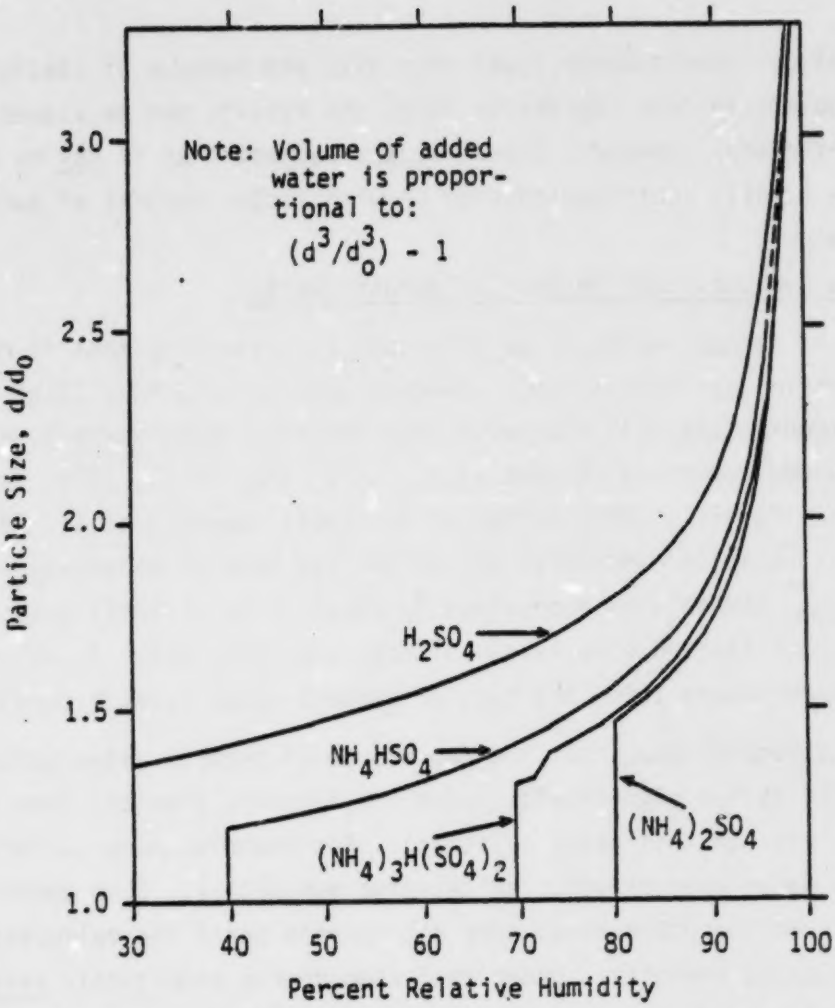

Figure 3.2 Growth curves for sulfate aerosols as a function of relative humidity (Tang 1981).

scatter approximately 1.7 times as much light per unit mass than does sulfate. Thus, if there is typically slightly more water mass than electrolyte mass in the aerosol, the total amount of light scattering from the water should be about twice that from the electrolyte. This hypothesis is supported by recent field studies comparing scattering levels from "wet" versus "dry" aerosols (Groblicki et al. 1980; Ferman et al. 1981).

Figure 3.3 illustrates the geographical pattern of average relative humidity in the Eastern U.S. Over most of the region, relative humidity averages about 70 to 75% annually (about 60 to 70% during daylight hours). On a day-to-day basis, relative humidity can reach very high levels at all

Reproduced from
best available copy.

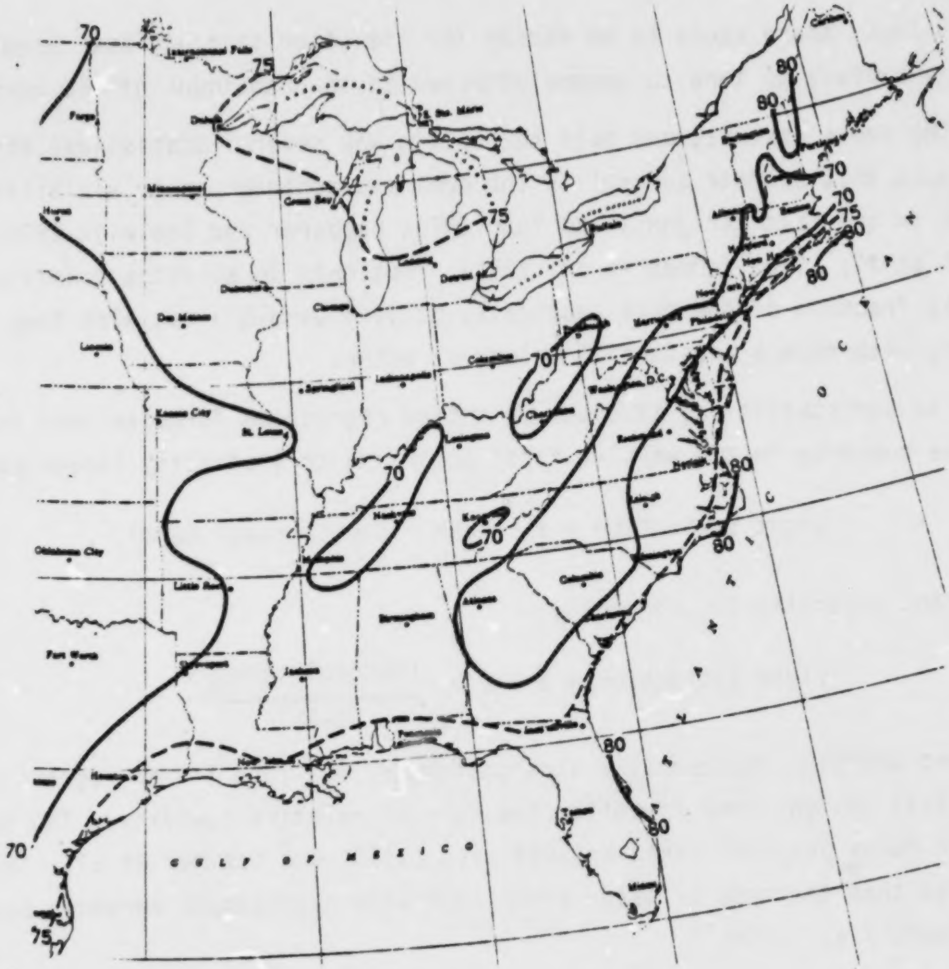
70
75
80
70
70
75
80
80
75
70
70
70
80
80
80
80
70
75
Fargo
Duluth
Green Bay
Des Moines
Kansas City
St. Louis
Oklahoma City
Fort Worth
D.C.
G U L F   O F   M E X I C O

Figure 3.3 Geographical distribution of annual average relative humidity (percent) in the Eastern U.S. (NOAA 1977).

locations in the region. Because of the fairly high humidity levels, water should be a very critical component of the ambient aerosol throughout the East.

Water should be regarded as an integral part of the aerosol to which it is attached. In other words, if the sulfate aerosol were eliminated, the water associated with the sulfate would also be eliminated from the aerosol phase. Transferring water from the aerosol to the gas phase produces essentially no change in relative humidity, because the total water in the gas phase is typically orders of magnitude greater than the total water in the particulate phase. Thus, there would be no reason for the water that had been associated with the sulfate to tend to become attached to the remainder of the aerosol.

The above observations help to explain why several statistical studies have found that sulfate aerosol is the dominant contributor to visibility reduction in the East (Trijonis and Yuan 1978; Leaderer and Stolwijk 1979; Pierson et al. 1980; Ferman et al. 1981). Not only do sulfates constitute a sizeable fraction of the fine (optically active) aerosol, but also they tend to carry with them a substantial volume of water.

In our statistical studies, we tested regression formulae that incorporated relative humidity in two ways -- first according to a strictly linear model,

$$\text{Light Extinction} = a + b_1 \text{RH} + \sum_i b_i \,(\text{aerosol term})_i \qquad (3\text{-}2)$$

and second according to the model,

$$\text{Light Extinction} = a + \sum_i b_i \,\frac{(\text{aerosol term})_i}{(1-\text{RH})}. \qquad (3\text{-}3)$$

The first approach represents a straightforward multiple linear regression with no physical insight used to define the role of relative humidity. The second approach makes physical sense because Cass (1979) and Latimer et al. (1978) have concluded that the mass of water associated with hygroscopic aerosols should vary approximately as $(1-\text{RH})^{-1}$.

As one might expect a priori, and as has been suggested in other studies (Trijonis and Yuan 1978; Trijonis 1979, 1980; Trijonis et al. 1982), our results show regression form (3-3) to be much superior to regression form (3-2). Equation (3-3) always produces higher correlation coefficients than Equation (3-2), despite the fact that Equation (3-3) has one less free parameter. Furthermore, we found that Equation (3-2) yields extinction efficiencies for sulfates that were nearly twice what would be expected on theoretical grounds. The most apparent reason for the badly inflated coefficients with Equation (3-2) is that the sulfate variable in Equation (3-2) represents not only sulfate compounds but also some of the water attached to those compounds [i.e. aerosol water is ambiguously represented in both the sulfate and linear RH terms in Equation (3-2)]. Thus, Equation (3-3) is obviously preferable empirically in addition to being best theoretically. Equation (3-3) correctly includes water within the aerosol terms and correctly approximates the hyperbolic dependence on relative humidity . For the above reasons, we will eliminate the strictly linear regression model, Equation (3-2), from all subsequent discussions.

3.2 LIGHT EXTINCTION FROM AEROSOL CONCENTRATIONS

Our analyses relating visibility to aerosol concentrations follows the statistical procedures established by Cass (1979), White and Roberts (1977), Trijonis and Yuan (1978), Trijonis (1979, 1981), and Trijonis et al. (1982). Regression equations are developed which relate daytime average extinction to daytime average relative humidity and 24-hour average particulate concentrations. The coefficients in the regression equations can be interpreted as estimates of "extinction coefficients per unit mass" or relative "extinction efficiencies" for each aerosol species. These extinction efficiencies can be used to estimate the fraction of visibility degradation attributable to individual aerosol components (e.g. sulfates).

3.2.1 Variable Definition and Regression Methodology

The parameters for the regression studies consist of visual range [miles], relative humidity [fraction, no units], and particulate concentrations [$\mu g/m^3$]. Before conducting the regressions, however, we must perform some simple transformations in the forms of the variables. For example, instead of using visual range (V) as the dependent variable, it is much more appropriate to use the extinction coefficient (B), which is inversely proportional to visual range. As explained in Section 1.1, the extinction coefficient is a linear sum of four components: light scattering by gases, light scattering by aerosols, light absorption by gases, and light absorption by aerosols. Extinction coefficient is most appropriate for use in linear regression models because each of the components of extinction should be directly proportional to aerosol or gas concentrations (assuming other factors, such as light wavelength, aerosol size distribution, particle shape, and refractive index remain constant).

We compute extinction coefficient from visual range data using a modified Koschmeider formula:[*]

$$B = \frac{3.0}{V}. \quad (3\text{-}4)$$

Equation (3-4) differs from the usual Koschmeider formula, $B = 3.9/V$, in the sense that Equation (3-4) assumes a 5% contrast detection threshold for the visibility observer rather than a 2% detection threshold. We have chosen the modified Koschmeider formula because recent studies (Allard and Tombach 1980; Malm et al. 1979; Trijonis 1979) suggest that airport visibility observations underestimate true instrumental visual range (defined as the distance at which the contrast for a perfectly black target is reduced to 2%). Several investigators specifically recommend using a contrast threshold of 5% (Koschmeider constant of 3.0) in order to obtain an unbiased estimate of extinction coefficient from human observations of visual range (Allard and Tombach 1980; Malm 1979; Middleton 1952; Douglas and Young 1945).

The choice of a Koschmeider constant has a proportional effect on the aerosol extinction efficiencies that we calculate from the regression analysis. The choice has no effect, however, on allocating total extinction among aerosol species, because total extinction and the extinction contributions from individual aerosol species are both changed in proportion.

Because one major goal of our analysis is to quantify the relative importance of TSP, IP, and FP as determinants of visibility, we have conducted entirely parallel regression studies for each of those three particulate parameters. In each case, we define the total mass concentration as X (where X denotes TSP, IP, or FP). Furthermore, in order to compare the effects of sulfate and nonsulfate particles, we subdivide total aerosol mass according to

$$X = XSULFATE + XNONSULFATE. \quad (3\text{-}5)$$

---

[*] For consistency with established convention, we change the units of extinction to $10^{-4}m^{-1}$ after applying Equation (3-4).

The variable, XSULFATE, is defined as 1.38 times the measured sulfate concentration in order to account for the mass of the cation, presumably ammonium as $(NH_4)_2SO_4$. The variable, XNONSULFATE, is computed simply by subtracting XSULFATE from the total mass.

Figure 3.4 illustrates the design of our regression studies. For each of TSP, IP, and FP, we start by regressing extinction (B) against total mass concentration. We then examine how the results change and improve as we add relative humidity, chemical composition (sulfate versus nonsulfate), or both to the model. All the bivariate regressions are run stepwise, retaining only those terms that are statistically significant at a 95% confidence level.

It should be noted that, in the final step with both relative humidity and chemical composition, we allow the regression model to include or exclude hygroscopicity (relative humidity in the aerosol term). That is, we permit the model to select either XSULFATE or XSULFATE/(1-RH) and either XNONSULFATE or XNONSULFATE/(1-RH). We find that, in all cases, the model includes relative humidity as part of the aerosol terms in order to obtain the best fit. Thus, the final step is essentially just a bivariate regression of extinction against XSULFATE/(1-RH) and XNONSULFATE/(1-RH).

Regression analysis is a purely statistical technique, and there is no guarantee that the observed relationships represent cause-and-effect. However, if -- as in the above analysis -- the regression is structured to reflect fundamental principles, the results will strongly suggest certain physical implications. In our analysis, the coefficients b_i or $b_i/(1-RH)$ of the aerosol concentration terms are readily interpreted as extinction coefficients per unit mass (extinction efficiencies) for the aerosol terms.

3.2.2 Overall Correlation Levels

Before presenting the regression results, it is useful to discuss the overall degree of correlation among the variables in the analysis. Table 3.1 lists the correlations between extinction coefficient (the dependent variable) and the set of independent variables. Several patterns are obvious in the table. First, as will be discussed later in more detail, extinction correlates

$$\begin{tikzcd}
\text{Simplest model:}\quad B = a + b_1X \arrow[r, "\text{Add relative humidity to model}"] \arrow[d, "\text{Add chemical composition to model}"'] \arrow[dr, "\text{Add relative humidity and chemical composition to model}"] & B = a + b_1 \dfrac{X}{(1\text{-}RH)} \\
B = a + b_1\ XSULFATE + b_2\ XNONSULFATE & B = a + b_1 \dfrac{XSULFATE}{(1\text{-}RH)} + b_2 \dfrac{XNONSULFATE}{(1\text{-}RH)}
\end{tikzcd}$$

NOTE: X stands for TSP, IP, or FP.

Figure 3.4 Design of the regression studies.

better with FP than IP, and better with IP than TSP. Second, each aerosol term attains a higher degree of correlation if the relative humidity factor, $(1\text{-RH})^{-1}$ is included. (The relative humidity factor itself correlates with extinction at a level of 0.52). Third, extinction correlates much better with the sulfate fraction than the non-sulfate fraction. In fact, of all the variables in Table 3.1, TSPNONSULFATE and IPNONSULFATE are the only two that do not correlate with extinction at a 99% confidence level.

TABLE 3.1 CORRELATION OF EXTINCTION COEFFICIENT
WITH THE INDEPENDENT VARIABLES

INDEPENDENT VARIABLE: CORRELATION COEFFICIENT TO EXTINCTION

TSP	TSP:	.30	TSPSULFATE:	.46	TSPNONSULFATE:	.05**
	TSP/(1-RH):	.54	TSPSULFATE/(1-RH):	.70	TSPNONSULFATE/(1-RH):	.48
IP	IP:	.51	IPSULFATE:	.52	IPNONSULFATE:	.27*
	IP/(1-RH):	.66	IPSULFATE/(1-RH):	.73	IPNONSULFATE/(1-RH):	.61
FP	FP:	.63	FPSULFATE:	.50	FPNONSULFATE:	.44
	FP/(1-RH):	.70	FPSULFATE/(1-RH):	.75	FPNONSULFATE/(1-RH):	.63

*Does not attain 99% confidence level for statistical significance

**Does not attain 95% confidence level for statistical significance

It is also worthwhile to examine the degree of intercorrelation (colinearty) between the "independent" variables that are linked together in multiple regressions. As indicated in Table 3.2, the various terms XSULFATE and XNONSULFATE correlate moderately with one another ($R \approx .40$). The terms XSULFATE/(1-RH) and XNONSULFATE/(1-RH), however, correlate strongly together ($R \approx .75$). These strong levels of intercorrelation among the independent variables can cause statistical problems in the sense that one of the independent variables may be given more weight in the regression at the expense of another. The colinearity problem will be discussed further in the later section dealing with limitations of the analysis.

TABLE 3.2 INTERCORRELATIONS AMONG INDEPENDENT VARIABLES
USED TOGETHER IN BIVARIATE REGRESSIONS

TSPSULFATE vs. TSPNONSULFATE: 0.34	$\frac{\text{TSPSULFATE}}{(1\text{-RH})}$ vs. $\frac{\text{TSPNONSULFATE}}{(1\text{-RH})}$: 0.72
IPSULFATE vs. IPNONSULFATE: 0.41	$\frac{\text{IPSULFATE}}{(1\text{-RH})}$ vs. $\frac{\text{IPNONSULFATE}}{(1\text{-RH})}$: 0.77
FPSULFATE vs. FPNONSULFATE: 0.48	$\frac{\text{FPSULFATE}}{(1\text{-RH})}$ vs. $\frac{\text{FPNONSULFATE}}{(1\text{-RH})}$: 0.74

3.2.3 Regression Results

Tables 3.3a, 3.3b, and 3.3c summarize the results of the regression analyses for TSP, IP, and FP, respectively. For each analysis, we have listed the regression equation, the standard error of the coefficients, the sample size, and the percent of variance explained (R^2, square of the correlation coefficient). As noted previously, only those variables that meet a 95% statistical significance level are retained in the equations.

The reader should be reminded that the units of extinction (B) are $\left[10^{-4}m^{-1}\right]$, and that the units of aerosol concentration are $\left[\mu g/m^3\right]$. Thus, the units of the regression coefficients are $\left[(10^4 m)^{-1}/(\mu g/m^3)\right]$.

Comparing the upper portions of Tables 3.3a, 3.3b, and 3.3c, it is obvious that FP is related significantly better to visibility than IP, which in turn is related significantly better to visibility than TSP. This makes good physical sense because light scattering by particles -- the dominant part of aerosol extinction in the East -- is distinctly a fine particle phenomenon. As shown previously in Figure 3.1, light scattering per unit mass by aerosols exhibits a pronounced peak near a particle size of 0.5 µm (at the wavelength of light). In addition, the absorption of light by aerosols is basically governed by fine elemental carbon (Groblicki et al. 1980; Ferman et al. 1981; Weiss and Waggoner 1981). For these reasons, the fine particle mass mode (typically residing in the 0.1-1.0 µm size range) usually dominates over the coarse particle mass mode (typically residing in the 3-50 µm size range) with respect to visibility reduction. It is not surprising that -- as we better approximate fine particle mass by going from $TSP < 50$ µm to $IP < 15$ µm to $FP < 2.5$ µm -- the correlation to light extinction improves significantly.

The upper right hand corners of Tables 3.3a to 3.3c show that the performance of the regressions improves significantly if relative humidity is added to the model. The lower left hand corners of the tables indicate that the statistical fit does not improve very much (except in the case of

Reproduced from best available copy.

TABLE 3.3 RESULTS OF THE REGRESSION STUDIES

Table 3.3a TSP

$B = 1.12 + .013\ TSP$ $(\pm .0025)$ Sample Size: 254 Variance Explained: 9% (R=.30)	$B = 0.96 + .0062\,\frac{TSP}{(1-RH)}$ $(\pm .0006)$ Sample Size: 254 Variance Explained: 30% (R=.54)
$B = 1.09 + .064\ TSPSULFATE$ $(\pm .013)$ Sample Size: 92 Variance Explained: 21% (R=.46)	$B = 1.17 + .022\,\frac{TSPSULFATE}{(1-RH)}$ $(\pm .0024)$ Sample Size: 92 Variance Explained: 49% (R=.70)

Table 3.3b IP

$B = 0.77 + .030\ IP$ $(\pm .0032)$ Sample Size: 254 Variance Explained: 26% (R=.51)	$B = 0.91 + .011\,\frac{IP}{(1-RH)}$ $(\pm .0008)$ Sample Size: 254 Variance Explained: 43% (R=.66)
$B = 1.05 + .103\ IPSULFATE$ $(\pm .018)$ Sample Size: 93 Variance Explained: 27% (R=.52)	$B = 1.18 + .034\,\frac{IPSULFATE}{(1-RH)}$ $(\pm .0033)$ Sample Size: 93 Variance Explained: 54% (R=.73)

Table 3.3c FP

$B = 0.76 + .053FP$ $(\pm .0041)$ Sample Size: 254 Variance Explained: 40% (R=.63)	$B = 1.03 + .016\,\frac{FP}{(1-RH)}$ $(\pm .0010)$ Sample Size: 254 Variance Explained: 50% (R=.70)
$B = 0.82 + \underset{(\pm .020)}{.075}\ FPSULFATE + \underset{(\pm .016)}{.041}\ FPNONSULFATE$ Sample Size: 93 Variance Explained: 30% (R=.55)	$B = 1.04 + \underset{(\pm .0056)}{.034}\,\frac{FPSULFATE}{(1-RH)} + \underset{(\pm .0037)}{.0064}\,\frac{FPNONSULFATE}{(1-RH)}$ Sample Size: 93 Variance Explained: 58% (R=.76)

FORMAT

Simplest model, B vs. total concentration	Add RH to model B vs. conc./(1-RH)
Add chemical composition to model B vs. sulfate, nonsulfate	Add RH and chemical composition to model B vs. sulfate/(1-RH), nonsulfate/(1-RH)

TSP) if the particulate concentration is divided into sulfates and nonsulfates. When the sulfate/nonsulfate division is made, the sulfate fraction is the more important term and is, in fact, the only statistically significant term in the case of TSP and IP. The regression coefficients (extinction efficiencies) for sulfates in the lower left hand corners of the tables are significantly higher than one would expect for pure (dry) sulfates based on theoretical principles. The reason for this is obvious; the sulfate mass extinction efficiency reflects the effect of water as well as the effect of sulfates.

Examining the lower right hand corners of Tables 3.3a - 3.3c, it is apparent that the best statistical fits are obtained when both chemical composition (sulfates) and relative humidity are included in the regression models. The percent variance explained by these regressions is about 55% ($R \approx .75$). In the case of TSP and IP, the sulfate fraction is the only significant term. It is very noteworthy that, once sulfates and relative humidity are added to the model, the fit does not improve that much as one proceeds from TSP to IP to FP. These results suggest that the single most critical step in analyzing Eastern visibility is to distinguish the combined roles of sulfates and relative humidity. It is also noteworthy that the extinction efficiencies for "dry" sulfates in the lower right-hand corners of the tables agree very well with theoretical values of 2 to 4 m^2/g (Latimer et al. 1978; White and Roberts 1977).

The performance of the regression equations in Table 3.3 has also been evaluated against the independent "test" data set. Table 3.4 presents the results of this evaluation. Somewhat surprisingly, the equations fitted to the "development" data set usually achieve even higher percent variance explained with the "test" data set. This unusual and encouraging result indicates that there is not a serious "over-fitting" problem.

3.2.4 Conclusions Regarding Issues of Concern

The regression studies of Table 3.3 provide insights with respect to several issues of current interest. One such issue is the relative extinction efficiency per unit mass concentration of sulfates versus other aerosols. With respect to this issue, we will discuss only the regression equations

TABLE 3.4 REGRESSION EQUATION PERFORMANCE EVALUATED WITH THE INDEPENDENT TEST DATA SET

	PERCENT VARIANCE EXPLAINED	
EQUATION	DEVELOPMENT DATA SET	INDEPENDENT TEST DATA SET
$B = 1.12 + .013\ \mathrm{TSP}$	9%	10% (9%*)
$B = 1.09 + .064\ \mathrm{TSPSULFATE}$	21%	20%
$B = 0.96 + .0062\ \frac{\mathrm{TSP}}{1-\mathrm{RH}}$	30%	49% (49%*)
$B = 1.17 + .022\ \frac{\mathrm{TSPSULFATE}}{1-\mathrm{RH}}$	49%	53%
$B = 0.77 + .030\ \mathrm{IP}$	26%	21%
$B = 1.05 + .103\ \mathrm{IPSULFATE}$	27%	24%
$B = 0.91 + .011\ \frac{\mathrm{IP}}{1-\mathrm{RH}}$	43%	62% (64%*)
$B = 1.18 + .034\ \frac{\mathrm{IPSULFATE}}{1-\mathrm{RH}}$	54%	54%
$B = 0.76 + .053\ \mathrm{FP}$	40%	27%
$B = 0.82 + .041\ \mathrm{FPSULFATE} + .075\ \mathrm{FPNONSULFATE}$	30%	34%
$B = 1.03 + .016\ \frac{\mathrm{FP}}{1-\mathrm{RH}}$	50%	67% (71%*)
$B = 1.04 + .034\ \frac{\mathrm{FPSULFATE}}{1-\mathrm{RH}} + .0064\ \frac{\mathrm{FPNONSULFATE}}{1-\mathrm{RH}}$	58%	81%

*Values in parentheses are with removal of one outlier, 14 June 1980 at Tarrant City, from the test data set. This day, which barely managed to pass our data quality screen, had inconsistent values for particle concentrations: TSP = 167 $\mu g/m^3$, IP = 216 $\mu g/m^3$, and FP = 180 $\mu g/m^3$. The outlier had a fairly strong influence on the evaluation test because of the very high particle concentrations. It did not affect the evaluation of the chemically-resolved regression formulae because no chemical particulate data were available on that day.

involving the terms b_i(aerosol concentration)/(1-RH), with b_i representing the "dry" extinction efficiency and $(1\text{-RH})^{-1}$ indicating the growth of extinction efficiency with relative humidity.

With respect to relative extinction efficiencies, we must distinguish among three cases: sulfate versus nonsulfate TSP, nonsulfate IP, and nonsulfate FP. In the case of TSP, the dry sulfate extinction efficiency is 0.022 $10^{-4}m^{-1}/(\mu g/m^3)$ or 2.2 m^2/g. The TSPNONSULFATE coefficient is insignificant, and in fact turned out slightly negative in the bivariate regression with TSPSULFATE. However, total TSP has a dry extinction efficiency of 0.62 m^2/g. Because total TSP includes sulfates, the actual nonsulfate TSP coefficient should be significantly less than 0.62 m^2/g, much less than the 2.2 m^2/g for TSP sulfate. This conclusion agrees with the findings of many previous statistical studies that the extinction efficiency for sulfate is generally an order of magnitude greater than the extinction efficiency for the remainder of TSP (White and Roberts 1977; Trijonis and Yuan 1978; Cass 1979; Leaderer and Stolwijk 1979; Trijonis 1979, 1980, 1982c; Trijonis et al. 1982).

The case of IP is somewhat parallel to that of TSP. The extinction efficiency of IP sulfate is 3.4 m^2/g. The extinction efficiency of total IP is 1.1 m^2/g, implying a considerably lesser value for nonsulfate IP. Both nonsulfate IP and nonsulfate TSP are expected, on theoretical grounds, to have low extinction efficiencies because they include a coarse particle mode in the size range above 2 μm (see previous discussion).

The case of FP is less obvious and more interesting. In the bivariate regressions with FP, both the sulfate and nonsulfate terms are statistically significant. With the development data set, we obtain a dry extinction efficiency of 3.4 m^2/g for sulfate FP and 0.6 m^2/g for nonsulfate FP. This suggests that fine sulfates are much more efficient at light extinction than other fine particles. We are not, however, very confident of this conclusion. As noted in Section 3.2.2, the FPSULFATE/(1-RH) and FPNONSULFATE/(1-RH) variables are highly intercorrelated. It is very possible that the regression may have yielded an inflated sulfate coefficient at the expense of a deflated nonsulfate coefficient. This possibility seems all the more likely because a separate regression applied to our "test" data set produces dry extinction efficiencies of 2.8 m^2/g for sulfate FP and 1.7 m^2/g for nonsulfate FP (at a correlation of 0.92 for the sample size of 49). It seems very likely that sulfates are more efficient at visibility reduction than the remainder of fine particles, but we cannot quantify the difference very precisely at present.* A repeated analysis when more data are available should allow a more precise characterization of this issue.

As indicated by the above paragraphs, the extinction efficiency for TSPSULFATE (2.2 m^2/g) is significantly less than that for IPSULFATE and FPSULFATE (both 3.4 m^2/g). A major reason for this is that TSP sulfate concentrations are inflated due to artifact sulfate formation on Hi-Vol glass filters.

A second issue of concern is the fractional contribution of sulfates (and associated water) to total visibility reduction in the East. Several recent studies have found that sulfates contribute approximately 50 to 75% of light extinction in the East (Trijonis and Yuan 1978; Leaderer and Stolwijk 1979; Pierson et al. 1980; and Ferman et al. 1981). The regression equations in the lower right-hand corners of Tables 3.3a to 3.3c can be used to estimate sulfate contributions to extinction by plugging in average values for the variable "XSULFATE/(1-RH)". For the cases of TSP, IP, and FP, we obtain percentage sulfate contributions to extinction of 45%, 44%, and 40%, respectively. As discussed in the section on limitations of the analysis, these estimates are somewhat uncertain. Studies based on more detailed data sets suggest significantly higher percentage contributions from sulfates (Pierson et al. 1980; Ferman et al. 1981); however, the latter studies might be strongly seasonally biased because they were conducted in summer, when sulfates reach a distinct seasonal maximum.

A policy issue of major concern is the establishment of welfare standards to protect visibility. With respect to this issue, our results indicate a very simple but important conclusion. As recognized by EPA (1982), if welfare standards are to be established to protect visibility, such standards should be set for FP and/or sulfates, not TSP or IP.

3.2.5 Geographical Variations

It is worthwhile to investigate whether the extinction/aerosol relationship varies geographically. In a recent California study (Trijonis et al.

---

*The reader should note that one specific subcomponent of nonsulfate FP, elemental carbon, is known to have a very high extinction efficiency, about 12 m^2/g, most of which is absorption. At a relative humidity of 70%, the "dry" sulfate coefficient of 3.4 m^2/g increases to 11 m^2/g, still slightly below the extinction efficiency for elemental carbon.

1982), we found that aerosol extinction efficiencies showed significant and physically reasonable geographical variations. For example, sulfate extinction efficiency exhibited consistent regional differences by a factor two or more. These geographical differences were explained by region-specific aerosol size distributions within the fine particle mode. In agreement with theory (Faxvog and Roessler 1981; Ouimette 1981), regions where sulfates had a relatively large average diameter (e.g. 0.6 μm) showed much greater extinction efficiencies than regions where sulfates had a relatively small average diameter (e.g. 0.2 μm).

In order to investigate geographical variations in the East, the regressions of Table 3.3 were run individually for each of the six study cities (Birmingham, Washington, Philadelphia, Buffalo, Boston, and Minneapolis). The equations did change considerably from city to city, both in terms of the variables chosen as statistically significant and in terms of the specific regression coefficients (extinction efficiencies). Using these results, we formed a "geographically resolved prediction model" (based on six equations, one specific to each city) and compared the performance of that model to the aggregate model (based on the single overall equation listed in Table 3.3). Table 3.5 summarizes the comparison for the three approaches of B vs. concentration (X), B vs. X(1-RH), and B vs. XSULFATE/(1-RH) and XNONSULFATE/(1-RH). Comparing the first two columns, it is obvious that the geographically resolved model performs much better on the development data set than the aggregate Eastern model. However, when the geographically resolved model is applied to the independent data set, there is essentailly no gain at all in performance. This strongly implies that the geographical variations essentially just represent an "overfit" to the development data set. That an overfit problem exists is not surprising considering the very limited sample size per city, especially with respect to chemical composition (see Table 2.4a). Based on these results, we conclude that sufficient data are not now available to study geographical variations in the relationships. Significant geographical variations may actually exist, but they cannot be quantified until considerably more data are compiled from the EPA IP Network.

TABLE 3.5 EVALUATION OF GEOGRAPHICAL RESOLVED MODEL

REGRESSION TYPE	PERCENT VARIANCE EXPLAINED IN DEVELOPMENT DATA SET		PERCENT VARIANCE EXPLAINED IN INDEPENDENT TEST DATA*	
	Aggregate One Equation Model	Geographical Six Equation Model	Aggregate One Equation Model	Geographical Six Equation Model
B vs. TSP	9%	37%	10%	15%
B vs. TSP/(1-RH)	30%	52%	49%	20%
B vs. TSPSULFATE/(1-RH) and TSPNONSULFATE/(1-RH)	49%	85%	53%	74%
B vs. IP	26%	48%	21%	24%
B vs. IP/(1-RH)	43%	69%	62%	46%
B vs. IPSULFATE/(1-RH) and IPNONSULFATE/(1-RH)	54%	83%	54%	58%
B vs. FP	40%	58%	27%	13%
B vs. FP/(1-RH) and	50%	74%	67%	49%
B vs. FPSULFATE/(1-RH) and FPNONSULFATE/(1-RH)	58%	88%	81%	77%

Note: The equations applied to the independent test data are the equations derived from the development data set.

3.2.6 Limitations of the Analysis

There are several noteworthy limitations in using regression models to quantify the dependence of extinction on aerosol concentrations. One limitation involves random errors in the data base produced by imprecision in the measurement techniques (for airport visibility or particulate concentrations) and by the fact that the airport and particulate monitor are often located several kilometers apart. Random errors in the data tend to weaken the statistical relationships, leading to lower correlation coefficients and lower regression coefficients. This causes an underestimate of the extinction efficiencies for the aerosol species (e.g. sulfates) and, therefore, an underestimate of the contributions of the aerosol species to total extinction.

Incompatibilities between the airport visibility data base and the particulate data base can lead to at least two types of systematic bias. The particulate measurements, usually made at center-city locations, may be systematically higher than the aerosol concentrations averaged over the visual range surrounding the airports (usually suburban). The bias caused by relatively high particulate concentrations would result in an underestimate of extinction efficiencies for the aerosol species. A reverse type of bias, e.g. an overestimate of extinction efficiencies, would result if daytime aerosol levels (corresponding to the time period of the visibility measurements) were higher than the 24-hour average aerosol levels measured by the particulate monitors. Although these systematic errors could bias the extinction efficiencies, they should not bias the allocation of extinction among aerosol species (which is based on a multiplication of extinction efficiencies times the measured mass of the aerosol).

Artifact sulfate, formed by SO_2 collection on glass-fiber filters, is a systematic error affecting the Hi-Vol (TSP) data. Artifact sulfate should cause a slight to moderate underestimation of the extinction efficiency for sulfates but, again, should not distort the allocation of total extinction among sulfates and other aerosols.

Perhaps the most important difficulty in the regression analysis is the problem of colinearity, i.e. the intercorrelations that exist among the "independent" aerosol variables. Multiple regression is designed to estimate the individual effect of each variable, discounting for simultaneous effects of other variables, but the colinearity problem can still lead to distortions in the results. Specifically, in some cases, it is possible that nonsulfate particles are assigned lower regression coefficients or even statistical insignificance because they are colinear with sulfate which bears a stronger relation to extinction.

Although not a conceptual limitation, data availability was certainly a practical limitation in this study. As indicated in the discussions above, we think that many of our results can be made more certain and more precise when larger data sets become available. The size of the data set could be increased somewhat by moderately relaxing our criteria that eliminate days with fog or precipitation. Also, another year or two of measurements from the EPA IP Network would be extremely useful.

3.3 PREDICTION OF DICHOTOMOUS FP AND IP FROM AIRPORT DATA AND HI-VOL DATA

As demonstrated in the previous sections of this chapter, visibility is closely related with fine particle concentrations and, to a lesser extent, with inhalable particle concentrations. In fact, in the next chapter, we will show that -- because of this close relationship -- visibility can be used qualitatively to study the spatial/temporal extent, transport patterns, and origins of large scale fine particle episodes. It is also worthwhile to investigate if the relationship can be carried even further. Specifically, it is of interest to examine the feasibility of using airport data for visibility and relative humidity, in conjunction with Hi-Vol data for TSP, as quantitative predictors of FP and IP. The reason for the interest is that the geographical and historical record of dichotomous data is quite small compared to the available record of airport and Hi-Vol data. Empirical formulae for predicting dichotomous parameters from airport and Hi-Vol data would greatly augment historical information regarding FP and IP and would ease the expansion from TSP standards and monitoring to TSP/IP/FP standards and monitoring.

A study of relevance to this issue was recently reported by Trijonis and Davis (1981) and Trijonis (1983b). The prior study differed from the current investigation in three major respects. First, the prior study used a large national data base (930 simultaneous dichotomous and Hi-Vol samples at 75 nationwide locations), rather than a smaller Eastern data set. Second, the prior study related FP and IP to Hi-Vol data for TSP, $SO_4^=$, and Pb, rather than to Hi-Vol data for TSP in conjunction with airport data for extinction (visibility) and relative humidity. Third, the predictive formulae of the prior study were based on a hybrid methodology -- prespecifying the $SO_4^=$ and Pb coefficients based on physico-chemical principles, and fitting just one free statistical coefficient to the remainder of TSP through a zero-intercept regression -- rather than on a purely statistical approach.

To facilitate comparisons, we will use the same performance measure as the prior study -- percent error, which is simply the standard error of the predictions (appropriately adjusted for degrees of freedom) divided by the mean value of FP or IP. This is a very appropriate performance measure because the absolute predictive error increases nearly in proportion with the magnitude of FP or IP (Trijonis and Davis 1981; Trijonis 1983b).

In order to put our current results in perspective, it is worthwhile to briefly summarize the findings of the prior study. It was found that a Hi-Vol measurement of TSP alone is not a good predictor of FP. The national aggregate equation,

$$FP = 0.30\ TSP, \qquad (3\text{-}6)$$

yielded a 56% error for individual daily values of FP and a 30% error for annual mean values. Predictions of FP were improved substantially by adding sulfate and lead data. The national aggregate equation,

$$FP = 1.1\ SO_4^= + 11\ Pb + 0.14\ (TSP - 1.4\ SO_4^= - 15\ Pb), \qquad (3\text{-}7)$$

had a 40% error for daily values of FP and 17% error for annual mean values of FP. Disaggregating the FP predictive scheme by region and season did not further reduce the error significantly. Concentrations of IP were predicted fairly well from TSP data alone, the national aggregate equation,

$$IP = 0.61\ TSP, \qquad (3\text{-}8)$$

achieving a 31% error for daily values of IP and a 16% error for annual mean values. The error for IP could be further reduced marginally, to 26% for daily values and 13% for annual mean values, by adding the $SO_4^=$ and Pb variables and by disaggregating the predictive scheme by region and season.

3.3.1 Prediction of FP

Table 3.6 summarizes the results of predictive schemes for FP based on the following types of data (i.e. independent variables):

A. Hi-Vol data for TSP,
B.1 Airport data for extinction (visibility),
B.2 Airport data for extinction and relative humidity,
C.1 Hi-Vol data for TSP with airport data for extinction,
and C.2 Hi-Vol data for TSP with airport data for extinction and relative humidity.

Furthermore, to serve as a reference point, the first row of the table lists the "coefficient of variation" for FP, defined as

$$\frac{\text{standard deviation of FP concentrations (over all sites and all days or years)}}{\text{average FP concentration (over all sites and all days or years)}}$$

The coefficient of variation, about 60% for daily values of FP and about 25% for annual mean values of FP, represents the standard error if the composite mean (over all sites and days) were used as the most simplistic predictor of FP concentrations.

It should be noted that, in addition to the linear terms and simple combinations of variables in Table 3.6, various other polynomial terms were tried in the regression equations. The other polynomial terms did not yield significantly better statistical fits to the data. Thus, the equations in Table 3.6 represent about the best predictive accuracy possible for each set of independent variables.

There are several important conclusions evident in Table 3.6. The first is that TSP alone is not a good predictor FP (Scheme A). This is especially apparent in the poor performance of Equation A against the independent daily and annual data sets. This finding is consistent with the conclusions of the study discussed earlier (Trijonis 1983b).

TABLE 3.6 PERFORMANCE OF VARIOUS PREDICTIVE SCHEMES FOR FP CONCENTRATIONS

PREDICTIVE SCHEME AND EQUATION	PERCENTAGE ERROR IN PREDICTING DAILY FP VALUES		PERCENTAGE ERROR IN PREDICTING ANNUAL MEAN FP
	Development Data Set	Independent Test Data Set	(For ~ 40 Samples Per Year)
Coefficient of Variation	61%	67% (54%*)	25%
A. Prediction based on Hi-Vol data for TSP, Linear regression formula: FP = 0.3 + .34 TSP	45%	62% (54%)	25%
B.1 Prediction based on airport data for extinction (visibility). Linear regression formula: FP = 8.4 + 7.5 B	48%	57% (41%)	19%
B.2 Prediction based on airport data for extinction and relative humidity. Stepwise regression considering B, B(1-RH), B/RH, (1-RH), and 1/RH as potential variables: FP = 22.8 + 21.1 B(1-RH) - 38.2 (1-RH)	45%	53% (37%)	19%
C.1 Prediction based on data for TSP and extinction.			
C.1.a. Linear regression formula: FP = -5.9 + 5.6 B + .26 TSP	36%	55% (45%)	20%
C.1.b. Linear regression formula with ratio of B and TSP coefficients pre-specified based on zero-intercept regressions: FP = -4.1 + .68(10 B + 3 TSP)	37%	53% (41%)	16%
C.2 Prediction based on data for TSP, extinction, and relative humidity. Stepwise regression considering TSP, B, B(1-RH), B/RH, (1-RH), and 1/RH as potential variables: FP = 8.0 + 15.4 B(1-RH) - 33.2 (1-RH) + .25 TSP	35%	53% (42%)	20%

*Values in parentheses are with removal of one outlier, 14 June 1980 at Tarrant City, from the test data set. This day, which barely managed to pass our data quality screen, had inconsistent values for particulate concentrations: TSP = 167 $\mu g/m^3$, IP = 216 $\mu g/m^3$, and FP = 180 $\mu g/m^3$. The outlier had a fairly strong influence on the independent test data set because of the very high particulate concentrations on that day.

The second notable conclusion is that airport data for extinction and relative humidity (Schemes B.1 and B.2) do not yield good quantitative predictions of FP (at least on a daily basis). This conclusion deserves an extended discussion because it is somewhat surprising, considering that we earlier found extinction to be fairly closely related to fine particles and relative humidity. Basically, there are two fundamental impediments to predicting FP accurately from airport data. The first impediment concerns the intrinsically high fluctuation in daily FP concentrations -- a coefficient of variation of about 60%. In order to reduce this standard error down to a more reasonable value, such as 20-30%, we would require a regression result with 75-89% variance explained* (R = .87 - .94). As indicated by the following discussion, achieving such a good fit with the airport data alone seems impossible. The second impediment is that the inverse process of predicting fine particles from extinction and relative humidity is not as physically straightforward or statistically well-fitting as the more direct process of predicting extinction from fine particles and relative humidity. For example, based on atmospheric optics considerations, we found that it was very reasonable to propose the relationship:

$$B = a + b_1 \frac{FP}{(1-RH)} . \qquad (3\text{-}9)$$

Indeed, Equation (3-9) yielded a good statistical fit, about 50 to 70% variance explained (R = .70 - .84) based on the development and test data sets. But, how does one invert that relationship physically to serve as a predictor of FP? If we conduct an algebraic manipulation and try zero-intercept regressions of the form,

$$FP = C_1 B(1-RH) - C_2(1-RH) \qquad (3\text{-}10)$$

we find that such an equation achieves a poor statistical fit, explaining very little of the variance in FP. Adopting a blind statistical approach, and performing multiple regressions relating FP to an extensive list of potential predictors (Scheme B.2), we find fair but not excellent statistical fits, about 45% variance explained for FP (R = .68). To illustrate the difficulty involved, we note that -- in the direct process -- FP/(1-RH) explains 50% of the variance in B (R =.70) with the development data set, but that -- in the inverse process -- B(1-RH) explains only 35% of the variance in FP (R = .59).

---

*Note that the standard error is the square root of the variance. Thus, to reduce the standard error by one-half, one must explain 75% of the variance (R=.87).

As a corollary to the above conclusion, we note that -- if FP were to be predicted from airport data alone -- then including relative humidity adds rather little (as long as the data are pre-screened for precipitation and fog as are our data). The complicated regression including relative humidity (Scheme B.2) does not perform much better than the simple linear regression of FP versus extinction (Scheme B.1).

The third major conclusion is that we can obtain fairly reasonable predictions of FP using airport visibility data in conjunction with Hi-Vol particulate data. The linear regression equation of FP versus B and TSP (Scheme C.1.a) yields only a 36% standard error for daily FP with the development data set. There appears, however, to be an "overfitting" problem in this equation, as evidenced by the poorer performance with the annual and independent daily data sets. In an attempt to overcome the overfitting problem, we reduced the number of regression variables to one by pre-specifying the ratio of the B and TSP coefficients according to their individual (zero-intercept) relationships with FP. This produced a slightly greater error with the development data set (as it must) but improved performance considerably with the annual and independent daily data sets. As was the case with airport data alone, adding relative humidity (Scheme C.2) led to little improvement in predictive accuracy.

Because of limitations in the size and coverage of the current data set, the above evaluation of predictive schemes for FP cannot be regarded as fully definitive. At present, we only conclude that airport visibility data in conjunction with Hi-Vol TSP data can serve as a reasonably good predictor of FP, with an error of about 35-50% for daily FP values and about 15-20% for annual mean FP. These error levels are nearly identical with those achieved in the nationwide study using Hi-Vol data for TSP, $SO_4^=$, and Pb (Trijonis 1983b). When more data are available from the EPA IP Network, the error levels in Table 3.6 as well as the coefficients for the equations can be determined with greater precision.

3.3.2 Prediction of IP

Table 3.7 presents an evaluation of various predictive equations for IP. This table is similar to Table 3.6, except no results have been included for predictive schemes involving relative humidity data. We found that the relative humidity variable was even less significant for IP than it was for FP.

In agreement with the conclusions of the nationwide study (Trijonis 1983b), Table 3.7 indicates that IP concentrations can be predicted fairly well from TSP data alone (Scheme A). In fact, the regression coefficient, 0.61, is identical to that of the nationwide study. Furthermore, the predictive errors listed for Scheme A in Table 3.7 are generally consistent with those reported in the nationwide study (31% for daily IP and 16% for annual mean IP).

The results for Scheme B show that airport extinction alone is a poor predictor of IP concentrations. However, using both airport extinction data and Hi-Vol TSP data (Scheme C) does appear to improve performance somewhat over the predictions based on TSP alone. Table 3.7 suggests that IP can be estimated with less than a 30% error on a daily basis and less than a 15% error on an annual basis using TSP data in conjunction with airport extinction data. As was the case with the FP predictive schemes, the IP predictive schemes can be formulated and evaluated more precisely when more data become available.

TABLE 3.7 PERFORMANCE OF VARIOUS PREDICTIVE SCHEMES FOR IP CONCENTRATIONS

PREDICTIVE SCHEME AND EQUATION	PERCENTAGE ERROR IN PREDICTING DAILY IP VALUES		PERCENTAGE ERROR IN PREDICTING ANNUAL MEAN IP
	Development Data Set	Independent Test Data Set	(For ~40 Samples Per Year)
COEFFICIENT OF VARIATION	50%	52% (47%*)	27%
A. Prediction based on Hi-Vol data for TSP. Linear regression formula: $IP = -.9 + .61\, TSP$	26%	38% (35%)	17%
B. Prediction based on airport data for extinction (visibility). Linear regression formula: $IP = 23.8 + 8.7\, B$	43%	48% (42%)	25%
C. Prediction based on data for TSP and extinction.			
C.1. Linear regression formula: $IP = -6.2 + 4.7\, B + .55\, TSP$	23%	35% (32%)	15%
C.2. Linear regression formula with ratio of B and TSP coefficients pre-specified based on zero-intercept regressions. $IP = -.7 + .55\, (17\, B + .6\, TSP)$	28%	34% (29%)	12%

---

*Values in parentheses are with removal of one outlier, 14 June 1980 at Tarrant City, from the test data set. This day, which barely managed to pass our data quality screen, had inconsistent values for particulate concentrations: TSP = 167 $\mu g/m^3$, IP = 216 $\mu g/m^3$, and FP = 180 $\mu g/m^3$. The outlier had a fairly strong influence on the independent data set because of the very high particulate concentrations on that day.

4.0 CHARACTERIZATION OF PARTICULATE EPISODES USING AIRPORT DATA

The purpose of this chapter is to study the feasibility of using airport data to characterize the spatial extent, transport patterns, and origins of fine particle episodes. Section 3.1 discusses the information base and procedures for the analysis. Section 3.2 presents several case studies of fine particle episodes. Section 3.3 discusses our conclusions regarding the usefulness of the approach.

4.1 INFORMATION BASE

Three types of data are used in this chapter -- maps of daily particulate concentrations at EPA IP Network sites, maps of daily visibility levels at airports, and information on daily regional wind patterns. As indicated earlier in Section 2.4, the particulate concentration maps include only the 25 EPA IP Network sites (see previous Figure 2.1) that provided adequate amounts of data for the year, April 1980 - March 1981. Also, maps are prepared only on days when most of those 25 sites reported data. Each map basically consists of a listing of TSP, IP, FP, $SO_4^=$, and Pb concentrations at the monitoring sites. A single asterisk is used to denote concentrations a factor of 1.75 greater than the region wide annual mean, and a double asterisk indicates concentrations a factor of 2.50 greater than the region wide annual mean. Appendix A presents a complete tabulation of all the particulate maps.

Maps of average daytime visibility levels were prepared using data from 70 carefully selected airports (see previous Figure 2.2). We decided to use just visibility -- without discounting for relative humidity -- in these maps because, as discussed in Section 3.3, simple regressions of fine particle concentrations against extinction (i.e. visibility) alone yielded nearly as good a correlation as the more complicated and less physically interpretable regressions of fine particles against both extinction and relative humidity. The visibility maps are shaded to indicate areas where visual range is in the categories 0-3 miles, 3-6 miles, 6-10 miles, and above 10 miles. The process of shading the maps (done manually) is quite straightforward because the airport data are very consistent with respect to geographical variations. That is --

Preceding page blank

we usually find large areas containing many sites with low visibilities gradually blending into other large areas containing many sites with high visibilities. The consistency and quality of airport data with respect to geographical variations (Trijonis and Yuan 1978; Trijonis 1979, 1982a, 1982c; Husar et al. 1976a, b, 1979) is what makes this investigation possible and useful.

In the original study plan for this project, we did not intend to use wind data. However, we found that we could interpret transport patterns on the visibility maps much more meaningfully with some knowledge of overall wind conditions. To obtain an approximate indication of air flows, 24-hour average surface wind vectors at 35 airports were examined.* We then prepared a qualitative description of wind flows (direction and strength) based on the magnitude of the wind vectors and on the agreement among the various wind stations. These qualitative descriptions are included in the discussions of the next section and are summarized in rough surface wind maps presented along with the visibility maps. We recognize that surface wind data do not adequately represent synoptic scale transport conditions, but the surface wind study was the only wind study possible within the budget of the project.

The procedure for the case studies is as follows. First, episode days of high fine particle concentrations are identified using the particulate maps (Appendix A). Regional visibility maps are then prepared for several days surrounding the episode day. The spatial extent, transport patterns, and origins of the episode are interpreted using the visibility maps and knowledge of general wind conditions. A specific comparison is also made between the visibility map and particulate map on the episode day. It should be noted that our interpretation of the visibility maps and transport conditions is not without ambiguity. The uncertainties include the lack of a precise quantitative relationship between fine particles and visibility, the use of surface wind maps rather than synoptic trajectories, and the lack of a full, quantitative accounting of meteorological influences on visibility (Martinez 1983).

---

*In an attempt to avoid serious local distortions produced by sea breezes or mountain drainage flows, we excluded airports near large water bodies or in mountain ranges.

As part of the interpretive analyses, it is useful to know important emission source areas, especially for sulfates which are a major component of fine particles and which tend to dominate visibility in the East. Figure 4.1 illustrates approximate sulfur oxide emission density by state. The greatest emissions occur in the triangle from Illinois to Massachusetts to Tennessee. The large states in the upper Ohio Valley exhibit particularly strong SO_2 emission density.

It should be acknowledged that Husar et al. (1976a, b) were the first to show that haze episodes in the East could be successfully tracked with airport visibility data. The present study attempts to extend the work of Husar et al. by using more refined data sets (for both particulate matter and visibility) and by formulating an operational procedure for EPA to use in characterizing fine particle episodes.

4.2 EPISODE CASE STUDIES

This section presents several case studies to illustrate the use of visibility maps in characterizing fine particle episodes. In analyzing these case studies, we were generally very encouraged by the spatial correspondence between visibility maps and particulate maps as well as by the reasonable agreement between haze movement and wind direction. To avoid any confusion, the reader should note that all wind directions discussed below refer to winds from the specified direction.

4.2.1 30 June 1980 to 6 July 1980

The first particulate episode that we selected for study occurred on 2 July 1980. As shown in Figure 4.2, this day exhibited high fine particle levels and very high sulfate levels in western Ohio as well as moderately high sulfate and fine particle levels along the Eastern seaboard. As will be discussed below, this episode is interesting because of its dramatic and similar beginning and end.

Figures 4.3a to 4.3g present visibility maps for 30 June 1980 through 6 July 1980. As seen in Figure 4.3a, the East was relatively free of haze on

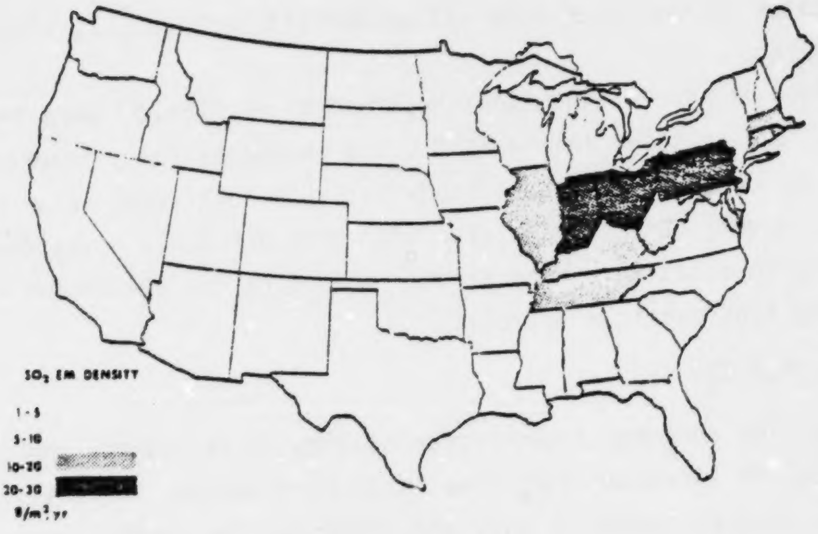
SO_2 EM DENSITY
1-5
5-10
10-20
20-30
g/m², yr

Figure 4.1 Sulfur oxide emission density map (NRC 1978; EPA 1976).

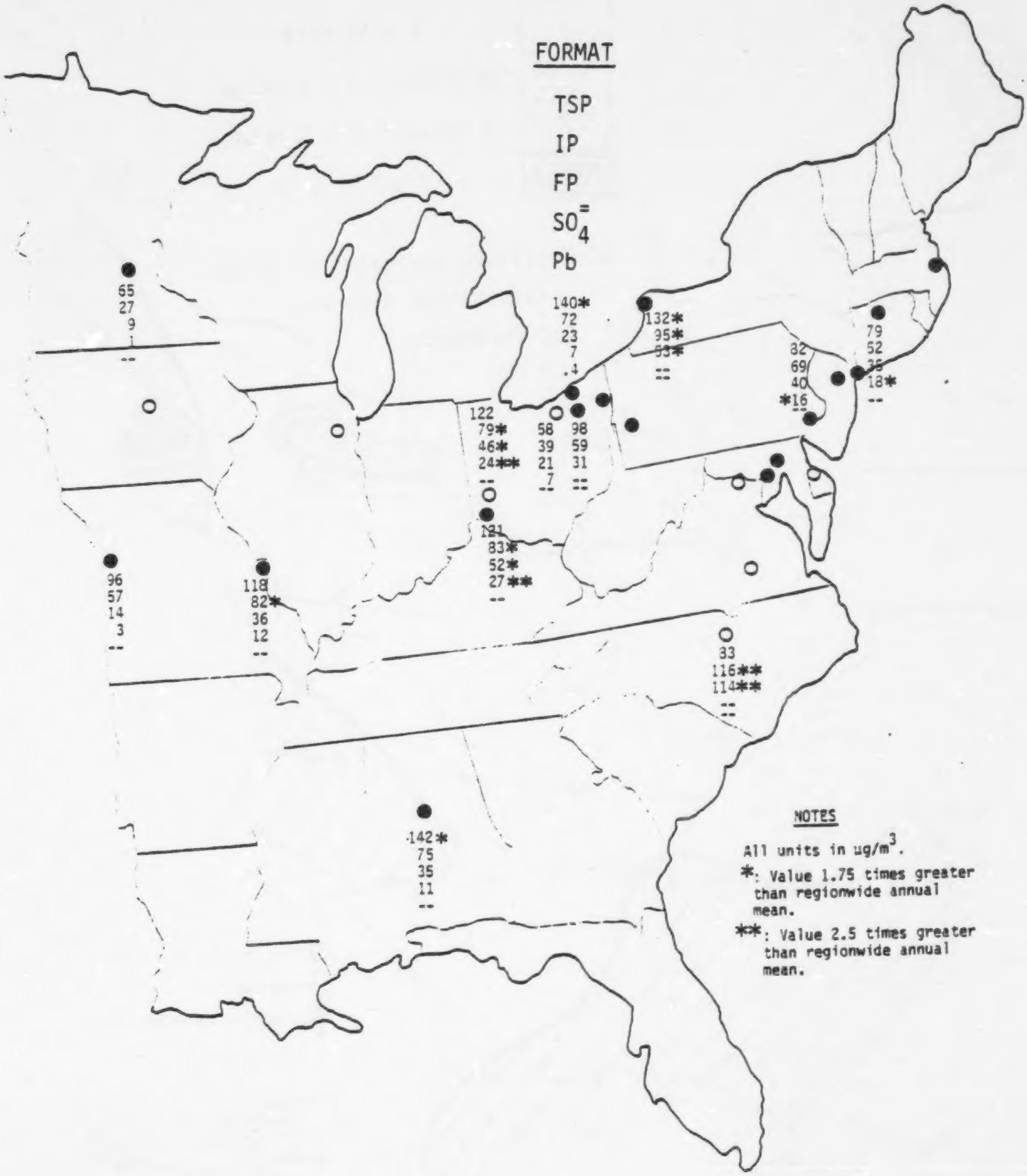
FORMAT
TSP
IP
FP
$SO_4^=$
Pb
65
27
9
1
--
140*
72
23
7
.4
132*
95*
53*
--
--
82
69
40
*16
--
79
52
35
18*
--
122
79*
46*
24**
--
58
39
21
7
--
98
59
31
--
--
121
83*
52*
27**
--
96
57
14
3
--
118
82*
36
12
--
33
116**
114**
--
--
142*
75
35
11
--

NOTES

All units in ug/m^3.

*: Value 1.75 times greater than regionwide annual mean.

**: Value 2.5 times greater than regionwide annual mean.

Figure 4.2 Particulate concentration map for 2 July 1980.

Reproduced from best available copy.

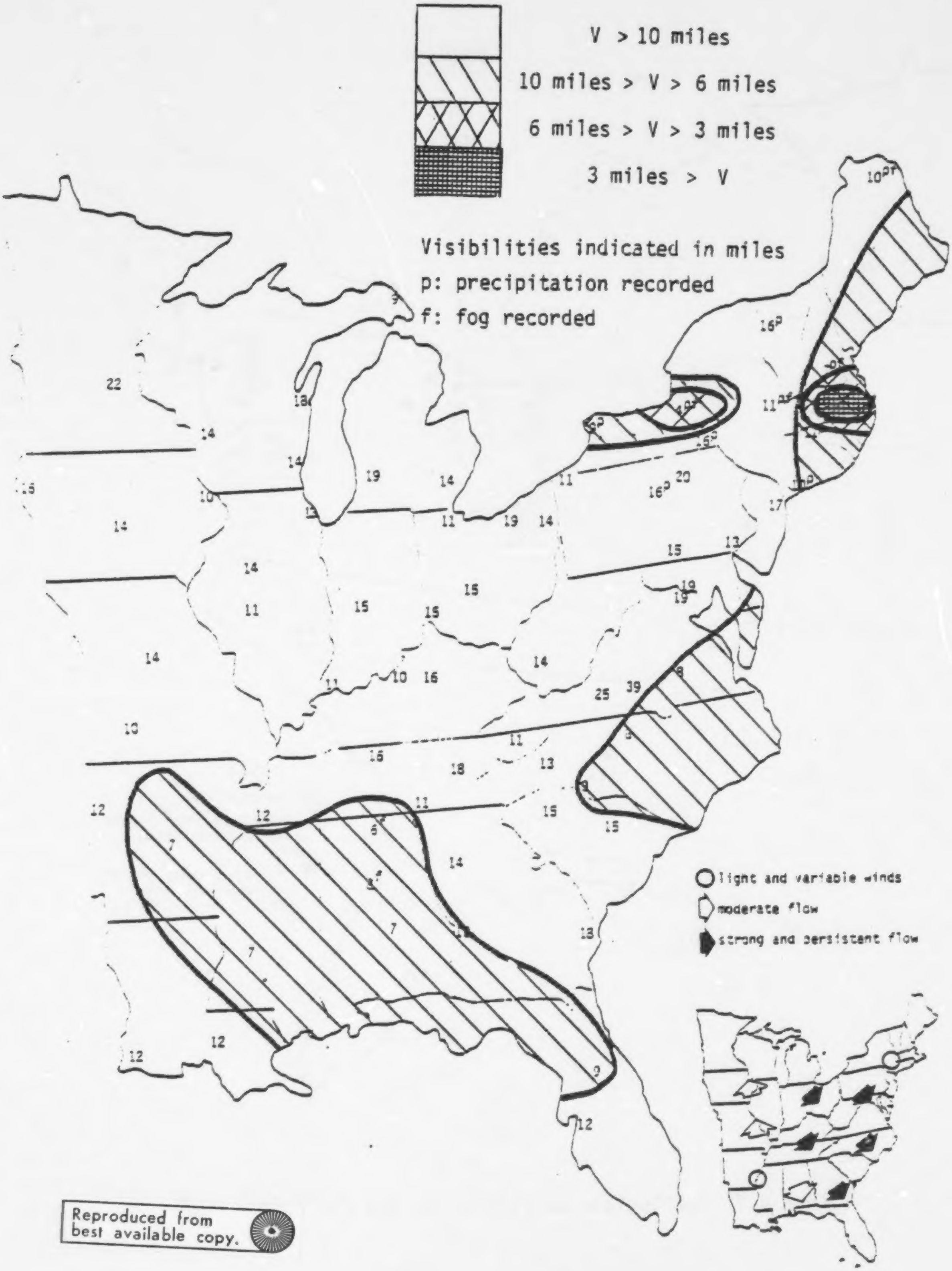
V > 10 miles
10 miles > V > 6 miles
6 miles > V > 3 miles
3 miles > V
Visibilities indicated in miles
p: precipitation recorded
f: fog recorded
light and variable winds
moderate flow
strong and persistent flow

Reproduced from best available copy.

Figure 4.3a Visibility map for 30 June 1980.

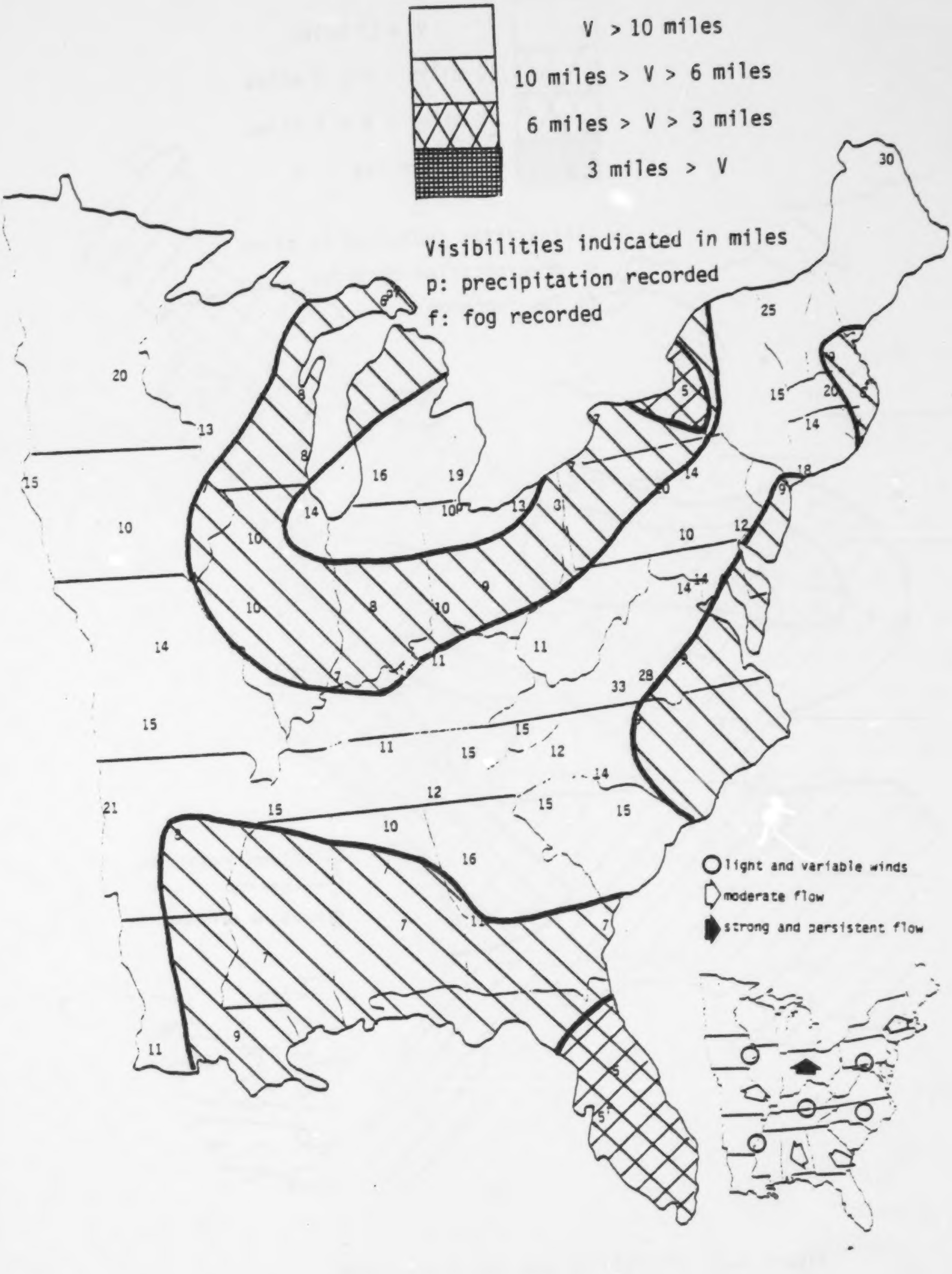
V > 10 miles
10 miles > V > 6 miles
6 miles > V > 3 miles
3 miles > V
Visibilities indicated in miles
p: precipitation recorded
f: fog recorded
light and variable winds
moderate flow
strong and persistent flow
30
25
20
15
20
14
18
9
13
15
16
19
14
10
13
3
14
10
12
10
10
9
8
10
14
14
14
11
11
33
28
15
15
11
15
12
14
21
15
12
15
15
10
16
7
11
7
7
11
9

Figure 4.3b Visibility map for 1 July 1980.

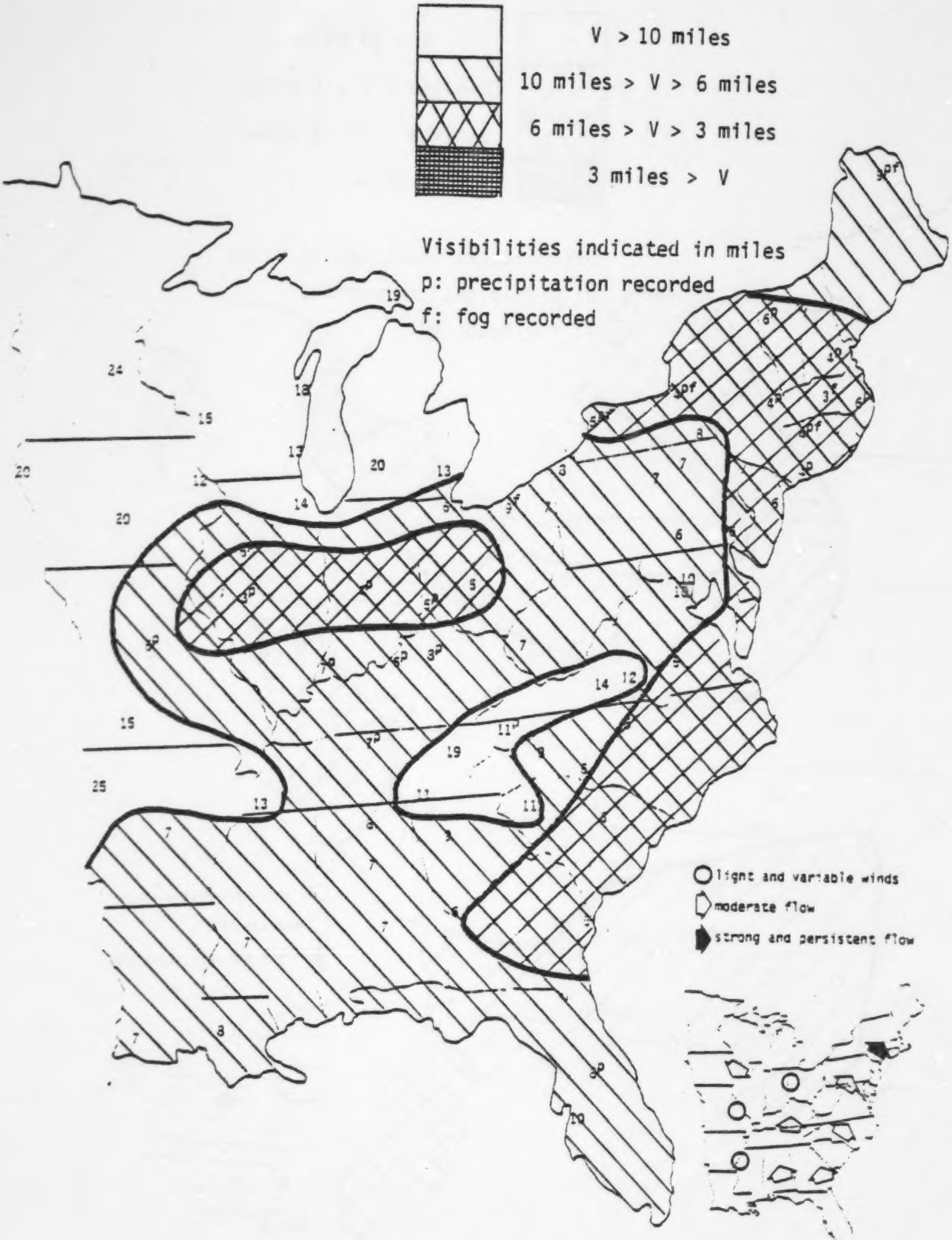
V > 10 miles
10 miles > V > 6 miles
6 miles > V > 3 miles
3 miles > V
Visibilities indicated in miles
p: precipitation recorded
f: fog recorded
light and variable winds
moderate flow
strong and persistent flow

Figure 4.3c Visibility map for 2 July 1980.

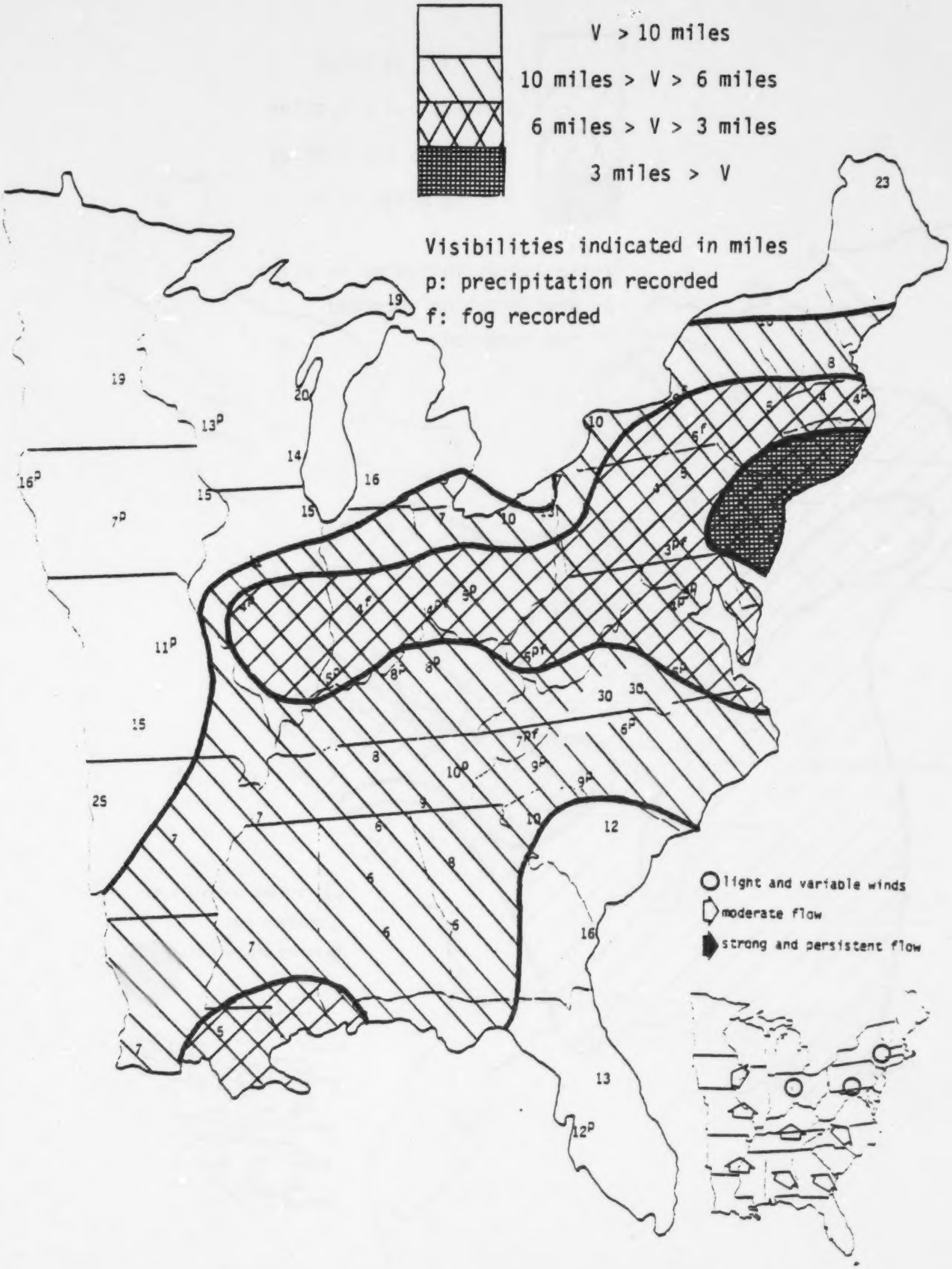
V > 10 miles
10 miles > V > 6 miles
6 miles > V > 3 miles
3 miles > V
Visibilities indicated in miles
p: precipitation recorded
f: fog recorded
light and variable winds
moderate flow
strong and persistent flow
23
19
19
20
13p
16p
14
16
7p
15
15
8
4p
10
6f
7
10
3pf
11p
30
30
15
6p
7pf
8
10p
9p
9p
25
7
9
12
6
10
7
8
6
6
6
7
16
5
7
13
12p

Figure 4.3d Visibility map for 3 July 1980.

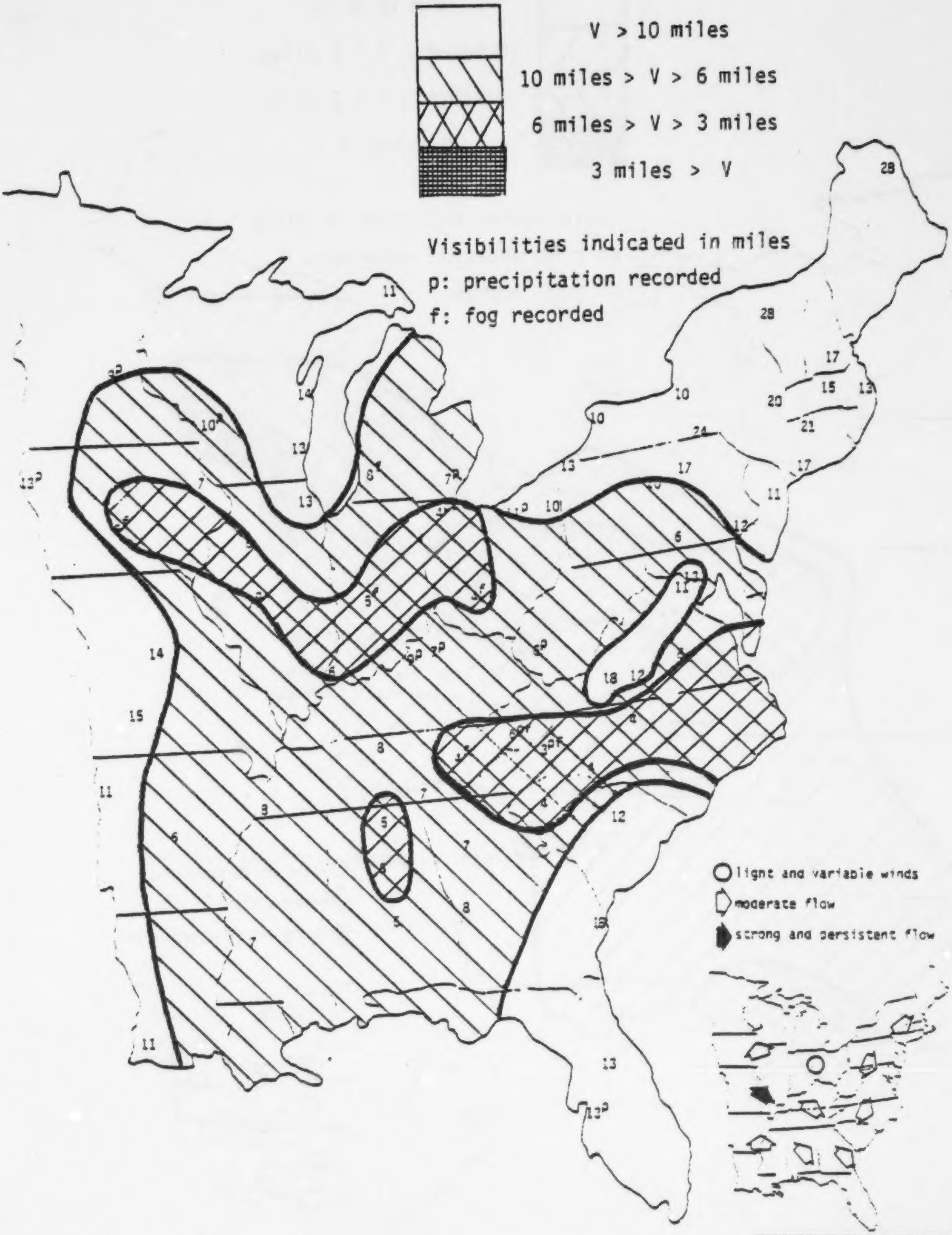
V > 10 miles
10 miles > V > 6 miles
6 miles > V > 3 miles
3 miles > V
Visibilities indicated in miles
p: precipitation recorded
f: fog recorded
light and variable winds
moderate flow
strong and persistent flow

Reproduced from best available copy.

Figure 4.3e Visibility map for 4 July 1980.

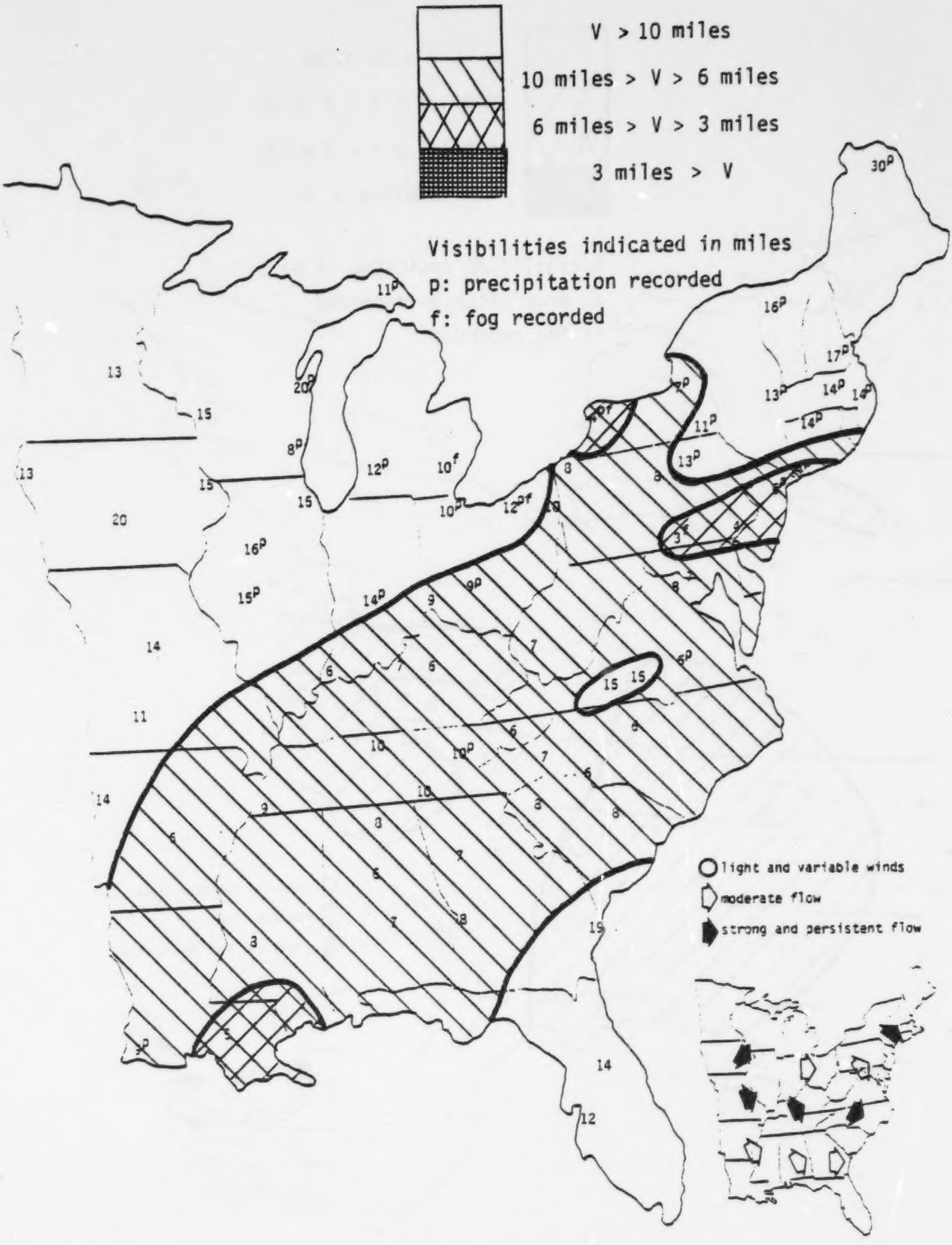
V > 10 miles
10 miles > V > 6 miles
6 miles > V > 3 miles
3 miles > V
Visibilities indicated in miles
p: precipitation recorded
f: fog recorded
light and variable winds
moderate flow
strong and persistent flow

Figure 4.3f Visibility map for 5 July 1980.

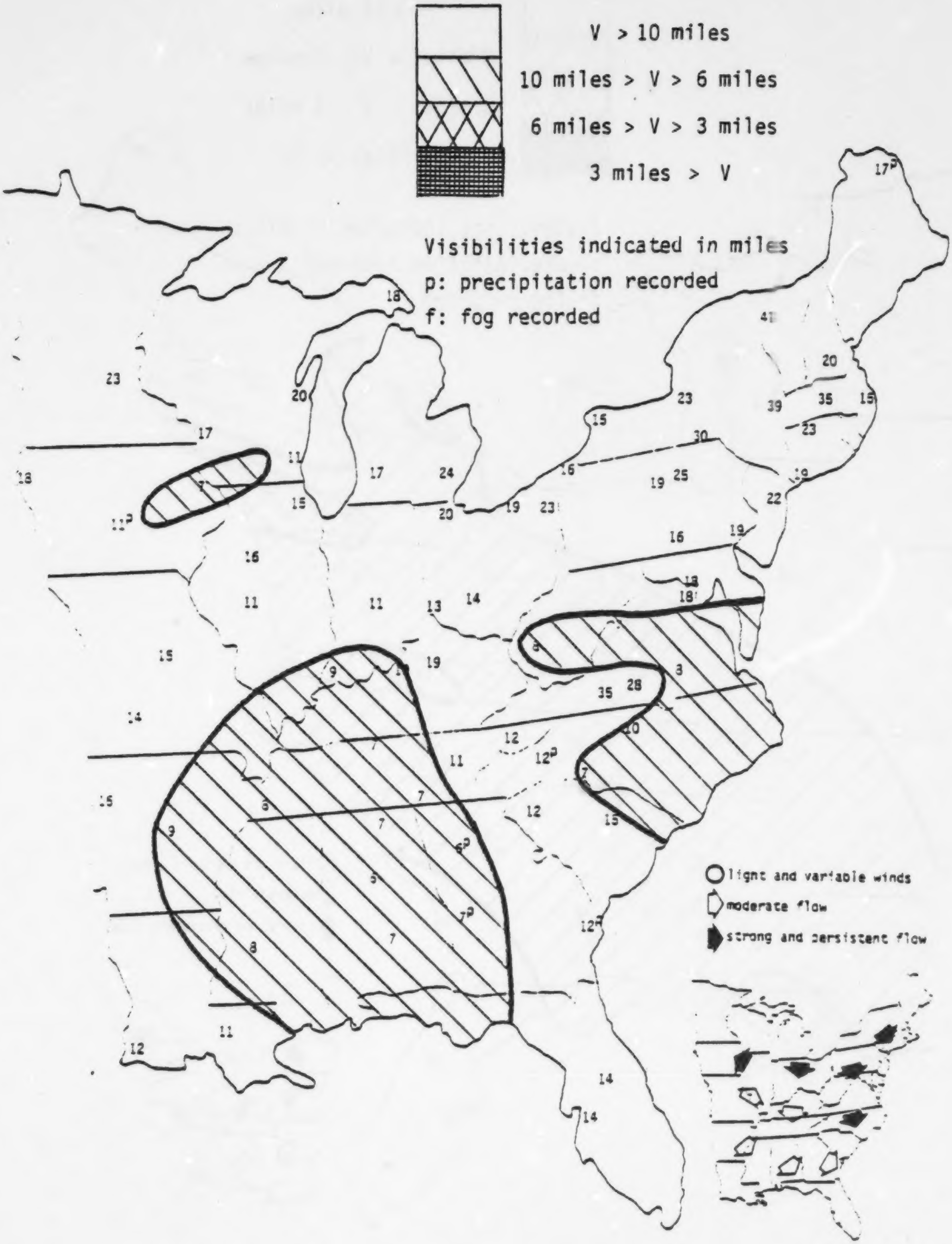
V > 10 miles
10 miles > V > 6 miles
6 miles > V > 3 miles
3 miles > V
Visibilities indicated in miles
p: precipitation recorded
f: fog recorded
17p
18
41
20
23
20
39
35
15
23
15
23
30
17
11
17
24
16
19
25
23
19
22
18
7
11p
15
20
19
23
16
19
16
11
11
13
14
18
18
15
9
19
6
3
35
28
14
10
12
11
12p
7
15
8
7
7
12
15
9
6p
6
7p
12p
8
7
11
12
14
14
light and variable winds
moderate flow
strong and persistent flow

Figure 4.3g Visibility map for 6 July 1980.

30 June. The wind pattern for this day was a very strong flow from the northwest, except for the Gulf States and New England where the flow was somewhat weaker. The strong northwesterly winds evidently had cleared the East of haze except for the latter two subareas.

On 1 July, the wind flow of the previous day stagnated. The only major transport evident was a southerly flow in the Great Lakes area. On this day, visibility began to decrease over much of the East.

Winds were again generally light on 2 July, the only notable flow being from the south up along the Appalachian and coastal area. The haziness increased to a moderate episode, with some of the haze possibly transported up to the New England area from the Central Atlantic states. Comparing 4.3c to 4.2, it is apparent that the visibility data conform rather well with the sulfate and fine particle data. At this point, the two most intense haze pockets in the Ohio Valley and along the Eastern seaboard appear to have accumulated separately from emissions in the two respective areas.

On 3 July, the relatively stagnant winds continued except for a minor drift from the southwest. The haziness continued to increase, reaching very high levels along the North Central Atlantic from New Jersey to Rhode Island. The haze pocket from the Ohio Valley has apparently connected with the seaboard pocket at this time.

A persistent northwesterly flow started to affect the New England and North Atlantic area on July 4th. This area was blown relatively free of haze. The remainder of the East experienced a less pronounced southerly flow, and the haze layer expanded toward the north.

July 5th witnessed a strong westerly wind over the East. The wind turned from westerly to southwesterly along the northeast seaboard. Apparently, this transport wind pushed the hazy air mass toward the east. The haze pocket in New Jersey on this day appears to be the remainder of the intense haze found on the previous day south of the Great Lakes.

By 6 July, a dominant northwesterly flow again prevailed over most of the area, bringing clear air over the Ohio Valley and Northeast. Very similar to 30 June, little haze was left in the region; the remainder of the episode seemed to be pushed to the south and east borders.

4.2.2 11 July 1980 to 18 July 1980

The second episode selected for a case study occurred on 14 July 1980. Figure 4.4 shows that this episode involved a band of moderately high fine particle levels down the center of the region, with very high sulfates in St. Louis. The far western and far eastern portions of the region exhibited rather low particulate concentrations. This day has a puzzling aspect in the sense that some locations in the eastern Great Lakes region recorded low concentrations while other nearby locations recorded high concentrations.

Figure 4.5a shows that, on 11 July, a moderately intense haze covered the entire area east of the Mississippi. Wind flows were from the west at moderate to strong intensity on this day.

On 12 July, the general wind pattern continued westerly at reduced strength, except in the New England/North Atlantic area where a strong northwesterly flow prevailed. The haze on 12 July appears to have shifted slightly toward the east from the previous day. Also, the New England and North Atlantic states appear to have been cleared by the strong northwesterly flow in that area.

On July 13th, the strong northwesterly winds continued in the North Atlantic and that area remained free of haze. Winds over the remainder of the area were moderately intense -- northeasterly over the Ohio Valley and westerly over the Gulf States. On this day, a severe haze pocket began to accumulate in the western Ohio Valley.

Winds stagnated on 14 July, except for a strong southerly flow from the Ohio Valley up through the Great Lakes area. This flow evidently transported haze from the Ohio Valley up to Lake Superior and produced the elongated pattern of Figure 4.5d. The spatial visibility pattern is generally consistent with the fine particle concentrations of Figure 4.4, especially with respect to the high sulfate in St. Louis and the low particulate concentrations in the far western and far eastern borders of the region. The only anomaly concerns the moderately high particulate concentrations near Lake Erie in Figure 4.4.

A strong southwesterly flow became established in the northern two-thirds of the study area on July 15th. This wind pattern evidently pushed the north-

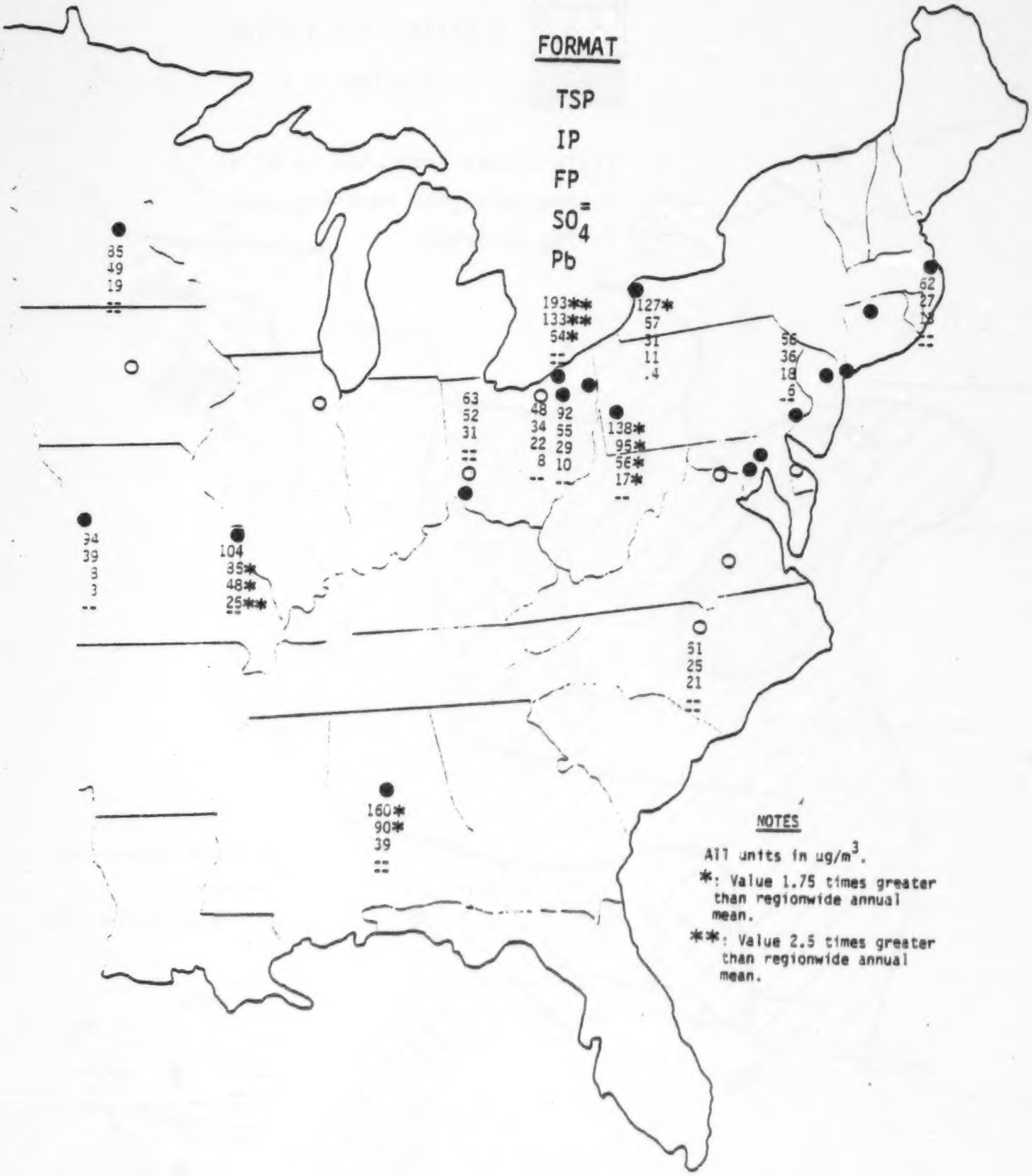
FORMAT
TSP
IP
FP
$SO_4^=$
Pb
85
49
19
--
34
39
3
3
--
104
35*
48*
25**
--
63
52
31
--
48
34
22
8
--
92
55
29
10
--
193**
133**
54*
--
127*
57
31
11
.4
138*
95*
56*
17*
--
56
36
18
6
--
62
27
13
--
51
25
21
--
160*
90*
39
--
NOTES
All units in ug/m^3.
*: Value 1.75 times greater than regionwide annual mean.
**: Value 2.5 times greater than regionwide annual mean.

Figure 4.4 Particulate concentration map for 14 July 1980.

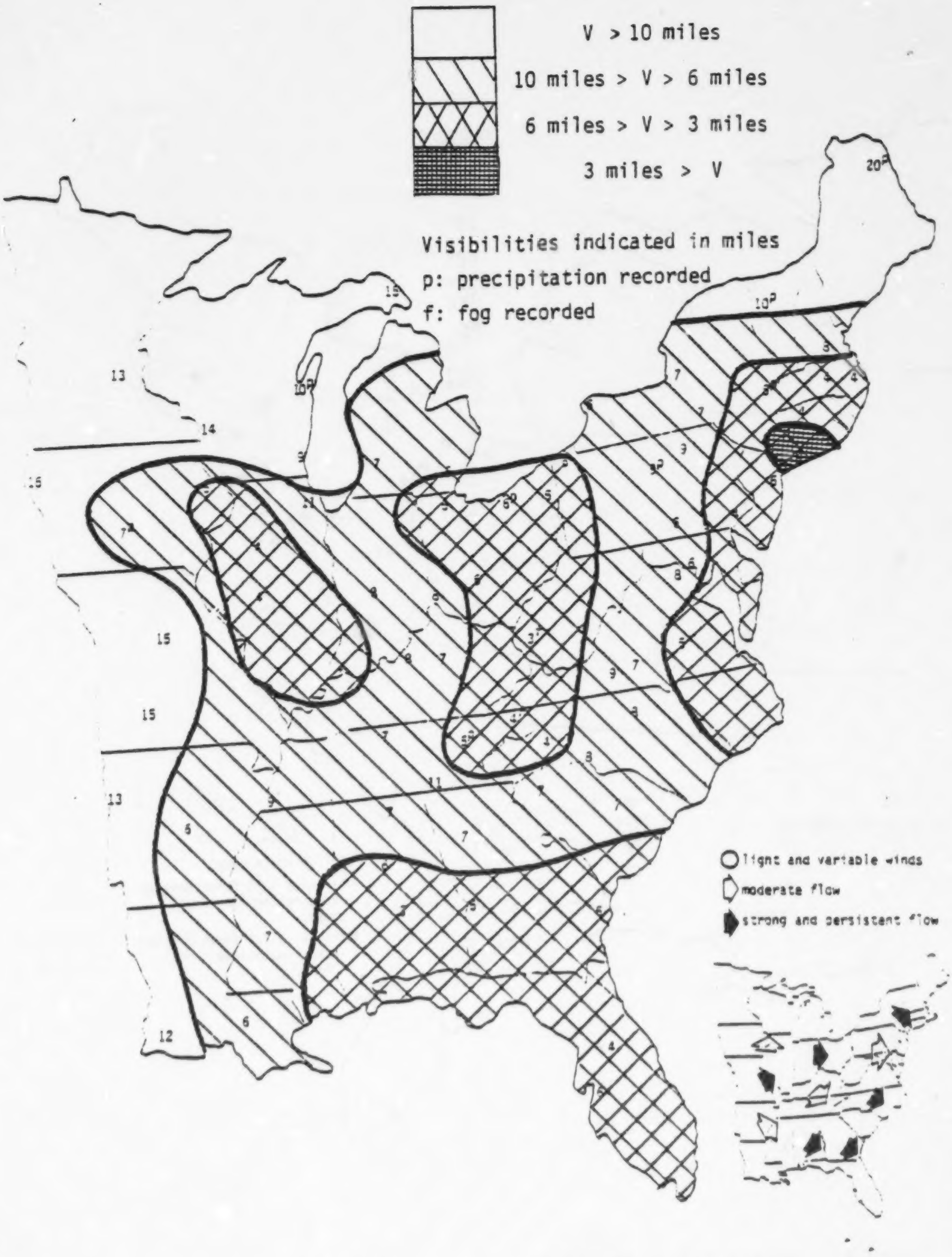
V > 10 miles
10 miles > V > 6 miles
6 miles > V > 3 miles
3 miles > V
Visibilities indicated in miles
p: precipitation recorded
f: fog recorded
light and variable winds
moderate flow
strong and persistent flow
20P
10P
15
13
14
15
15
15
13
12
6
4

Figure 4.5a Visibility map for 11 July 1980.

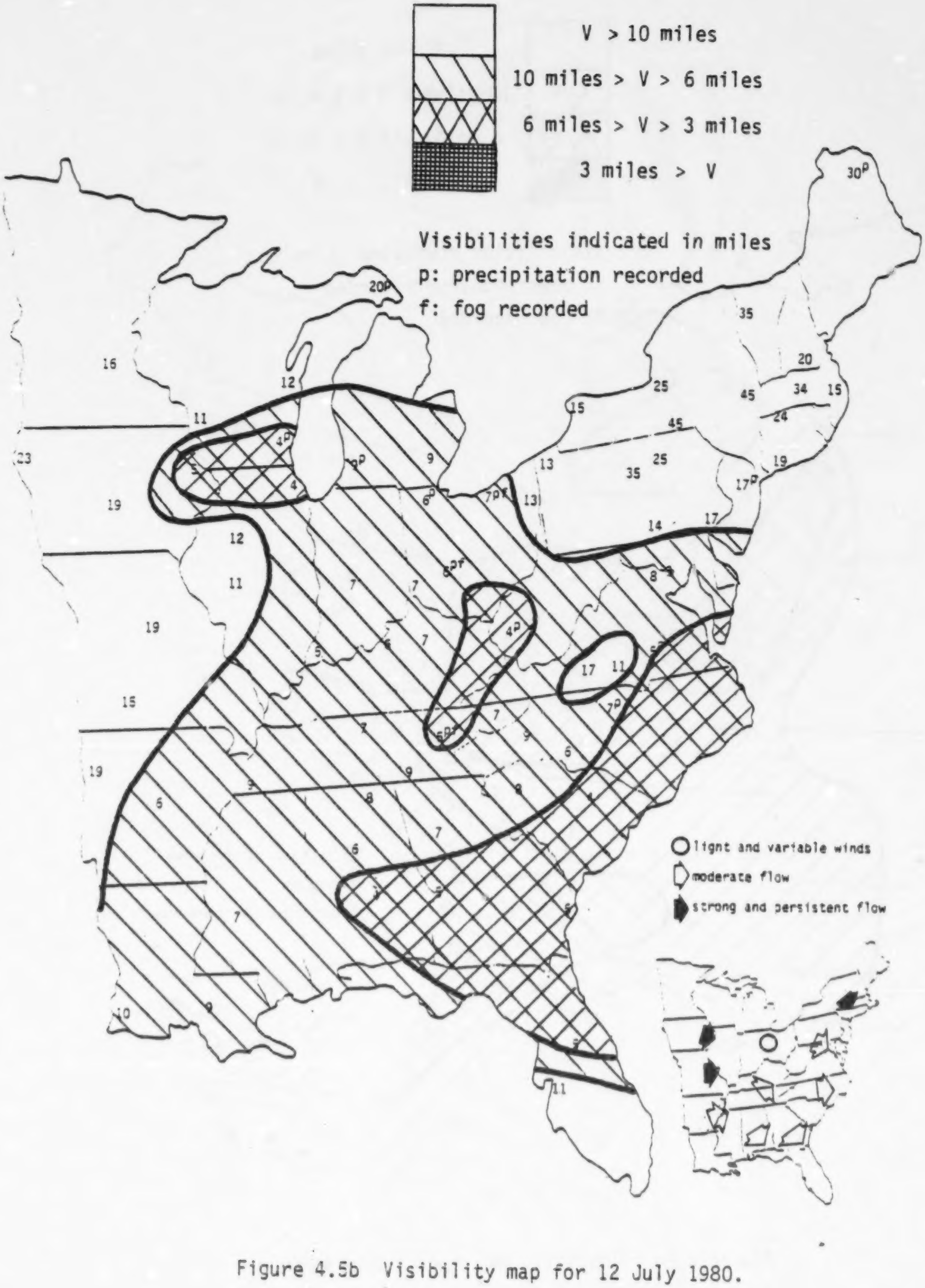
V > 10 miles
10 miles > V > 6 miles
6 miles > V > 3 miles
3 miles > V
Visibilities indicated in miles
p: precipitation recorded
f: fog recorded
light and variable winds
moderate flow
strong and persistent flow

Figure 4.5b Visibility map for 12 July 1980.

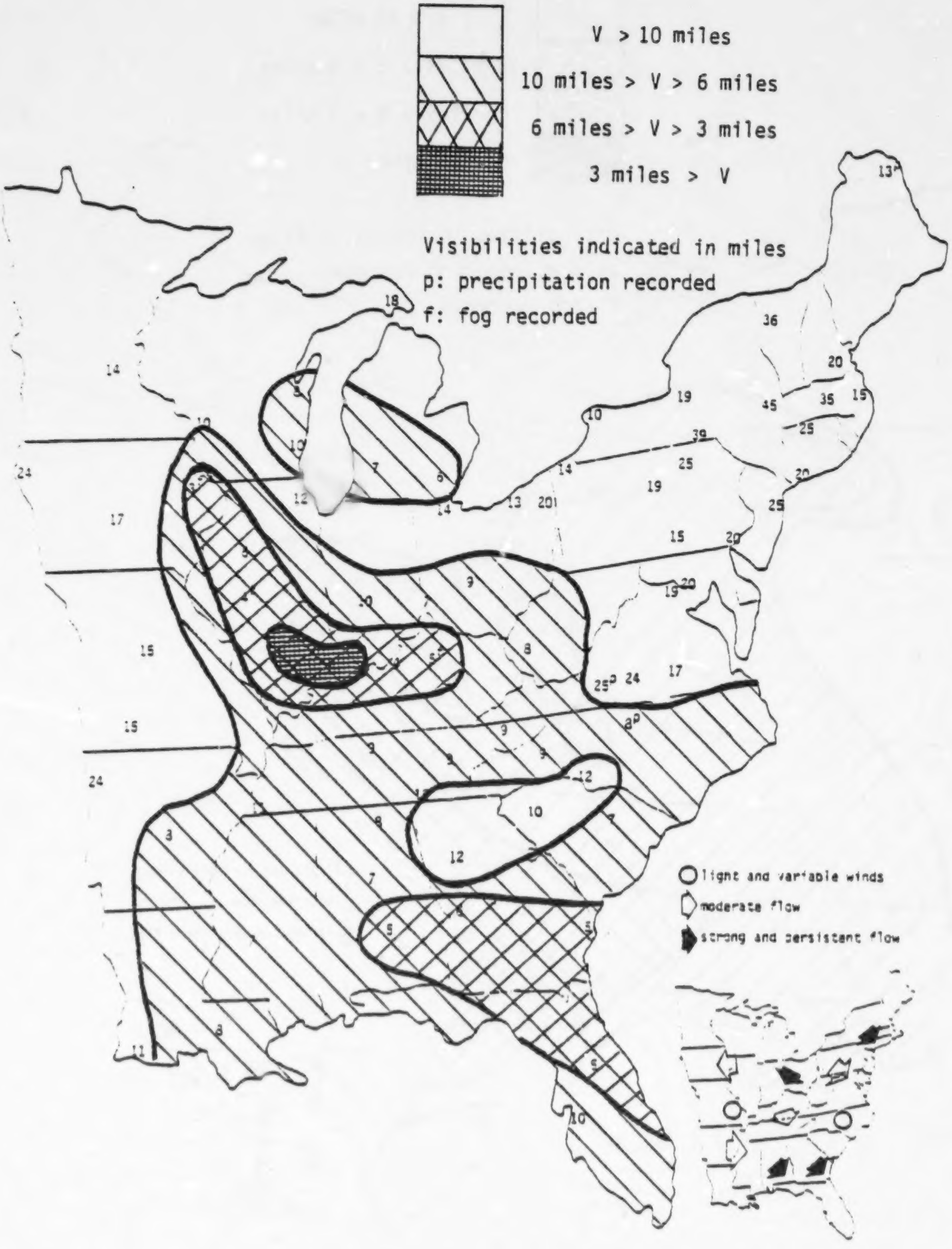
V > 10 miles
10 miles > V > 6 miles
6 miles > V > 3 miles
3 miles > V
Visibilities indicated in miles
p: precipitation recorded
f: fog recorded
light and variable winds
moderate flow
strong and persistent flow

Figure 4.5c Visibility map for 13 July 1980.

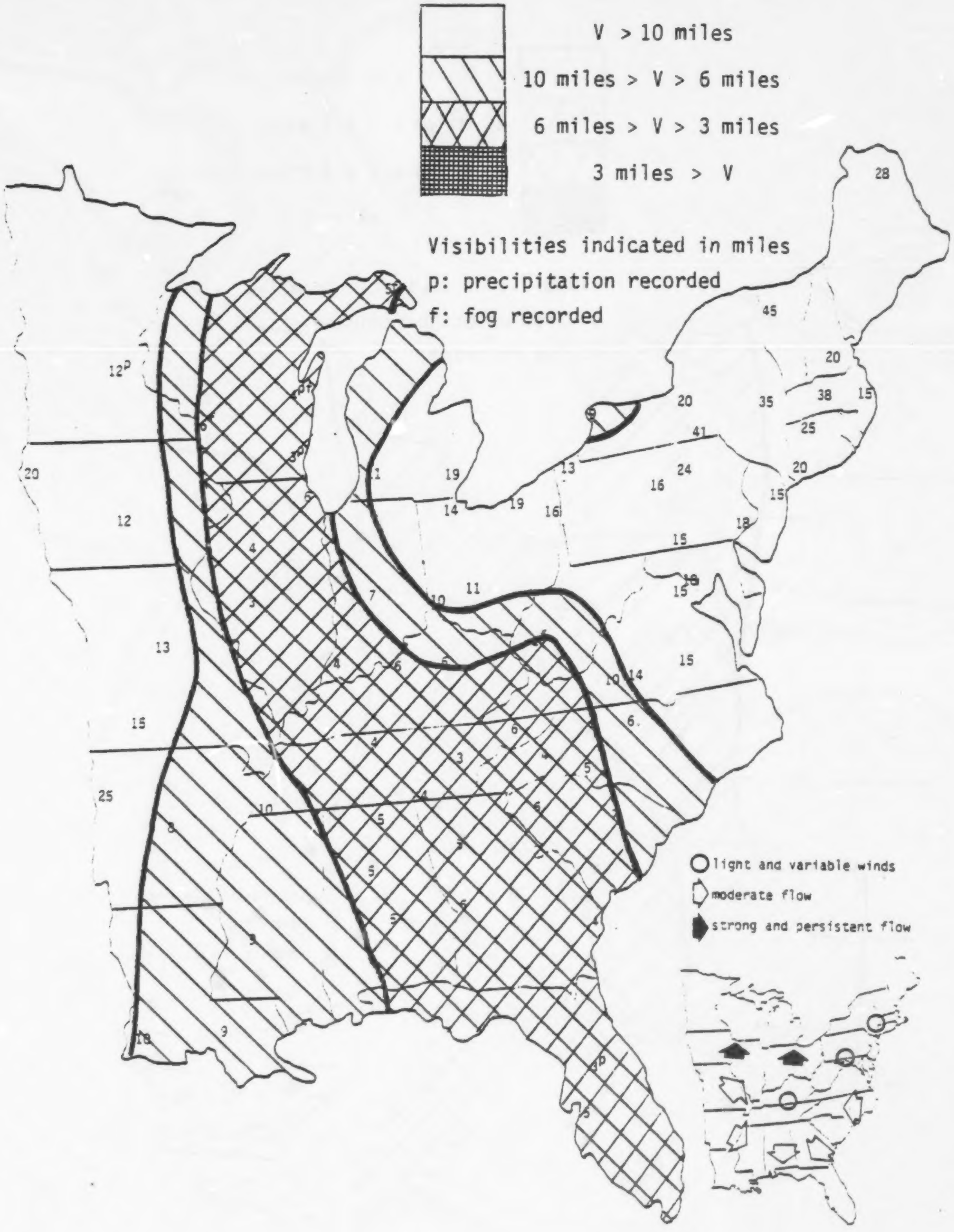
V > 10 miles
10 miles > V > 6 miles
6 miles > V > 3 miles
3 miles > V
Visibilities indicated in miles
p: precipitation recorded
f: fog recorded
light and variable winds
moderate flow
strong and persistent flow

Figure 4.5d Visibility map for 14 July 1980.

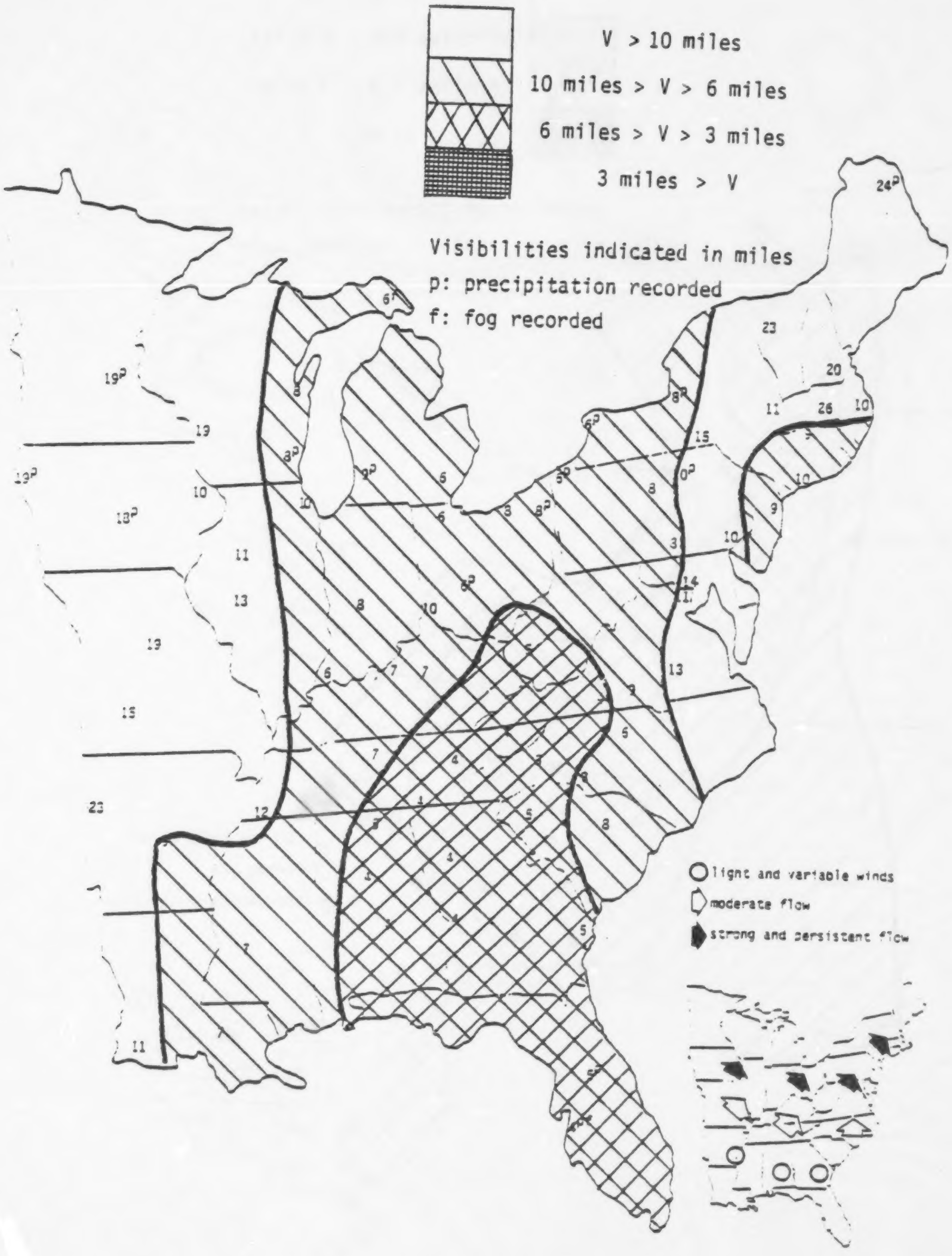
V > 10 miles
10 miles > V > 6 miles
6 miles > V > 3 miles
3 miles > V
Visibilities indicated in miles
p: precipitation recorded
f: fog recorded
light and variable winds
moderate flow
strong and persistent flow

Figure 4.5e Visibility map for 15 July 1980.

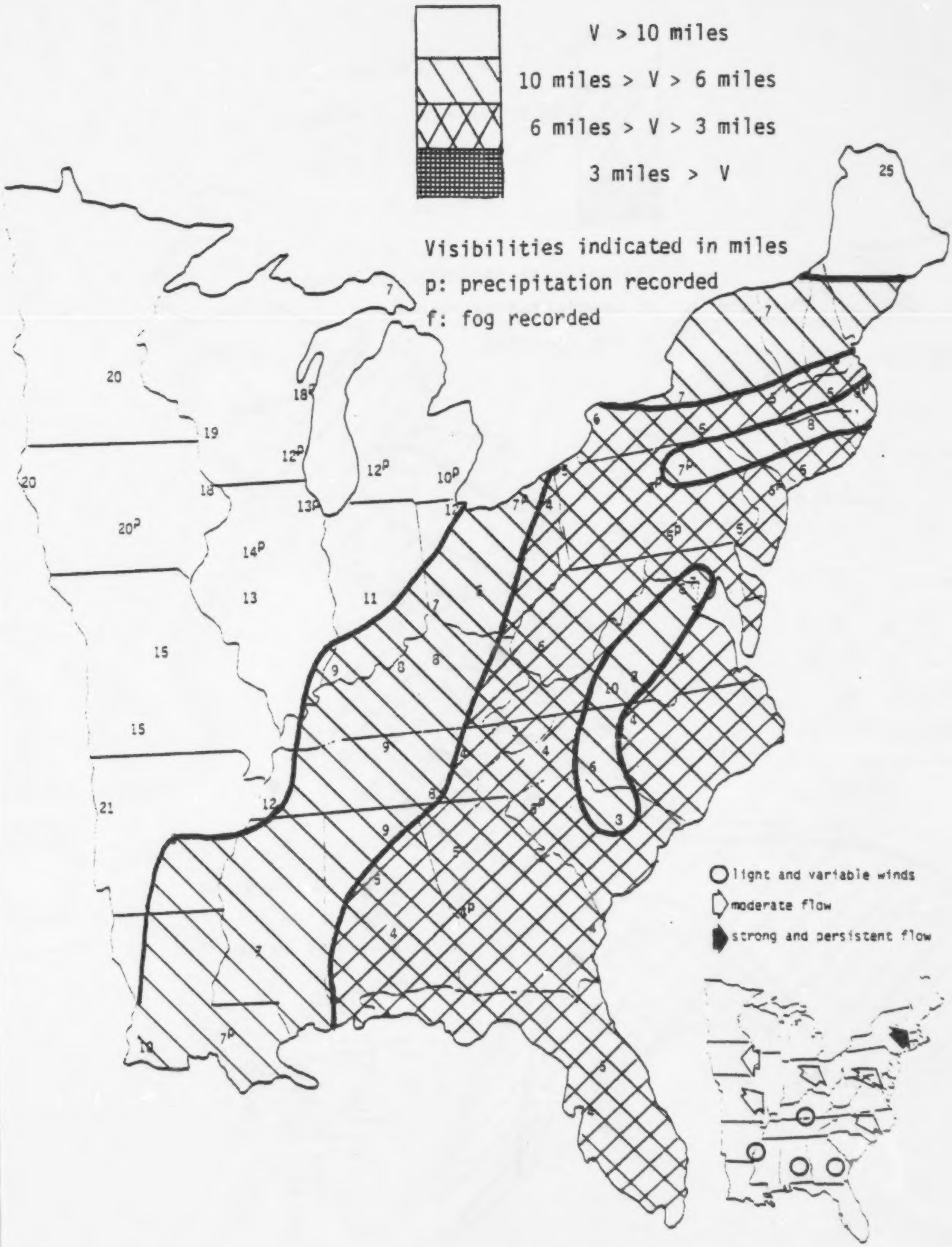
V > 10 miles
10 miles > V > 6 miles
6 miles > V > 3 miles
3 miles > V
Visibilities indicated in miles
p: precipitation recorded
f: fog recorded
light and variable winds
moderate flow
strong and persistent flow

Figure 4.5f Visibility map for 16 July 1980.

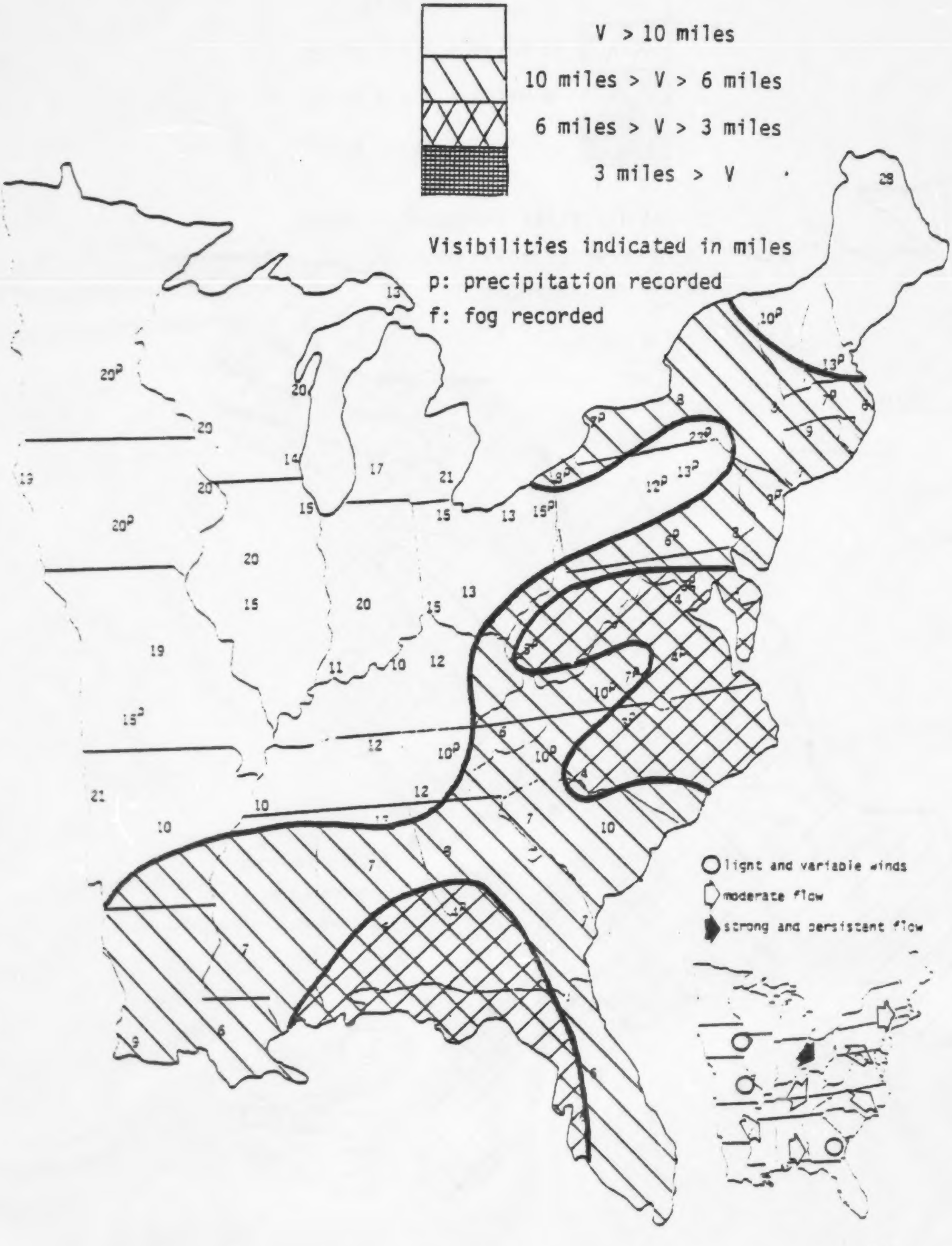
V > 10 miles
10 miles > V > 6 miles
6 miles > V > 3 miles
3 miles > V
Visibilities indicated in miles
p: precipitation recorded
f: fog recorded
light and variable winds
moderate flow
strong and persistent flow

Figure 4.5g Visibility map for 17 July 1980.

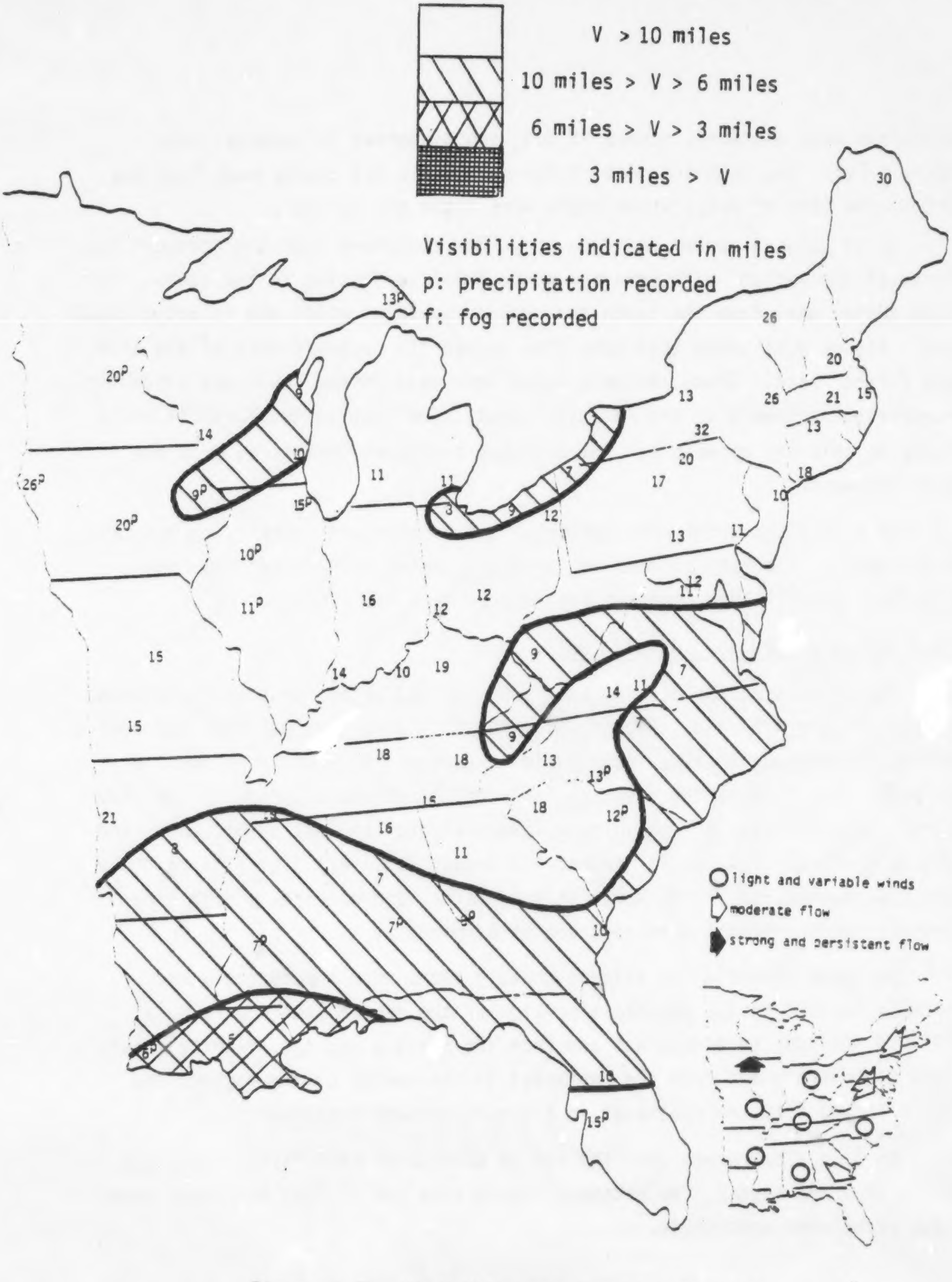
V > 10 miles
10 miles > V > 6 miles
6 miles > V > 3 miles
3 miles > V
Visibilities indicated in miles
p: precipitation recorded
f: fog recorded
light and variable winds
moderate flow
strong and persistent flow

Figure 4.5h Visibility map for 18 July 1980.

south haze band eastward, spread it out, and dispersed it somewhat (see Figure 4.5e). The southern part of the region did not change much from the 14th to the 15th of July; winds there were light and variable.

On 16 July, a weaker southwesterly flow continued over the northern two-thirds of the region, with variable winds still persisting in the south. The winds turned more from the south and grew in strength along the Atlantic coastline. Figure 4.4f shows that this flow pushed the northern part of the haze mass further east. Also, the more dense haze area in the south was evidently transported northward up the Atlantic coast. The haze in the North Atlantic states on this day appears to be a distinct transport phenomenon from the south and west.

On July 17th, winds were westerly in the north and westerly to variable in the south. The hazy airmass was evidently being shifted off into the Atlantic. By July 18th, most of the intense haze had left the region.

4.2.3 24 July 1980 to 3 August 1980

The third study period includes two sampling dates for the EPA IP Network -- 26 July (Figure 4.6) and 1 August (Figure 4.7). July 26th was the most severe particulate episode that we found during the year. As seen in Figure 4.6, extremely high fine particle and sulfate concentrations occurred in the Ohio Valley, with moderately high sulfate levels stretching west to St. Louis and east to the Central Atlantic states. On August 1st, very high fine particle levels were measured in the North Atlantic area, and moderately high fine particle concentrations were recorded at Birmingham, Al.

We began tracking the episode on July 24th, when a moderately hazy air mass resided in the southeast portion of the region (see Figure 4.8a). Winds on that day were moderate and from the north along the Atlantic coast, light to moderate and from the northeast in the center of the region, and fairly strong from the southeast in Missouri through Wisconsin.

On July 25th, winds over the entire study area were fairly light and mostly from the south. The haziness accumulated and shifted northward under these light wind conditions.

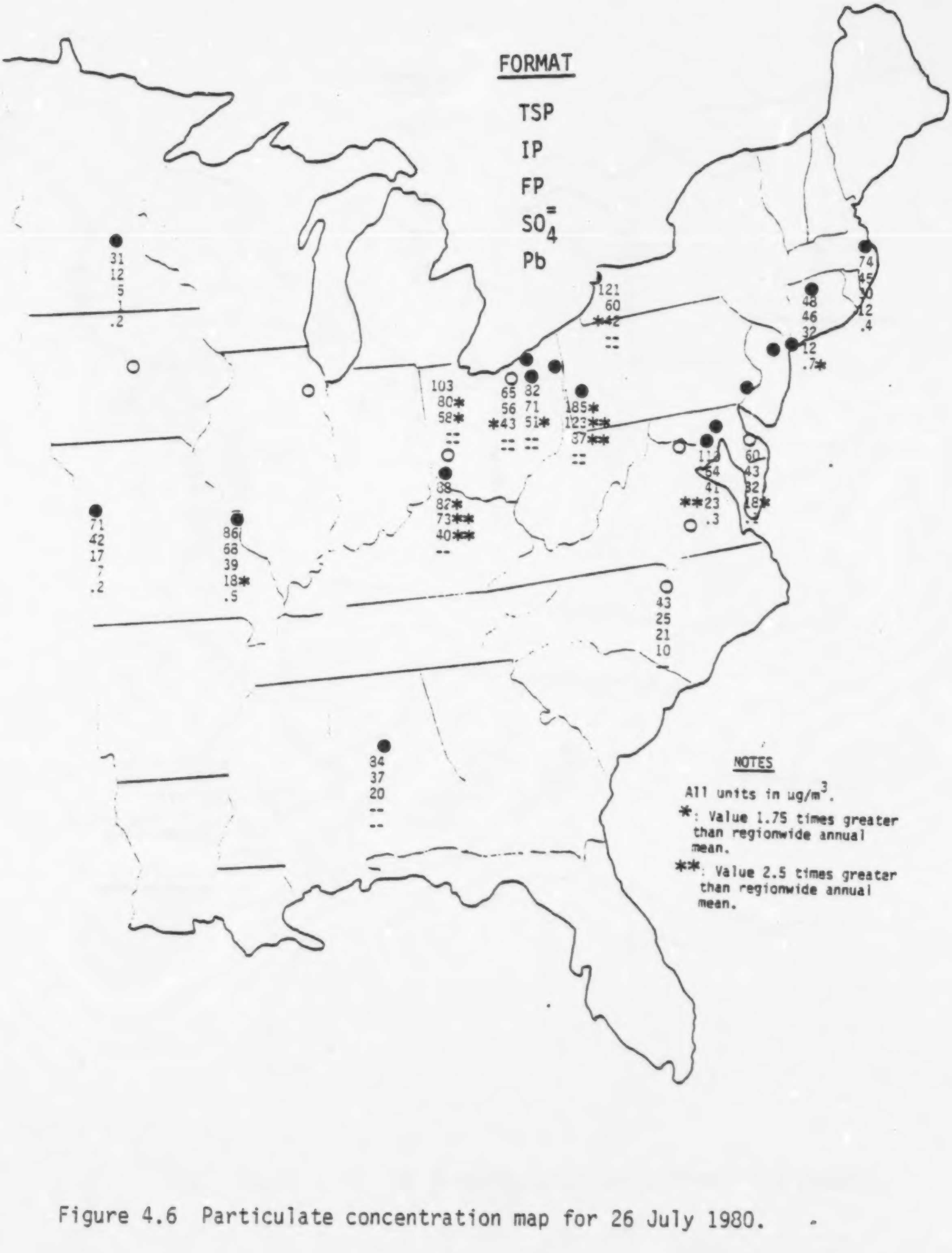
FORMAT
TSP
IP
FP
$SO_4^=$
Pb
31
12
5
1
.2
103
80*
58*
--
--
65
56
*43
--
--
82
71
51*
--
121
60
*42
--
--
185*
123**
37**
--
74
45
30
12
.4
48
46
32
12
.7*
88
82*
73**
40**
--
71
42
17
7
.2
86
68
39
18*
.5
113
54
41
**23
.3
60
43
32
18*
.2
43
25
21
10
84
37
20
--
--
NOTES
All units in ug/m^3.
*: Value 1.75 times greater than regionwide annual mean.
**: Value 2.5 times greater than regionwide annual mean.

Figure 4.6 Particulate concentration map for 26 July 1980.

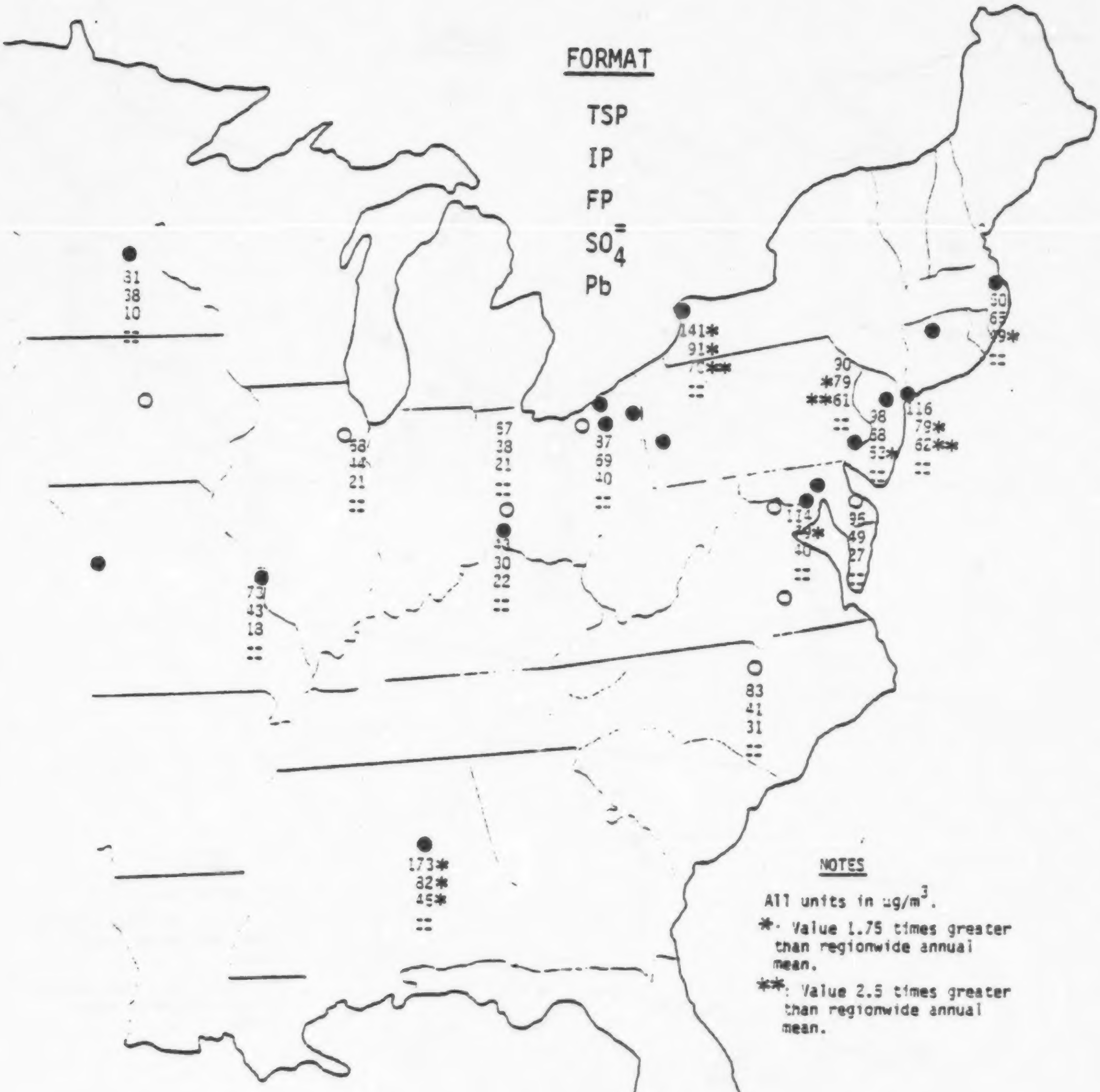
FORMAT
TSP
IP
FP
SO$_4^=$
Pb
31
38
10
::
58
14
21
::
57
38
21
::
43
30
22
::
73
43
13
::
37
69
40
::
141*
91*
70**
::
90
*79
**61
::
38
68
53*
::
116
79*
62**
::
80
65
39*
::
114
39*
40
::
95
49
27
::
83
41
31
::
173*
82*
45*
::
NOTES
All units in ug/m^3.
*: Value 1.75 times greater than regionwide annual mean.
**: Value 2.5 times greater than regionwide annual mean.

Reproduced from best available copy.

Figure 4.7 Particulate concentration map for 1 August 1980.

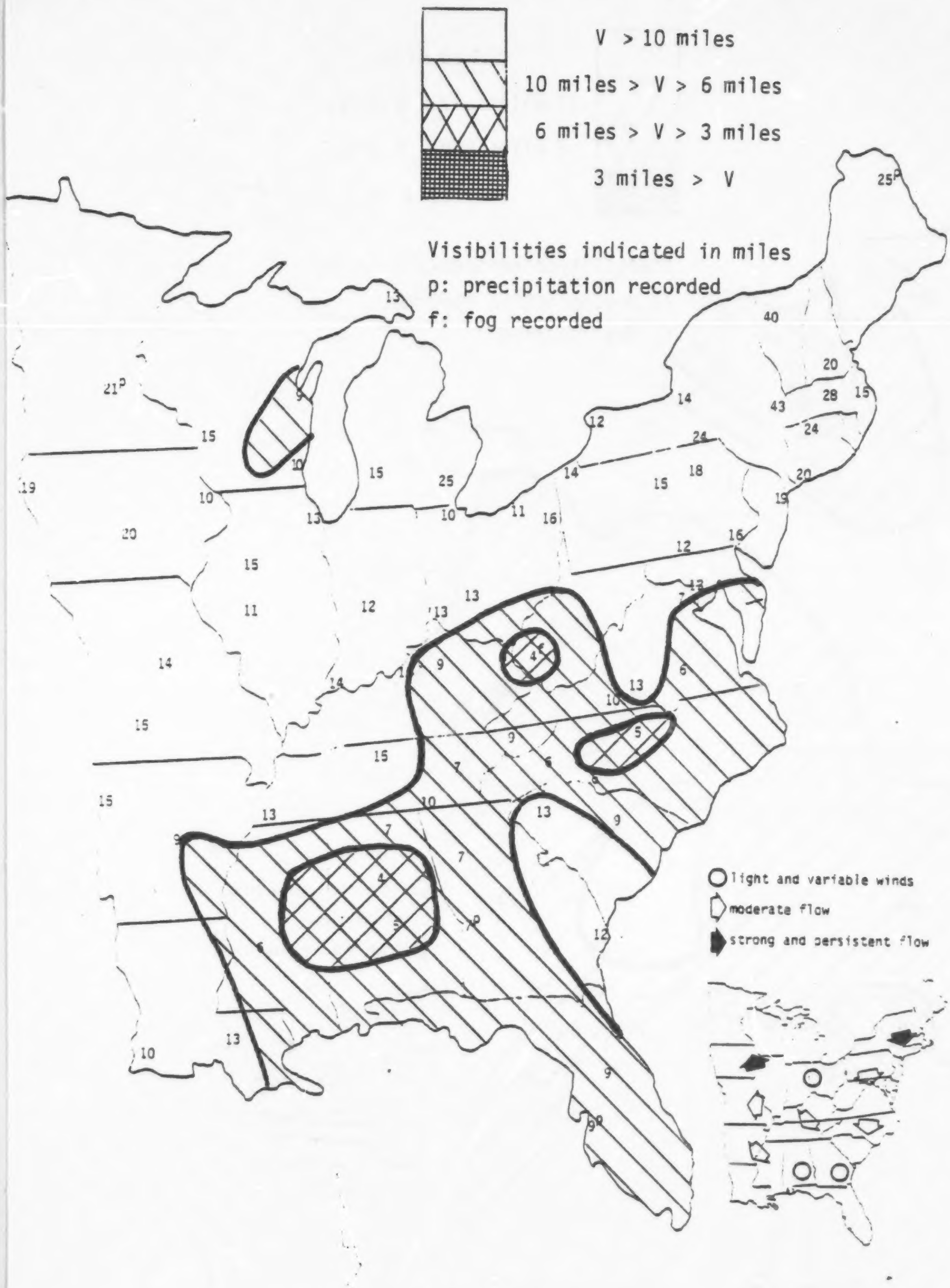
V > 10 miles
10 miles > V > 6 miles
6 miles > V > 3 miles
3 miles > V
Visibilities indicated in miles
p: precipitation recorded
f: fog recorded
light and variable winds
moderate flow
strong and persistent flow
25p
40
20
28
15
43
24
14
12
24
18
15
14
20
19
16
12
13
21p
15
9
10
19
10
15
25
10
11
16
13
20
15
11
12
13
13
14
14
9
4
6
13
10
5
15
9
6
15
7
10
13
9
15
13
9
7
4
7
5
p
12
6
9
13
10
9p

Figure 4.8a Visibility map for 24 July 1980.

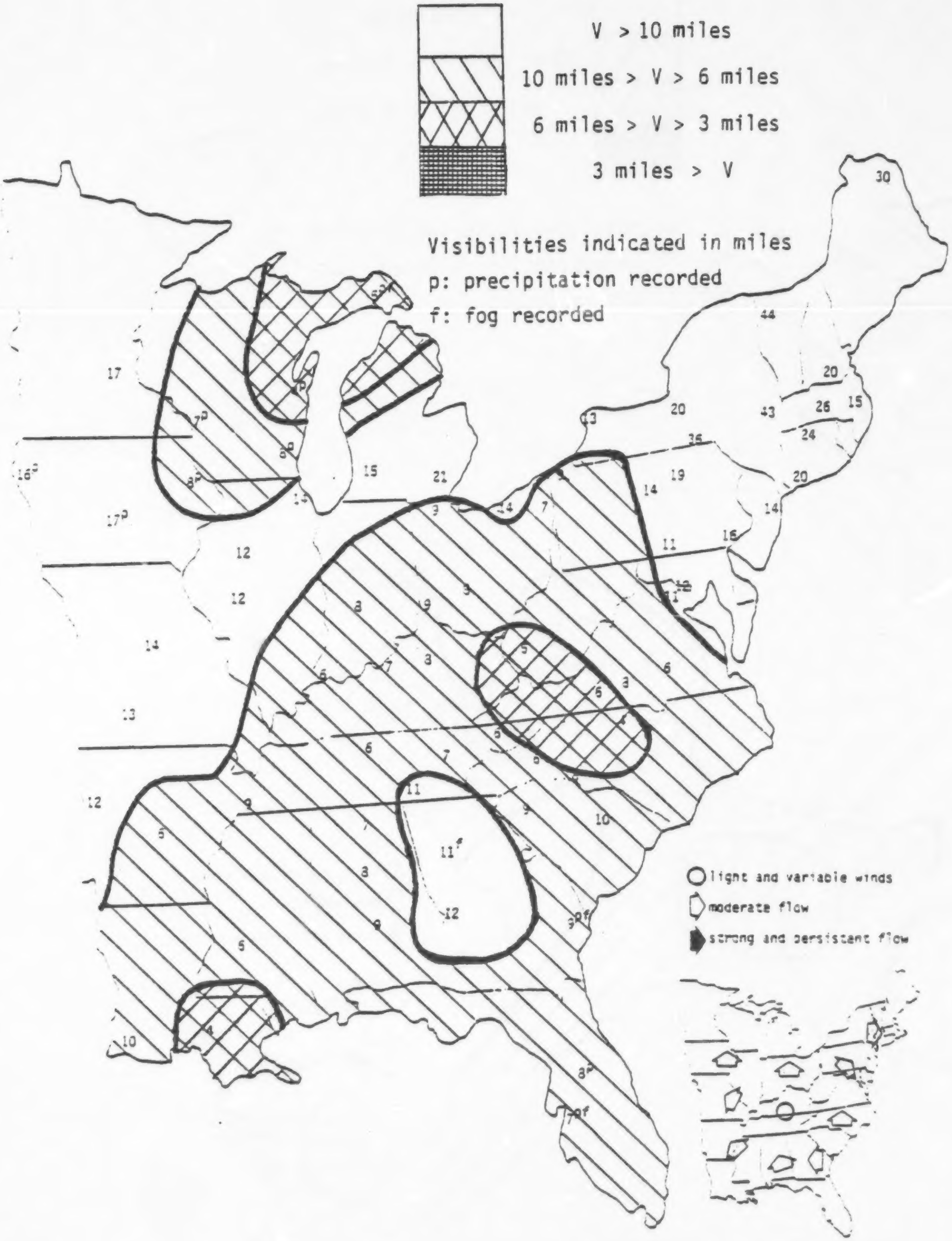
V > 10 miles
10 miles > V > 6 miles
6 miles > V > 3 miles
3 miles > V
Visibilities indicated in miles
p: precipitation recorded
f: fog recorded
light and variable winds
moderate flow
strong and persistent flow

Figure 4.8b Visibility map for 25 July 1980.

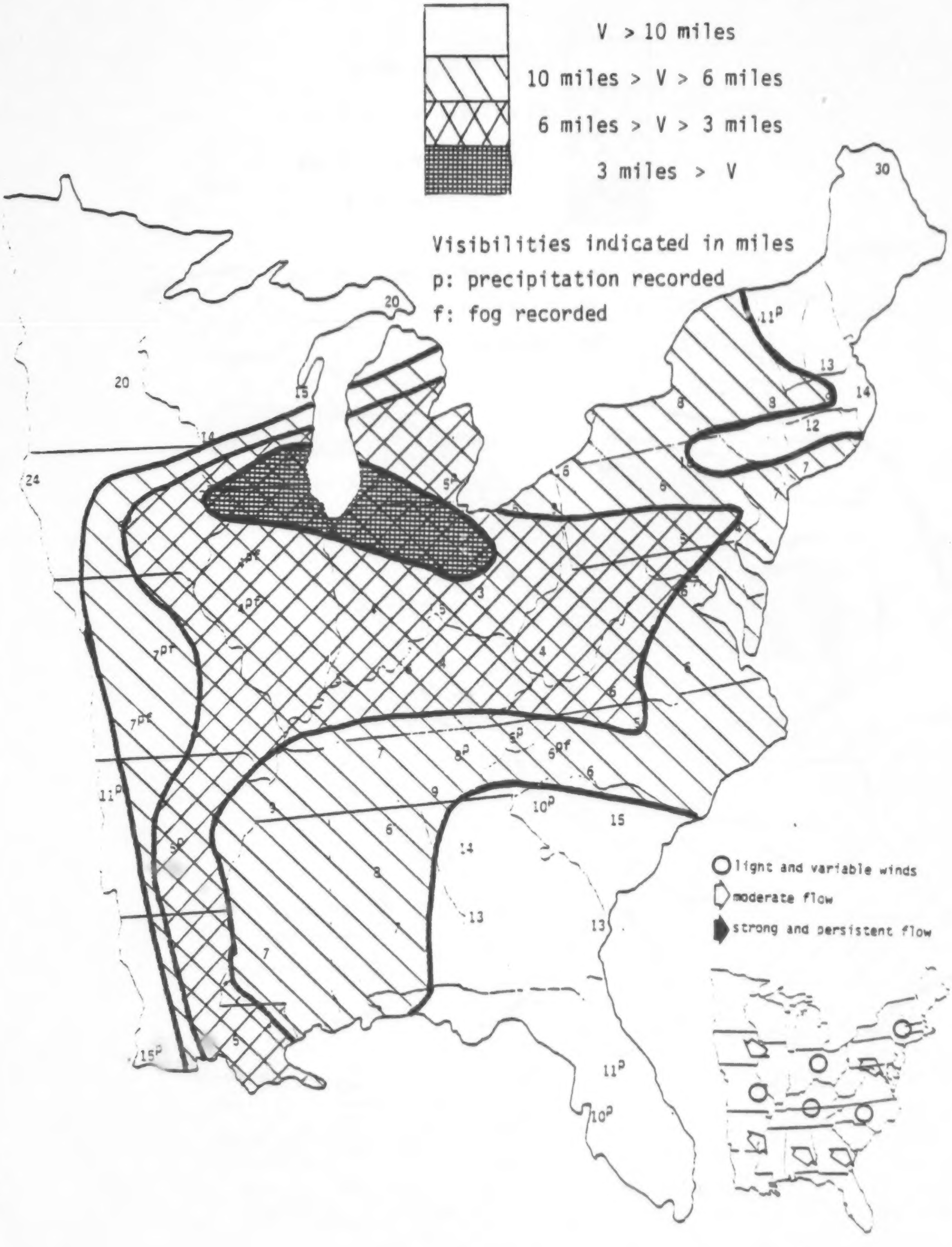
V > 10 miles
10 miles > V > 6 miles
6 miles > V > 3 miles
3 miles > V
Visibilities indicated in miles
p: precipitation recorded
f: fog recorded
light and variable winds
moderate flow
strong and persistent flow
30
20
20
15
14
24
11p
13
14
8
8
12
7
6
6
3
4
5
6
7pf
7pf
11p
5p
7
5
15p
9
6
8
14
13
13
15
10p
11p
10p

Figure 4.8c Visibility map for 26 July 1980.

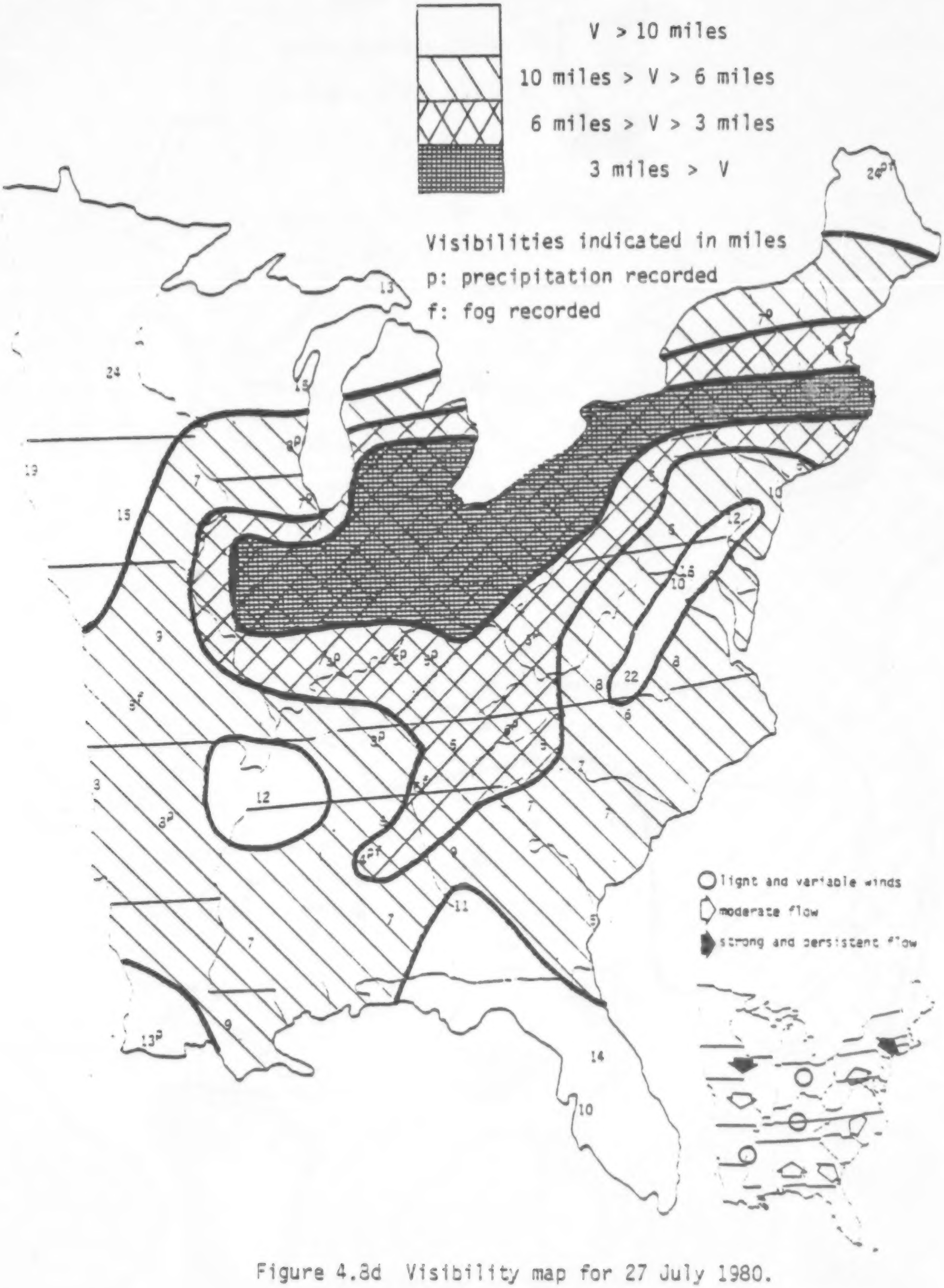
V > 10 miles
10 miles > V > 6 miles
6 miles > V > 3 miles
3 miles > V
Visibilities indicated in miles
p: precipitation recorded
f: fog recorded
light and variable winds
moderate flow
strong and persistent flow

Figure 4.8d Visibility map for 27 July 1980.

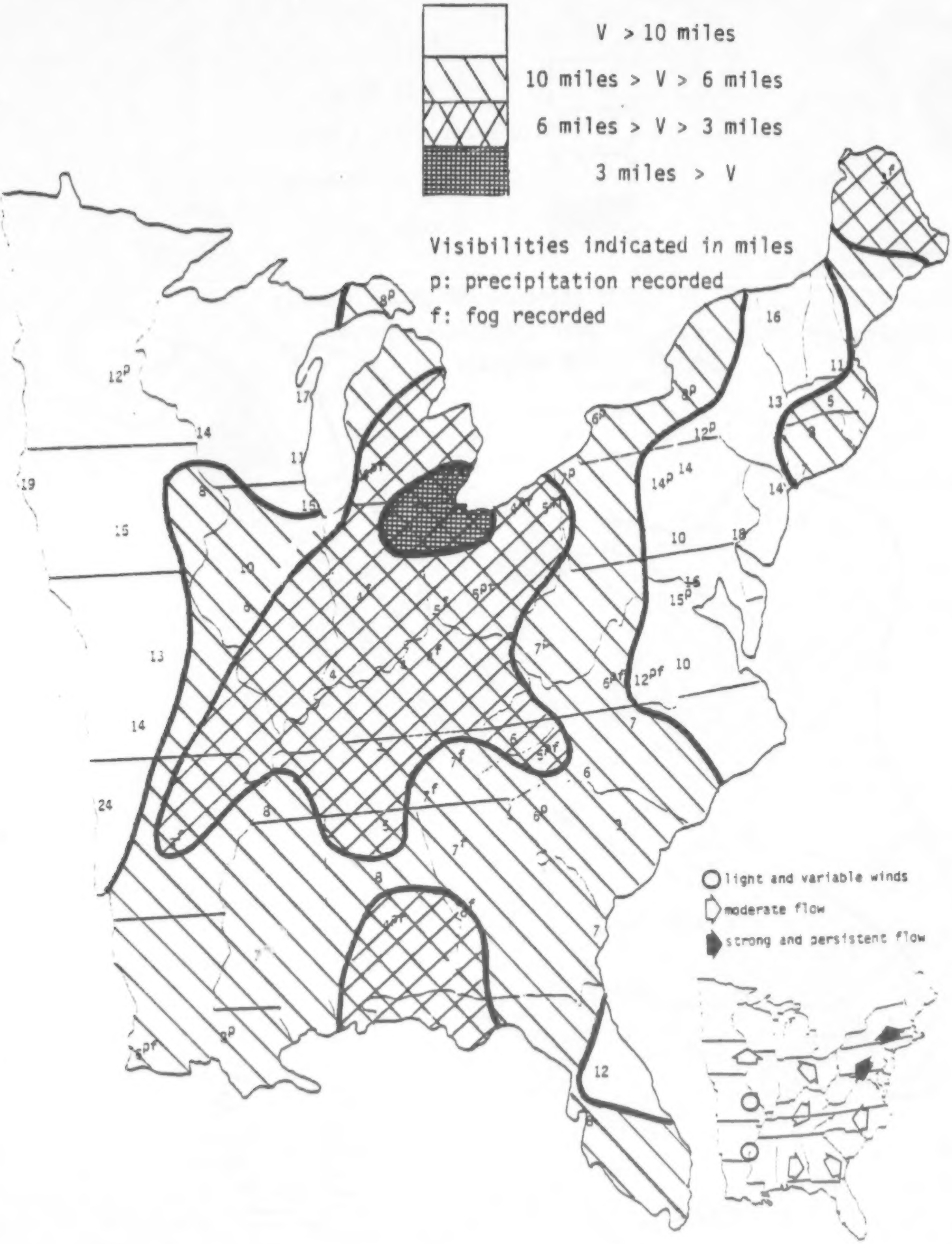
V > 10 miles
10 miles > V > 6 miles
6 miles > V > 3 miles
3 miles > V
Visibilities indicated in miles
p: precipitation recorded
f: fog recorded
light and variable winds
moderate flow
strong and persistent flow

Figure 4.8e Visibility map for 28 July 1980.

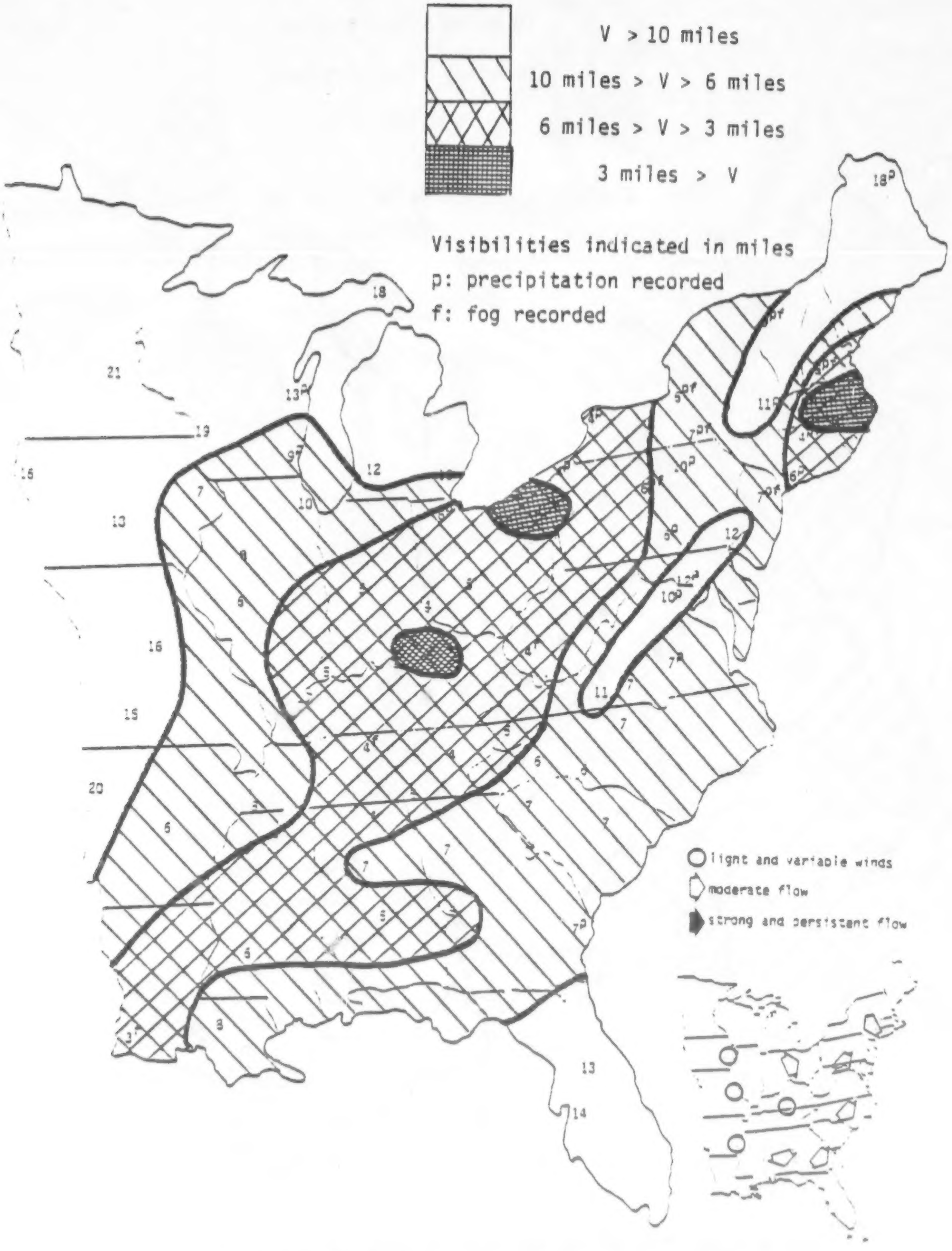
V > 10 miles
10 miles > V > 6 miles
6 miles > V > 3 miles
3 miles > V
Visibilities indicated in miles
p: precipitation recorded
f: fog recorded
light and variable winds
moderate flow
strong and persistent flow

Figure 4.8f Visibility map for 29 July 1980.

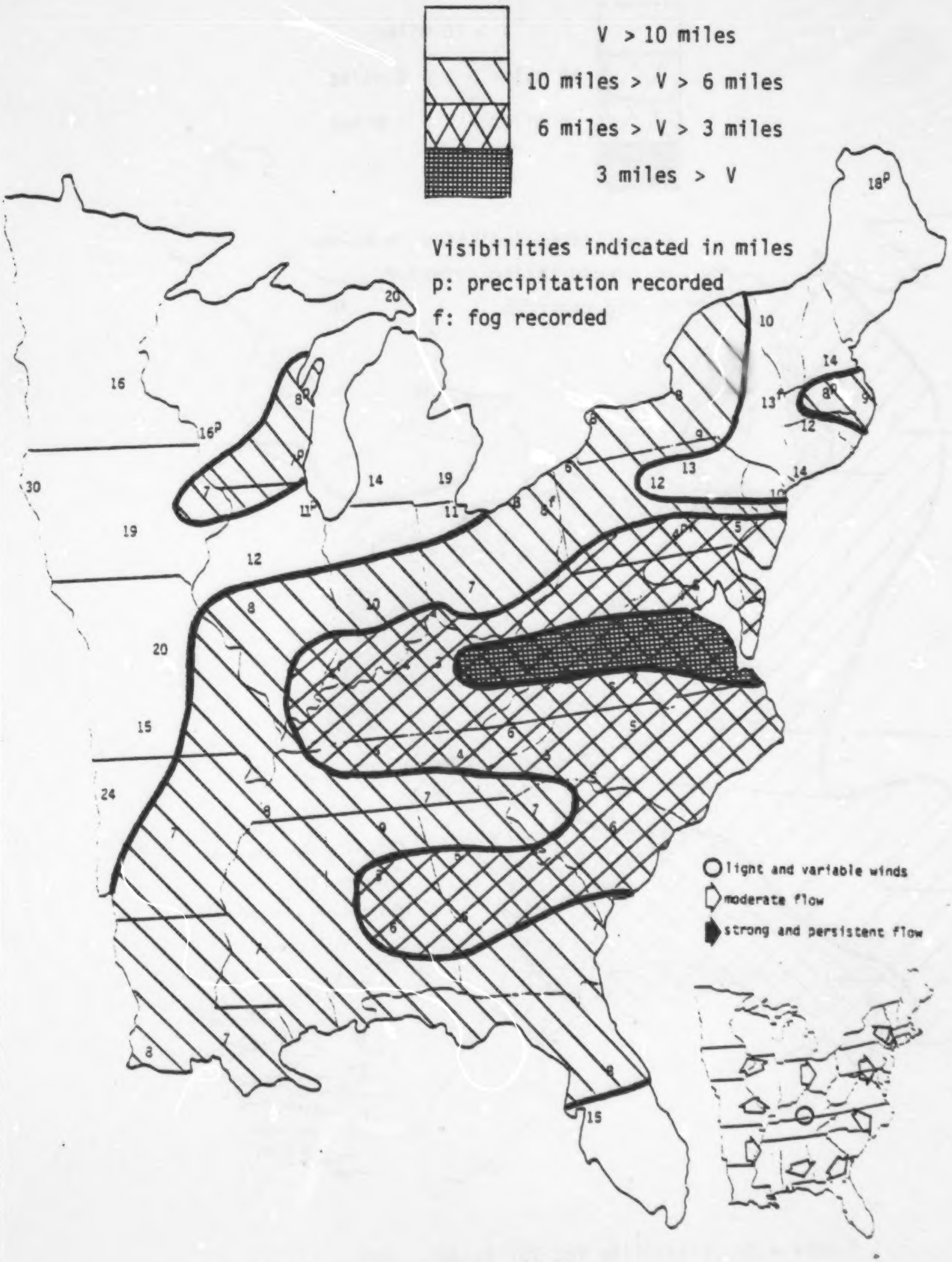
V > 10 miles
10 miles > V > 6 miles
6 miles > V > 3 miles
3 miles > V
Visibilities indicated in miles
p: precipitation recorded
f: fog recorded
18p
20
10
16
8p
14
16p
13f
8p
9
8
12
6
9
30
7
p
14
19
6
13
12
14
10
11p
11
8
8f
4p
5
19
12
7
8
10
20
15
6
5
4
6
5
24
8
7
7
7
9
5
6
6
7
8
7
8
15
light and variable winds
moderate flow
strong and persistent flow

Figure 4.8g Visibility map for 30 July 1980.

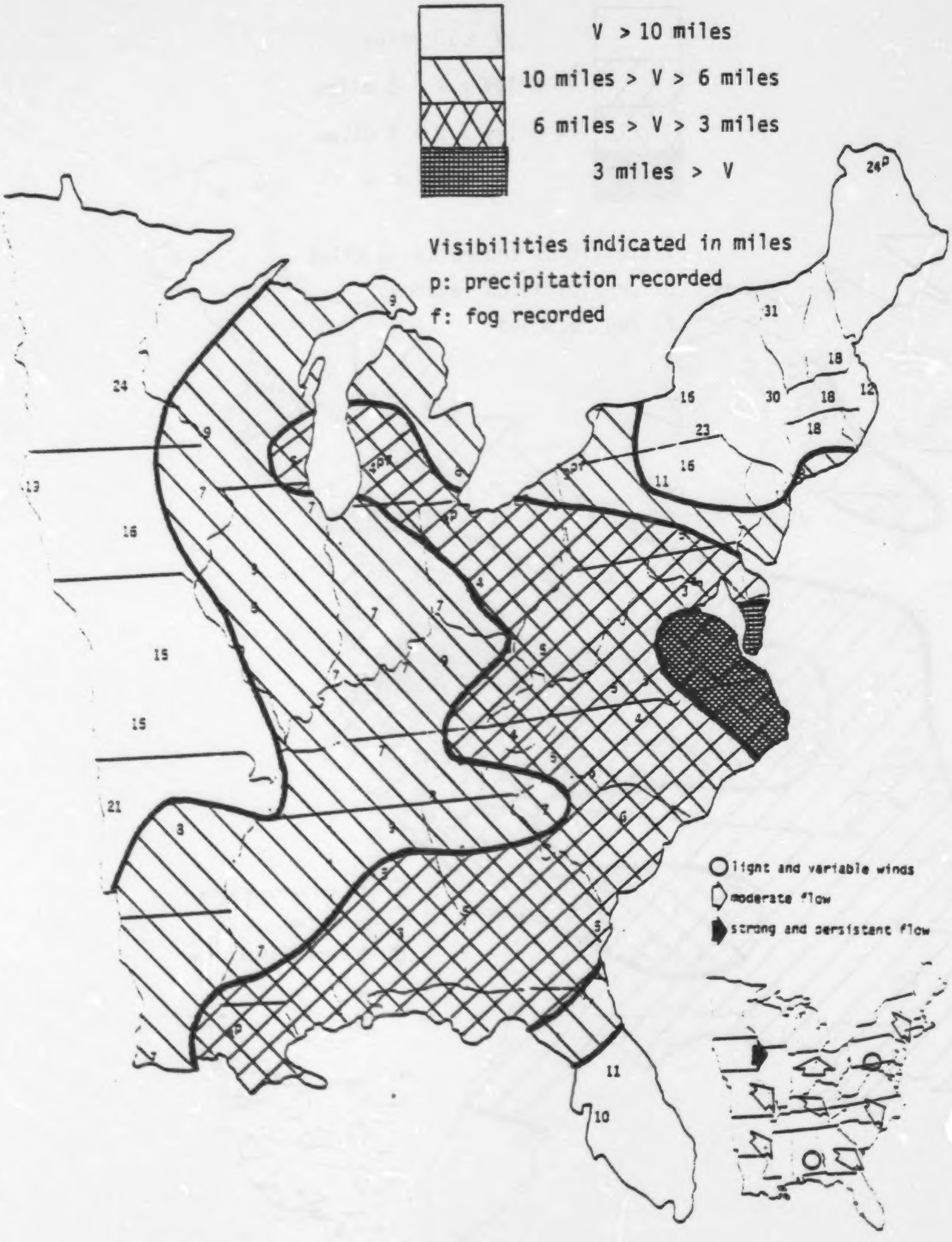
V > 10 miles
10 miles > V > 6 miles
6 miles > V > 3 miles
3 miles > V
Visibilities indicated in miles
p: precipitation recorded
f: fog recorded
light and variable winds
moderate flow
strong and persistent flow

Figure 4.8h Visibility map for 31 July 1980.

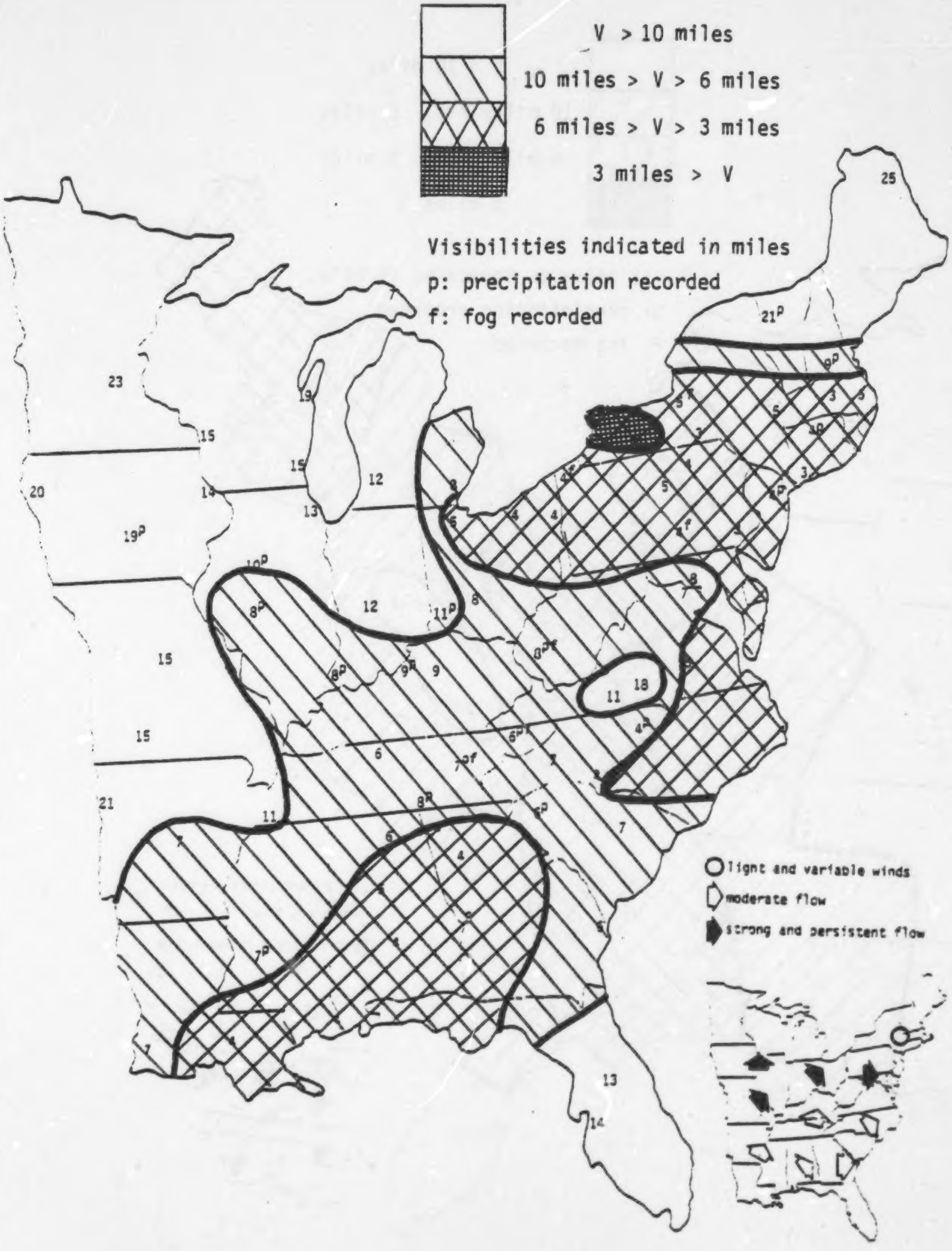
V > 10 miles
10 miles > V > 6 miles
6 miles > V > 3 miles
3 miles > V
Visibilities indicated in miles
p: precipitation recorded
f: fog recorded
light and variable winds
moderate flow
strong and persistent flow

Figure 4.8i Visibility map for 1 August 1980.

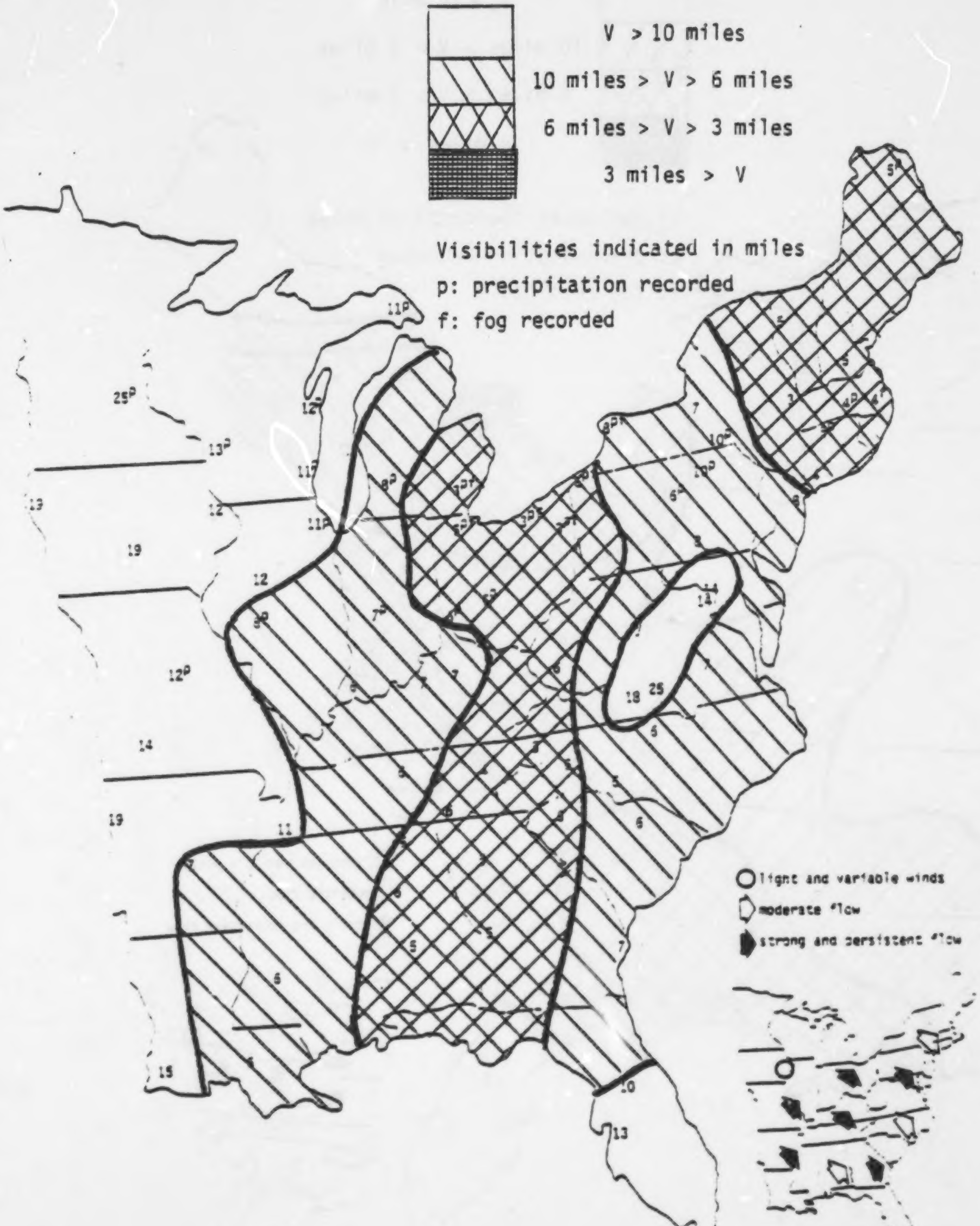
V > 10 miles
10 miles > V > 6 miles
6 miles > V > 3 miles
3 miles > V
Visibilities indicated in miles
p: precipitation recorded
f: fog recorded
light and variable winds
moderate flow
strong and persistent flow

Figure 4.8j Visibility map for 2 August 1980.

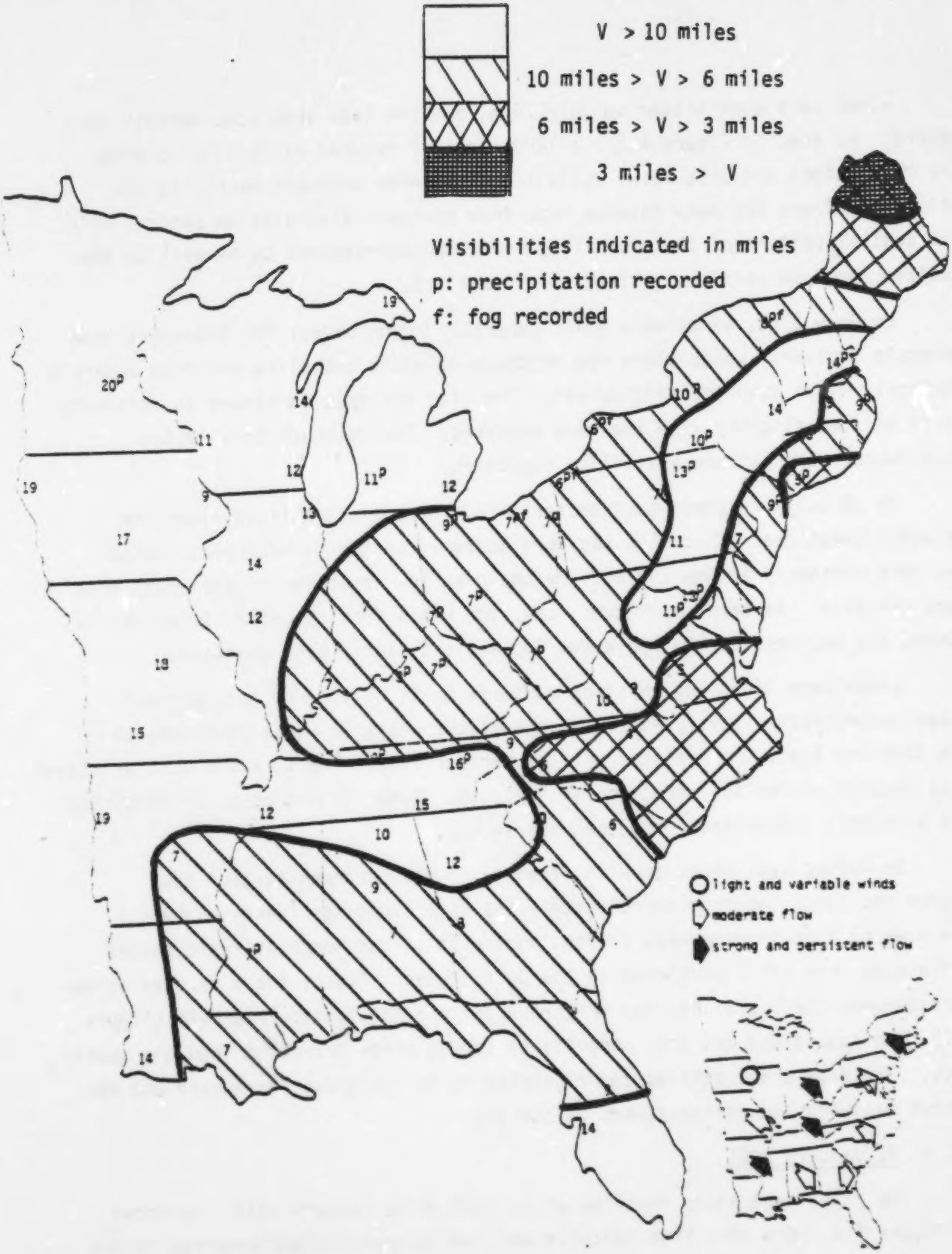
V > 10 miles
10 miles > V > 6 miles
6 miles > V > 3 miles
3 miles > V
Visibilities indicated in miles
p: precipitation recorded
f: fog recorded
light and variable winds
moderate flow
strong and persistent flow

Figure 4.8k Visibility map for 3 August 1980.

Winds were even milder on July 26th, and the haze grew considerably more severe. As seen in Figure 4.8c, a large area of reduced visibility covered the Mississippi and Ohio River Valleys and extended eastward nearly to the Atlantic. There was very intense haze from southern Wisconsin to central Ohio. The spatial pattern of the visibility reduction corresponds quite well to the sulfate and fine particle patterns of Figure 4.6.

On July 27th, winds were again generally light, except for transport from moderate southerly winds along the northern Atlantic coastline and from moderate northerly winds down the Mississippi. The hazy air mass continued to intensify as it shifted slightly with the wind patterns. The northern Ohio Valley experienced very extreme visibility reduction.

On 28 July, a strong southeasterly flow became established along the Atlantic coastline. This flow was more easterly in the mid-Atlantic States and more northerly in New England. Winds over the remainder of the study area were variable. As seen in Figure 4.8e, the winds from the Atlantic evidently pushed the haziness partly above New England and partly back westward.

Winds were light and shifting westerly on 29 July. The hazy airmass moved accordingly slightly east. As the slight westerly winds continued on the 30th and 31st, the haziness shifted further east. The 30th and 31st witnessed very intense visibility reduction in Virginia. Some, if not most, of this haze was evidently transported from the Ohio Valley.

On August 1st, winds grew in strength in the northern part of the region and continued from approximately the same direction (west-southwest). The area of most intense haze shifted northeast to the North Atlantic states while some haze still persisted in the Gulf States. Again, there is good agreement between the visibility map (Figure 4.8i) and the particulate data (Figure 4.7). On August 2nd and 3rd, moderate to strong winds prevailed from the southwest. The haze areas shifted and elongated to the northeast on August 2nd and pushed eastward and northeastward on the 3rd.

4.2.4 22 January 1981

The final case study involves an episode on 22 January 1981. As shown in Figure 4.9, very high fine particle and lead concentrations occurred in the

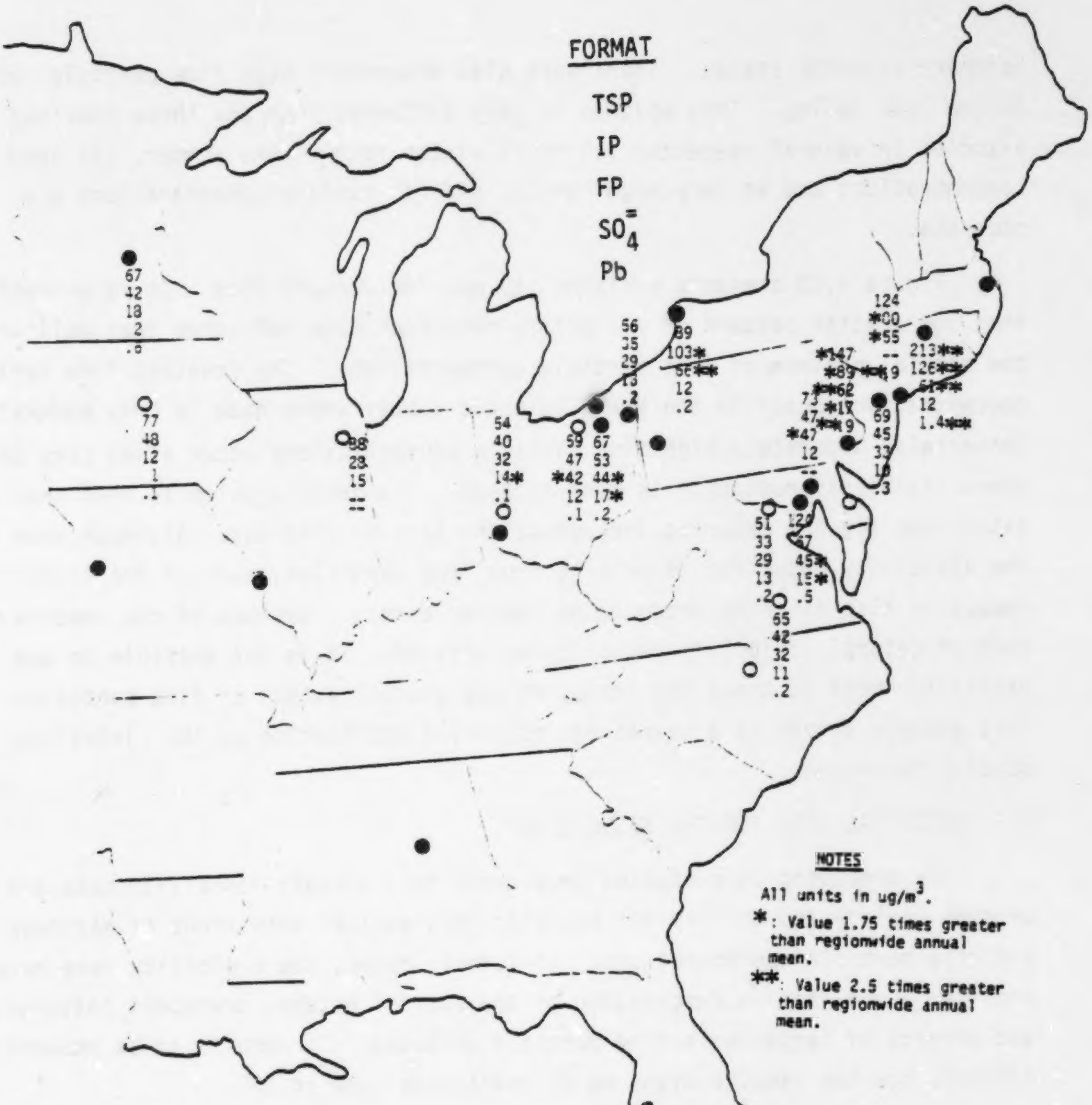
FORMAT
TSP
IP
FP
$SO_4^=$
Pb
67 42 18 2 .6
77 48 12 1 .1
88 28 15 -- --
54 40 32 14* .1
59 47 *42 12 .1
67 53 44* 17* .2
56 35 29 13 .2
89 103* 56** 12 .2
*147 *89 **62 *17 **9
73 47 *47 12 --
124 *00 *55 -- **19
69 45 33 10 .3
213** 126** 61** 12 1.4**
51 33 29 13 .2
120 67 45* 15* .5
65 42 32 11 .2
NOTES
All units in ug/m^3.
*: Value 1.75 times greater than regionwide annual mean.
**: Value 2.5 times greater than regionwide annual mean.

Figure 4.9 Particulate concentration map for 22 January 1981:

Northern Atlantic states. There were also moderately high fine particle levels in the Ohio Valley. This episode is very different from the three previous examples in several respects: (1) it is winter rather than summer, (2) lead concentrations are at very high levels, and (3) sulfate concentrations are moderate.

Figure 4.10 presents a visibility map for January 22nd. It is evident that the spatial pattern of visibility reduction does not agree that well with the spatial pattern of fine particle concentrations. The greatest fine particle concentrations occur in the North Atlantic states where haze is only moderate. Conversely, moderately high fine particle concentrations occur along Lake Erie where visibility reduction is very intense. The basic problem is that precipitation and fog are occuring throughout the East on this day. Although some of the visibility reduction is arising from fine particles, much of the visibility reduction also is being produced by weather events. Because of the important role of natural visibility reduction on this day, it is not possible to use visibility maps to trace the transport and spatial extent of fine particles. This example serves as a caveat against blind application of the visibility mapping technique.

4.3 POTENTIAL USES FOR THE METHODOLOGY

The preceding case studies have shown that airport visibility data are of good quality and utility for studying geographical variations of haziness and fine particle concentrations. In several cases, the visibility data have provided a qualitative description of the spatial extent, transport patterns, and origins of large-scale fine particle episodes. It remains to be answered, however, how the results might be of operational use to EPA.

One potential use of the approach is to establish the general necessity for interstate considerations in control regulations for fine particles or sulfates. Based upon our results and other previously cited publications, it is evident that sulfates and fine particles can accumulate and transport on a spatial scale that far transcends state boundaries. Controlling fine particles and sulfates requires a large-scale regional policy.

The approach may also be useful in some specific circumstances. One example involves regulations to achieve short term standards for fine or

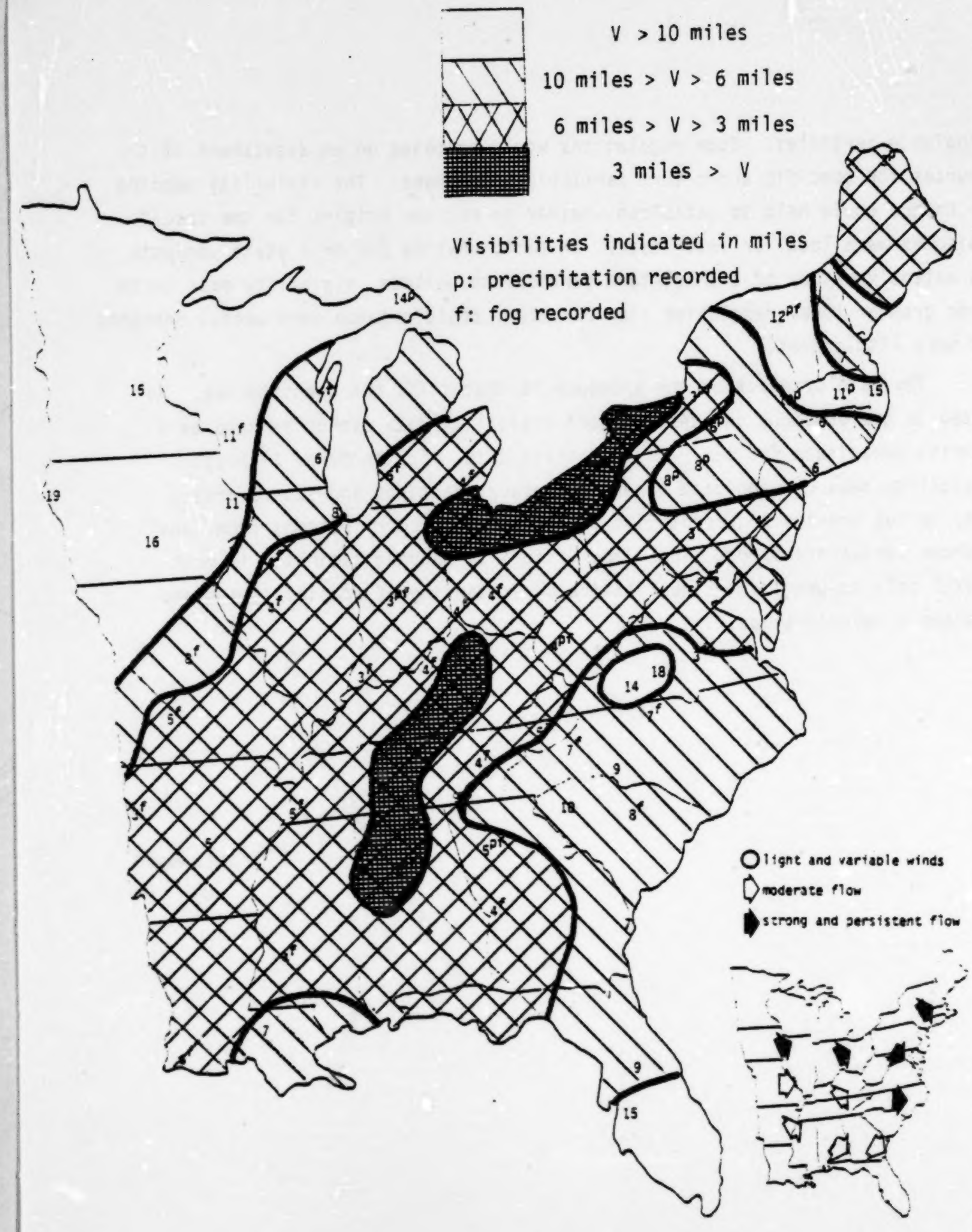
V > 10 miles
10 miles > V > 6 miles
6 miles > V > 3 miles
3 miles > V
Visibilities indicated in miles
p: precipitation recorded
f: fog recorded
light and variable winds
moderate flow
strong and persistent flow

Figure 4.10 Visibility map for 22 January 1981.

inhalable particles. Such regulations would be based on an assessment of the sources for specific short term particulate episodes. The visibility mapping technique could help to establish whether or not the origins for the specific episodes were local or interstate. In fact, anytime EPA or a state conducts an extensive study of a short-term particulate episode, visibility maps (with even greater local resolution than our maps) could provide very useful insights at very little cost.

The main drawback of the approach is that it is not quantitative. As noted in the previous chapter, airport visibility data cannot be used as a precise substitute for daily fine particle data. Furthermore, although visibility maps can indicate general transport patterns and source areas, they do not provide a quantitative breakdown as to contributions from local sources versus transport. Thus, the visibility mapping technique is most useful only in providing a qualitative understanding of spatial scales and transport relationships.

5. REFERENCES

Allard, D. and I. Tombach, "Evaluation of Visibility Measurement Methods in Eastern United States," Presented at the 73rd Annual Meeting of the Air Pollution Control Association, Montreal, June 22-27, 1980.

Cass, G.R., "On the Relationship Between Sulfate Air Quality and Visibility With Examples in Los Angeles," Atmospheric Environment, Vol. 13, pp. 1069-1084, 1979.

Cass, G.R., P.M. Boone, E.S. Macias, "Emission and Air Quality Relationships for Atmospheric Carbon Particles in Los Angeles," in Particulate Carbon: Atmospheric Life Cycle, G.T. Wolff, R.L. Klimisch, eds., Plenum Press, New York, 1981.

Conklin, M.C., Cass, G.R., Chu L-C, and Macias, E.S., "Wintertime Carbonaceous Aerosols in Los Angeles, An Exploration of the Role of Elemental Carbon," in Atmospheric Aerosol: Source/Air Quality Relationships, eds. Macias, E.S. and Hopke, P.K., ACS Symposium Series, 167, American Chemical Society, Washington, D.C., 1981.

Countess, R.J., S.H. Cadle, P.J. Groblicki, and G.T. Wolff, "Chemical Analysis of Size-Segregated Samples of Denver's Ambient Particulate," Journal of the Air Pollution Control Association, 31, pp. 247-252, 1981.

Covert, D.S., R.J. Charlson, and N.C. Ahlquist, "A Study of the Relationship of Chemical Composition and Humidity to Light-Scattering by Aerosols," Journal of Applied Meteorology, 11, pp. 968-976, 1972.

Douglas, C.A and L.L. Young, "Development of a Transmissometer for Determining Visual Range, " U.S. C.A.A. Technical Development Report No. 47, 1945.

EPA, "National Emissions Report for 1973," EPA 450/2-76/007, Research Triangle Park, North Carolina, 1976.

EPA, "Review of the National Ambient Air Quality Standards for Particulate Matter: Assessment of Scientific and Technical Information," EPA 450/5-82-001, Research Triangle Park, North Carolina, January 1982.

Faxvog, F.R. and D.M. Roessler, "Carbon Aerosol Visibility Vs. Particle Size Distribution," Applied Optics, Vol. 17, 1978.

Ferman, M.A., G.T. Wolff, and N.A. Kelly, "The Nature and Sources of Haze in the Shenandoah Valley/Blue Ridge Mountains Area," Journal of the Air Pollution Control Association, 1981.

Groblicki, P.J. et al., "Visibility-Reducing Species in the Denver 'Brown Cloud', Part I: Relationships Between Extinction and Chemical Composition," Presented at the Symposium on Visibility": Measurements and Model Components, Grand Canyon, November 10-14, 1980.

Hidy, G.M. et al., "Characterization of Aerosols in California," Rockwell International Science Center Report, California Air Resources Board, Contract No. 358, 1974.

Ho, W.W., G.M. Hidy, and R.M. Govan, "Microwave Measurements of the Liquid Water Content of Atmospheric Aerosols," Journal of Applied Meteorology, 13, pp. 871-879, 1974.

Husar, R.B. et al., "Trends of Eastern U.S. Haziness Since 1948," Presented at the 4th Symposium on Atmospheric Turbulence, Diffusion and Air Pollution, Reno, Nevada, January 15-18, 1979.

Husar, R.B., N.V. Gillani, J.D. Husar, and D.R. Patterson, "A Study of Long Range Transport from Visibility Observations, Trajectory Analysis and Local Air Pollution Monitoring Data," Presented at the 7th International Technical Meeting on Air Pollution Modeling and its Application, Sept. 1976a.

Husar, R.B., D.E. Patterson, C.C. Paley, N.V. Gillani, "Ozone in Hazy Air Masses," Presented at the International Conference on Photochemical Oxidant and its Control, Raleigh, N.C., Sept. 12-17, 1976b.

Latimer, D.A., R.W. Bergstrom, S.R. Hayes, M.T. Liu, J.H. Seinfeld, G.F. Whitten, M.A. Wojcik, and M.J. Hillyer, "The Development of Mathematical Models for the Prediction of Atmospheric Visibility Impairment," EPA-450/3-78-110a,b,c, 1978.

Leaderer, B.P. and J.A. Stolwijk, "Optical Properties of Urban Aerosol and Their Relation to Chemical Composition," Presented at the New York Academy of Science Symposium on Aerosols: Anthropogenic and Natural Sources and Transport, January 9-12, 1979.

Malm, Wm. C., "Visibility: A Physical Perspective," Proceedings of the Workshop in Visibility Values, Fort Collins, Colorado, January 28-February 1, 1979.

Malm, Wm. C., M.L. Pitchford, and S.F. Archer, "Comparison of Electro-Optical Measurements Made by Various Visibility Monitoring Instruments," Proceedings of Conference on View on Visibility -- Regulatory and Scientific, pp. 222-231, 1979.

Martinez, E.L., EPA Office of Air Quality Planning and Standards, Personal Communication, January 1983.

NRC (National Research Council), Sulfur Oxides, National Research Council, National Academy of Sciences, Washington, D.C., 1978.

NOAA (National Oceanic and Atmospheric Administration), Climatic Atlas of the United States, National Climatic Center, Asheville, NC, 1977.

Ouimette, J.R., Chemical Species Contributions to the Extinction Coefficient, Ph.D. Thesis, California Institute of Technology, Pasadena, California, 1981.

Pierson, W.R., W.W. Brachaczek, T.J. Truex, J.W. Butler, and T.J. Korinski, "Ambient Sulfate Measurements on Allegheny Mountain and the Question of Atmospheric Sulfate in the Northeastern United States," Annals of the New York Academy of Sciences, 338, pp. 145-173, 1980.

Pitchford, M., "The Relationship of Regional Visibility to Coarse and Fine Particle Concentration in the Southwest," Journal of the Air Pollution Control Association, pp. 814-821, August 1982.

Rodes, C., Personal Communication, U.S. Environmental Protection Agency, Research Triangle Park, North Carolina, 1981.

Stelson, A.W. and J.H. Seinfeld, "Chemical Mass Accounting of Urban Aerosol," Envir. Sci. Techno., 15, pp. 671-679 , 1981.

Tang, I.N., "Deliquescence Properties and Particle Size Change of Hygroscopic Aerosols," Generation of Aerosols and Facilities for Exposure Experiments, Ann Arbor Science Publishers Inc., Ann Arbor, Michigan, 1981.

Trijonis, J., "Existing and Natural Background Levels of Visibility and Fine Particles in the Rural East," Atmospheric Environment, Volume 16, pp. 2431-2445, 1982a.

Trijonis, J.,"Impact of Light-Duty Diesels on Visibility in California," Journal of Air Pollution Control Association, October, 1982b.

Trijonis, J. "Effect of Diesel Vehicles on Visibility in California," prepared under contract A2-072-21 for the California Air Resources Board, 1983a.

Trijonis, J.,"Development and Application of Methods for Estimating Inhalable and Fine Particle Concentrations from Routine Hi-Vol Data," Atmospheric Environment, Volume 17, pp. 999-1008, 1983b.

Trijonis, J., "Visibility in California," Journal of the Air Pollution Control Association, February, 1982c.

Trijonis, J., "Visibility in California," prepared under contract A7-181-30 for the California Air Resources Board, 1980.

Trijonis, J., "Visibility in the Southwest - An Exploration of the Historical Data Base," Atmospheric Environment, Vol. 13, pp. 833-843, 1979.

Trijonis, J., G. Cass, G. McRae, Y. Horie, W. Lim, N. Chang, and T. Cahill, "Analysis of Visibility/Aerosol Relationships and Visibility Modeling/ Monitoring Alternatives for California," prepared under Contract #A9-103-31 for the California Air Resources Board, 1982.

Trijonis, J. and M. Davis, "Development and Application of Methods for Estimating Inhalable and Fine Particle Concentrations from Routine Hi-Vol Data," prepared under Contract #A0-076-32 for the California Air Resources Board, 1981.

Trijonis,J. and D. Shapland, "Existing Visibility Levels in the U.S., Isopleth Maps of Visibility in Suburban/Nonurban Areas During 1974-1976," EPA-450/5-79-010, 1979.

Trijonis, J. and K. Yuan, "Visibility in the Northeast: Long-Term Visibility Trends and Visibility/Pollutant Relationships," EPA-600/3-78-075, 1978.

Weiss, R.E. and A.P. Waggoner, "The Importance of Aerosol Absorption and Graphitic Carbon in Visibility and Atmospheric Optics," Presented at the 74th Annual Meeting of the Air Pollution Control Association, Philadelphia, Pennsylvania, June 21-26, 1981.

White, W.H. ed., "Plumes and Visibility: Measurements and Model Components," Atmospheric Environment (Special Issue, 15-10/11, pp. 1785-2406, 1981.

White, W.H. and P.T. Roberts, "On the Nature and Origins of Visibility-Reducing Aerosols in the Los Angeles Air Basin," Atmospheric Environment Vol. 11, p. 803, 1977.

Williamson, S.J., Fundamentals of Air Pollution, Addison Wesley, Reading, Massachusetts, 1973.

Wolff, G.T., R.J. Countess, P.J. Groblicki, M.A. Ferman, C.H. Cadel, and J.L. Mulbaer, "Visibility Reducing Species in Denver Brown Cloud, Part II, Sources and Temporal Patterns," General Motors Research Laboratory Publication GMR-3391, 1980.

APPENDIX A

PARTICULATE CONCENTRATION MAPS FOR THE EPA IP NETWORK

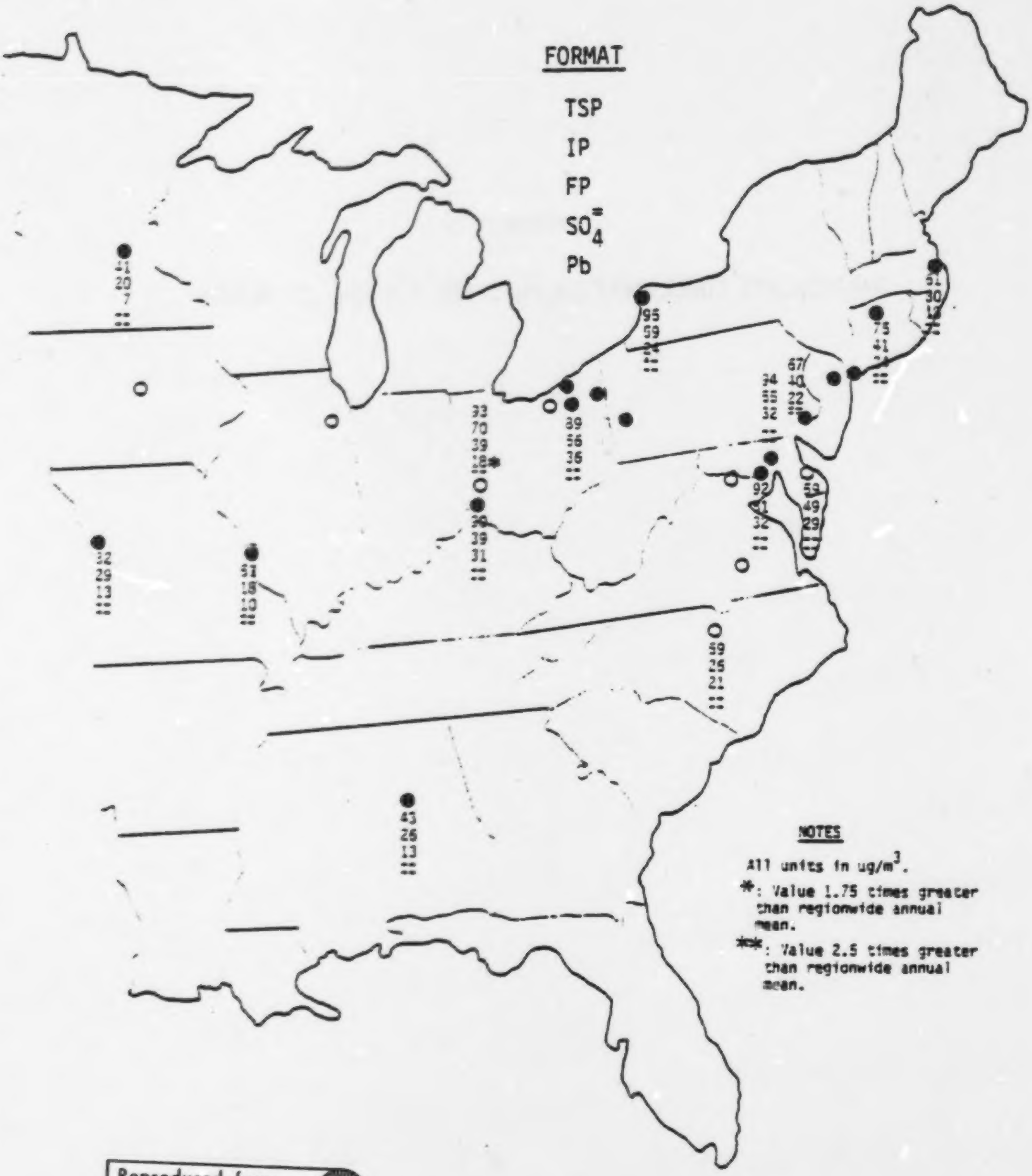
41
20
7
--
95
59
24
--
33
70
39
18*
--
39
56
36
--
30
39
31
--
32
29
13
--
51
18
10
--
34
55
32
--
67
40
22
--
75
41
24
--
51
30
12
--
92
41
32
--
53
49
29
--
59
25
21
--
43
26
13
--

FORMAT

TSP
IP
FP
$SO_4^=$
Pb

NOTES

All units in ug/m^3.

*: Value 1.75 times greater than regionwide annual mean.

**: Value 2.5 times greater than regionwide annual mean.

Reproduced from best available copy.

3 April 1980

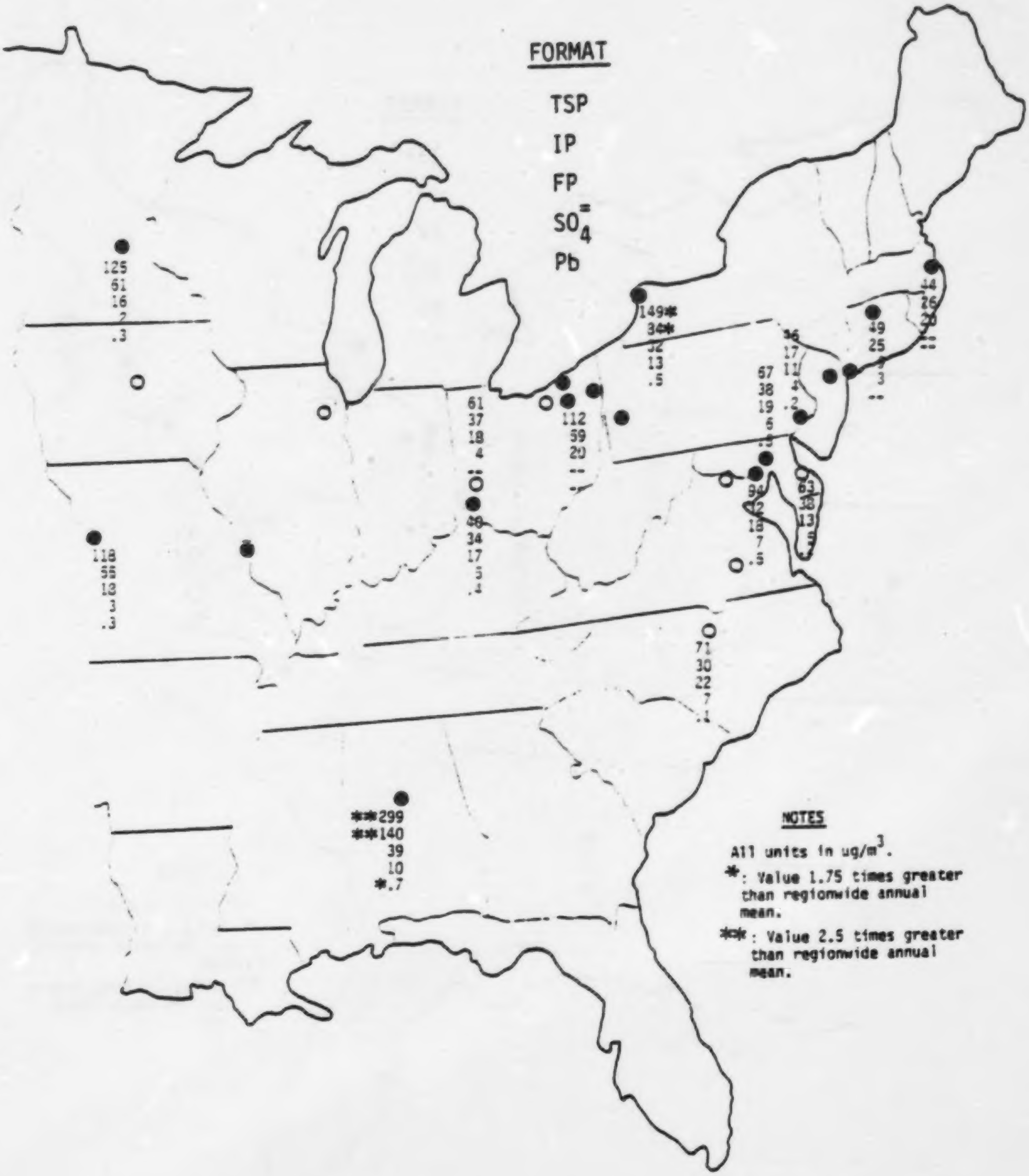
125
61
16
2
.3
61
37
18
4
149*
34*
32
13
.5
112
59
20
--
--
36
17
11
4
.2
67
38
19
6
.5
49
25
9
3
--
44
26
20
--
--
40
34
17
5
.4
118
55
18
3
.3
94
42
18
7
.5
63
38
13
5
71
30
22
7
.1
**299
**140
39
10
*.7

FORMAT

TSP
IP
FP
$SO_4^=$
Pb

NOTES

All units in ug/m^3.

*: Value 1.75 times greater than regionwide annual mean.

**: Value 2.5 times greater than regionwide annual mean.

21 April 1980

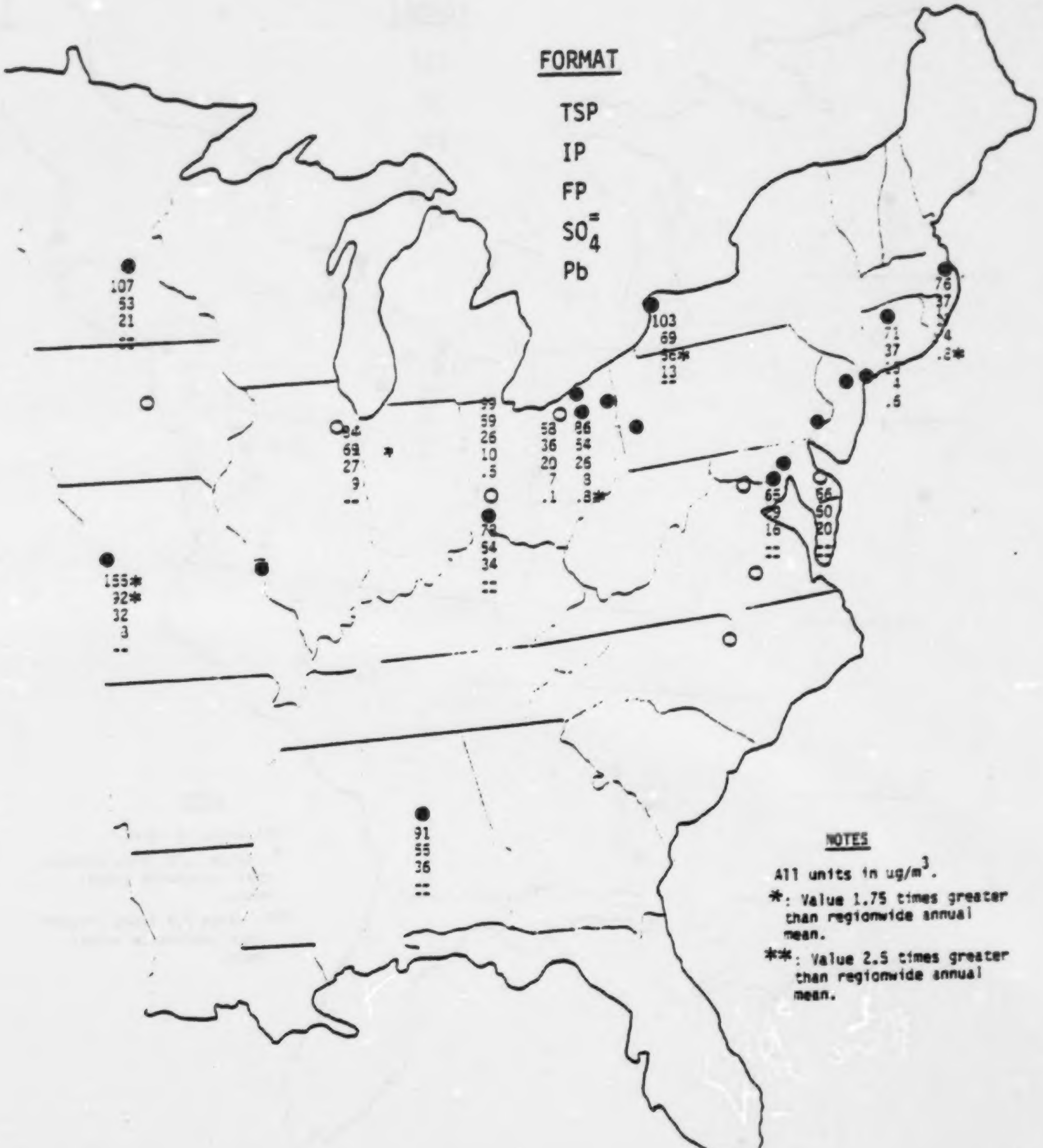
FORMAT
TSP
IP
FP
$SO_4^=$
Pb
107
53
21
155*
92*
32
3
64
69
27
9
99
59
26
10
.5
72
54
34
58
36
20
7
.1
86
54
26
8
.8*
103
69
36*
13
65
16
66
50
20
71
37
4
.6
76
37
4
.2*
91
55
36

NOTES

All units in ug/m^3.

*: Value 1.75 times greater than regionwide annual mean.

**: Value 2.5 times greater than regionwide annual mean.

3 May 1980

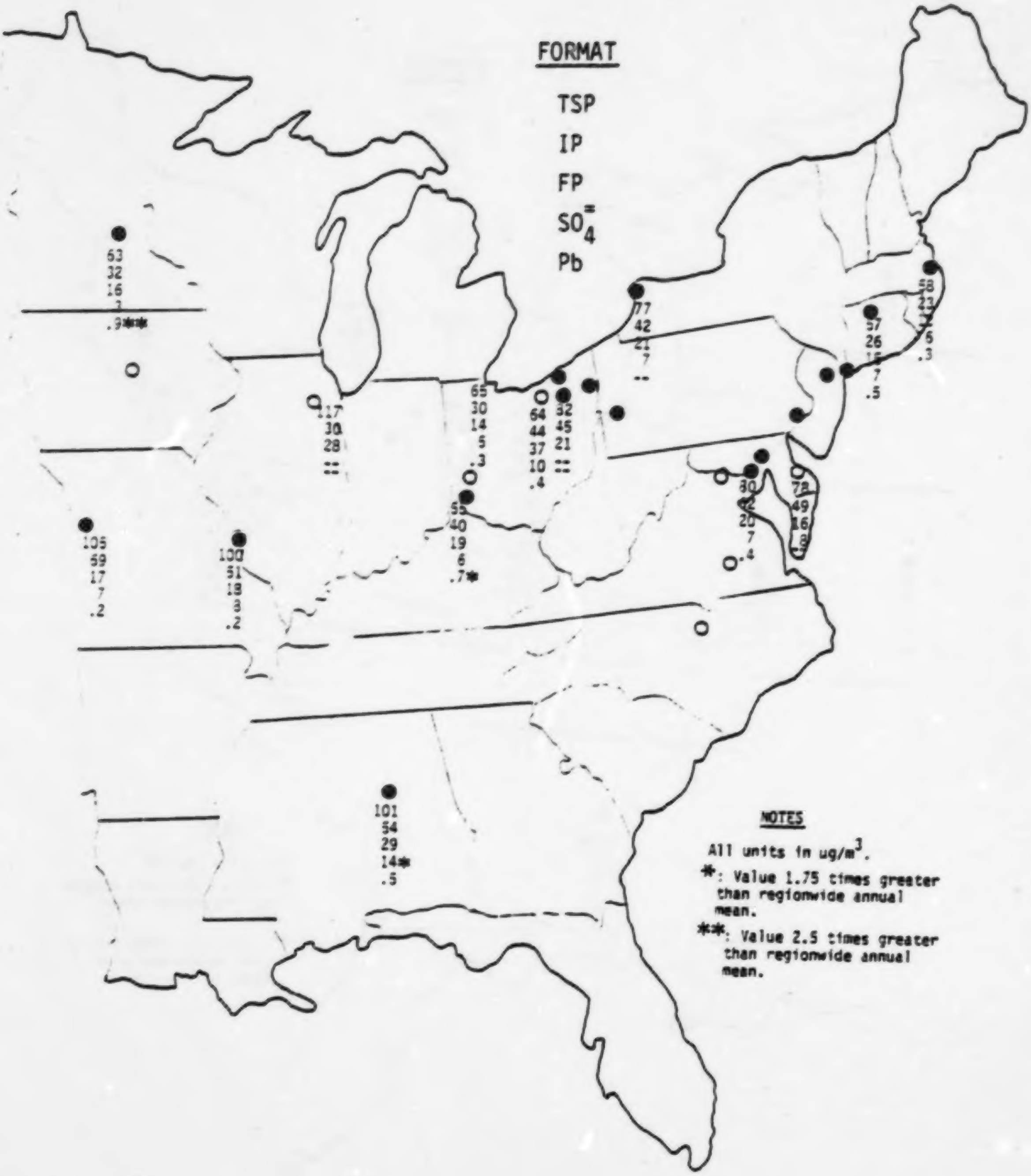
63
32
16
3
.9**
117
30
28
--
65
30
14
5
.3
64
44
37
10
.4
32
45
21
--
77
42
21
7
--
58
23
[illegible]
6
.3
57
26
16
7
.5
80
42
20
7
.4
78
49
16
8
105
59
17
7
.2
100
51
18
3
.2
55
40
19
6
.7*
101
54
29
14*
.5

FORMAT

TSP
IP
FP
$SO_4^=$
Pb

NOTES

All units in ug/m^3.

*: Value 1.75 times greater than regionwide annual mean.

**: Value 2.5 times greater than regionwide annual mean.

15 May 1980

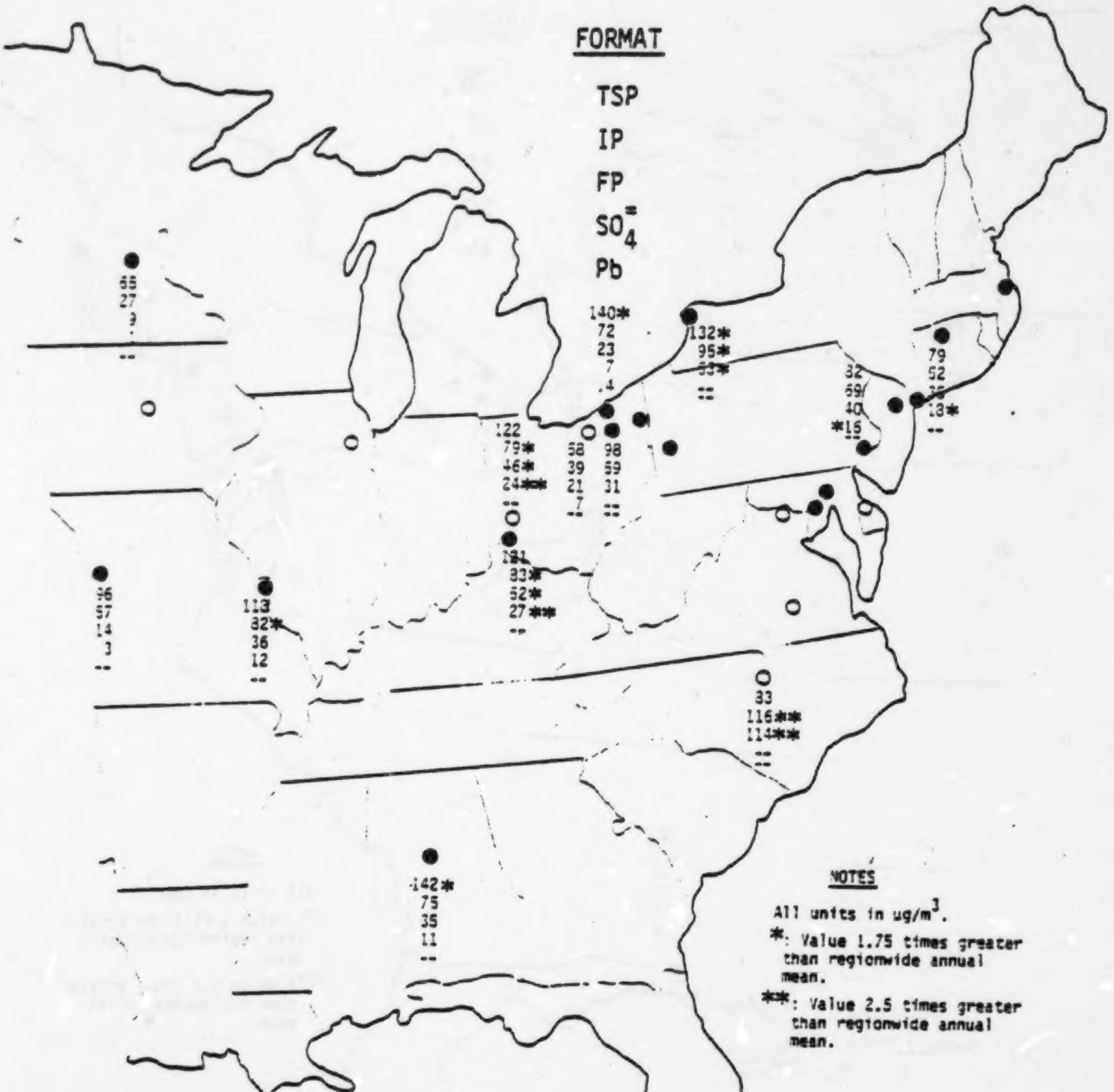
FORMAT
TSP
IP
FP
$SO_4^=$
Pb
69
27
9
--
140*
72
23
7
.4
132*
95*
53*
--
122
79*
46*
24**
--
58
39
21
7
--
98
59
31
--
32
69
40
*15
--
79
52
35
18*
--
96
57
14
3
--
113
82*
36
12
--
131
83*
52*
27**
--
33
116**
114**
--
142*
75
35
11
--

NOTES

All units in ug/m^3.

*: Value 1.75 times greater than regionwide annual mean.

**: Value 2.5 times greater than regionwide annual mean.

2 July 1980

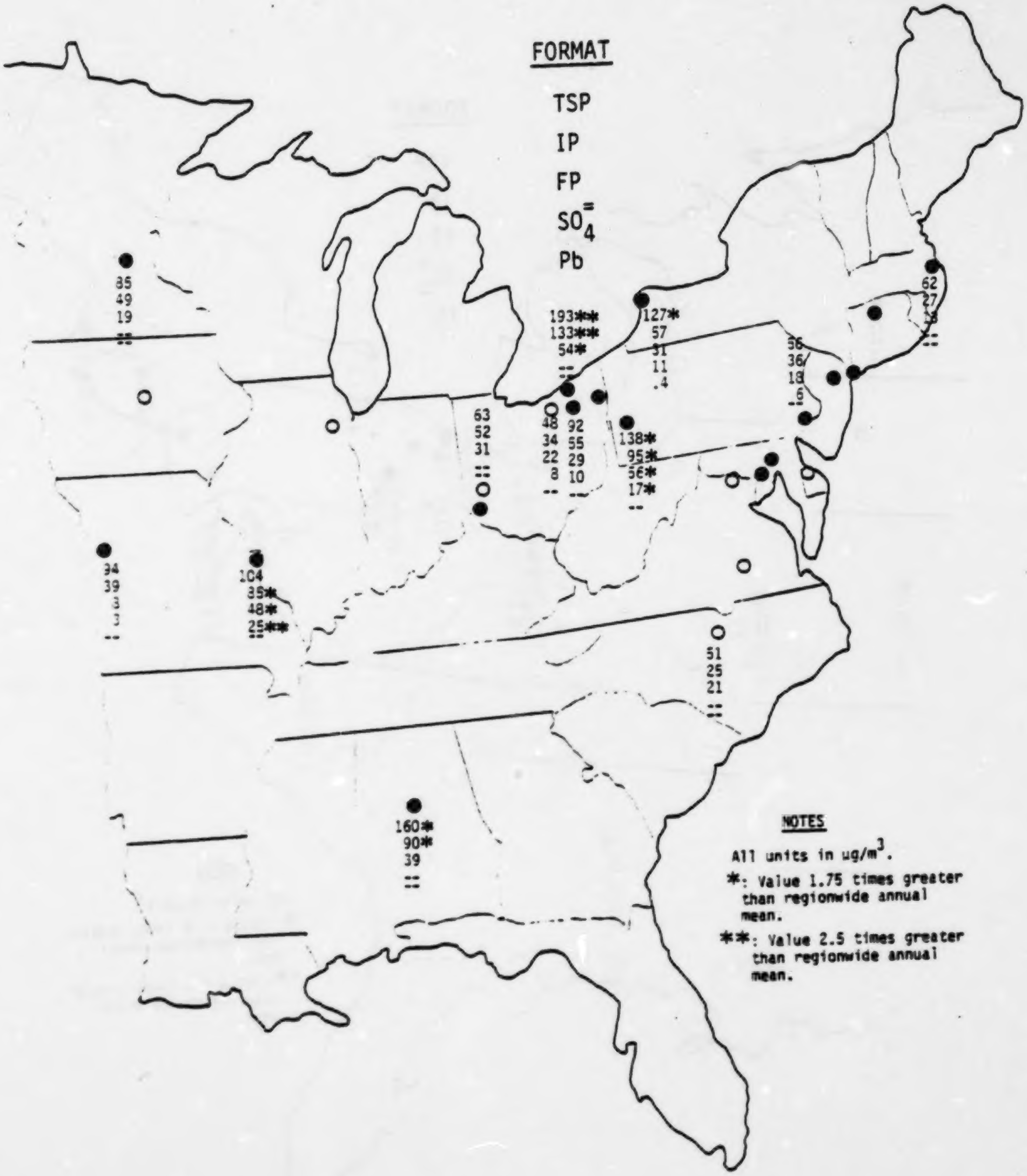
FORMAT
TSP
IP
FP
$SO_4^{=}$
Pb
85 49 19 --
193** 133** 54* --
127* 57 31 11 .4
56 36 18 6 --
62 27 13 --
63 52 31 --
48 34 22 8 --
92 55 29 10 --
138* 95* 56* 17* --
94 39 3 3 --
104 35* 48* 25** --
51 25 21 --
160* 90* 39 --

NOTES

All units in ug/m^3.

*: Value 1.75 times greater than regionwide annual mean.

**: Value 2.5 times greater than regionwide annual mean.

14 July 1980

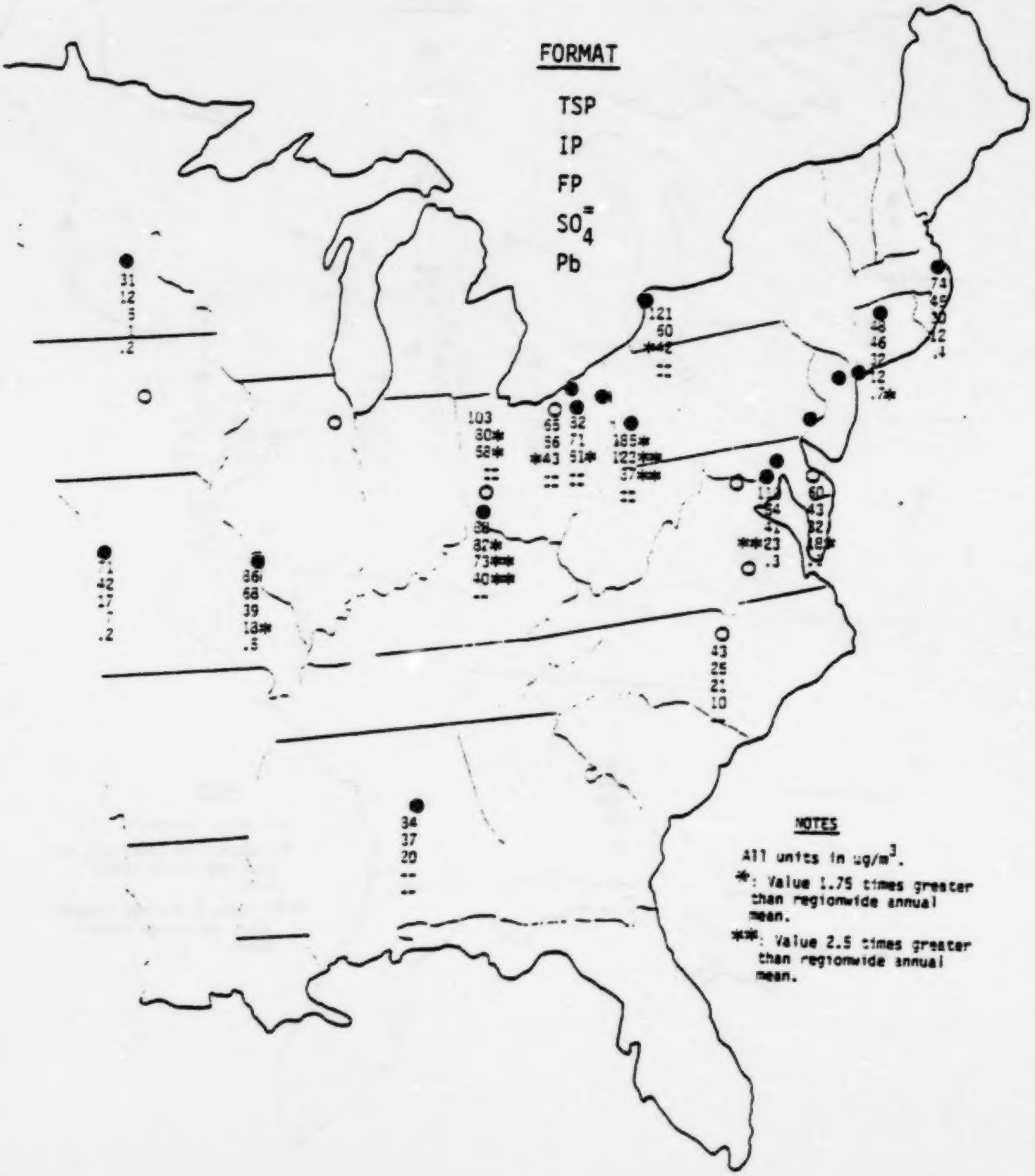
FORMAT
TSP
IP
FP
SO$_4^=$
Pb
31
12
5
.2
121
60
*42
--
--
74
45
30
12
.4
48
46
32
12
.7*
103
30*
52*
--
--
65
56
*43
--
--
32
71
51*
--
--
185*
123**
37**
--
--
88
82*
73**
40**
--
42
17
.2
86
68
39
18*
.5
54
**23
.3
60
43
32
18*
43
25
21
10
34
37
20
--
--

NOTES

All units in ug/m^3.

*: Value 1.75 times greater than regionwide annual mean.

**: Value 2.5 times greater than regionwide annual mean.

26 July 1980

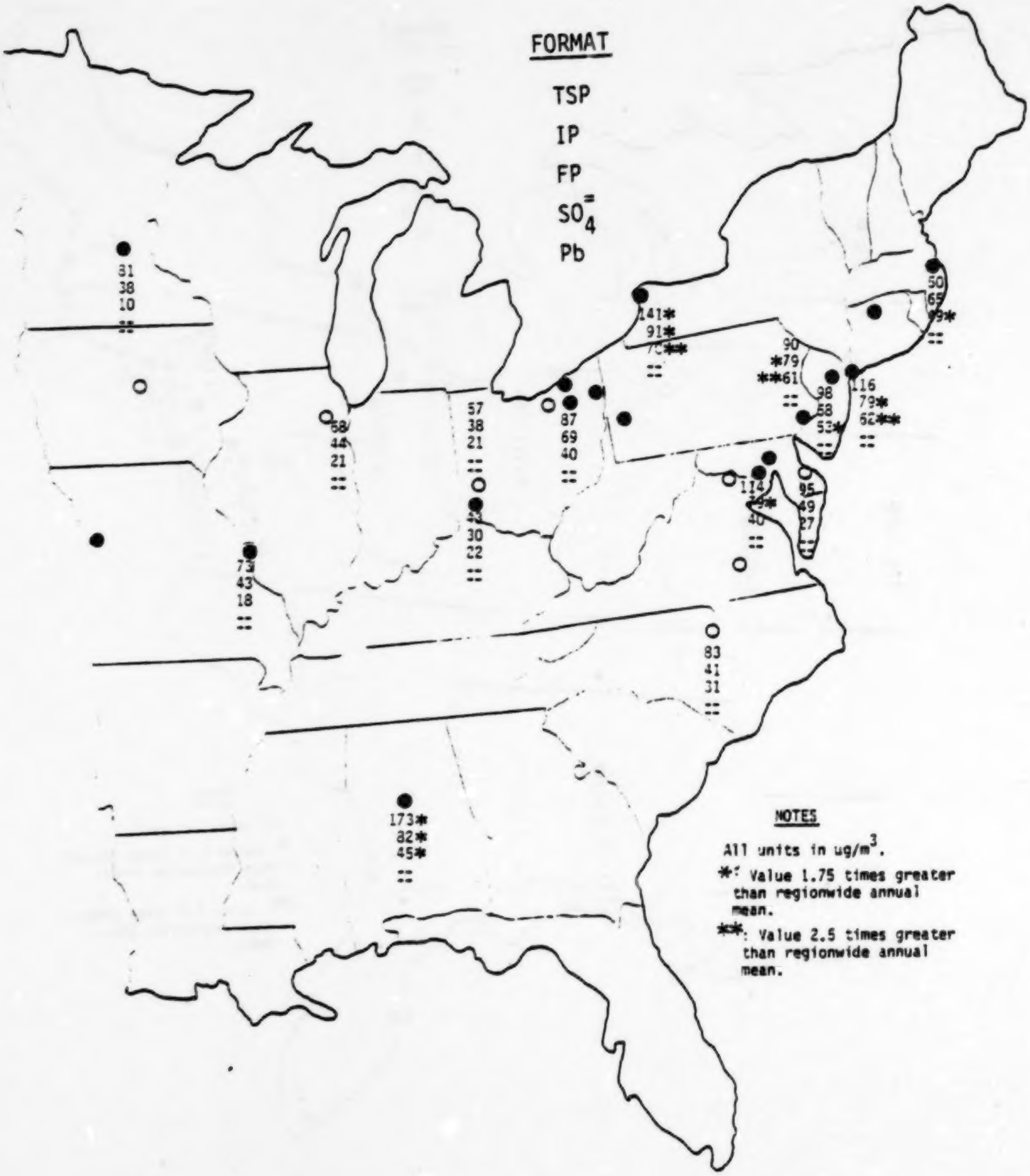
FORMAT
TSP
IP
FP
$SO_4^=$
Pb
81 38 10 ::
58 44 21 ::
57 38 21 ::
87 69 40 ::
141* 91* 75** ::
90 *79 **61 ::
98 58 53* ::
116 79* 62** ::
50 65 69* ::
114 79* 40 ::
95 49 27 ::
43 30 22 ::
73 43 18 ::
83 41 31 ::
173* 82* 45* ::

NOTES

All units in ug/m^3.

*: Value 1.75 times greater than regionwide annual mean.

**: Value 2.5 times greater than regionwide annual mean.

August 1 1980

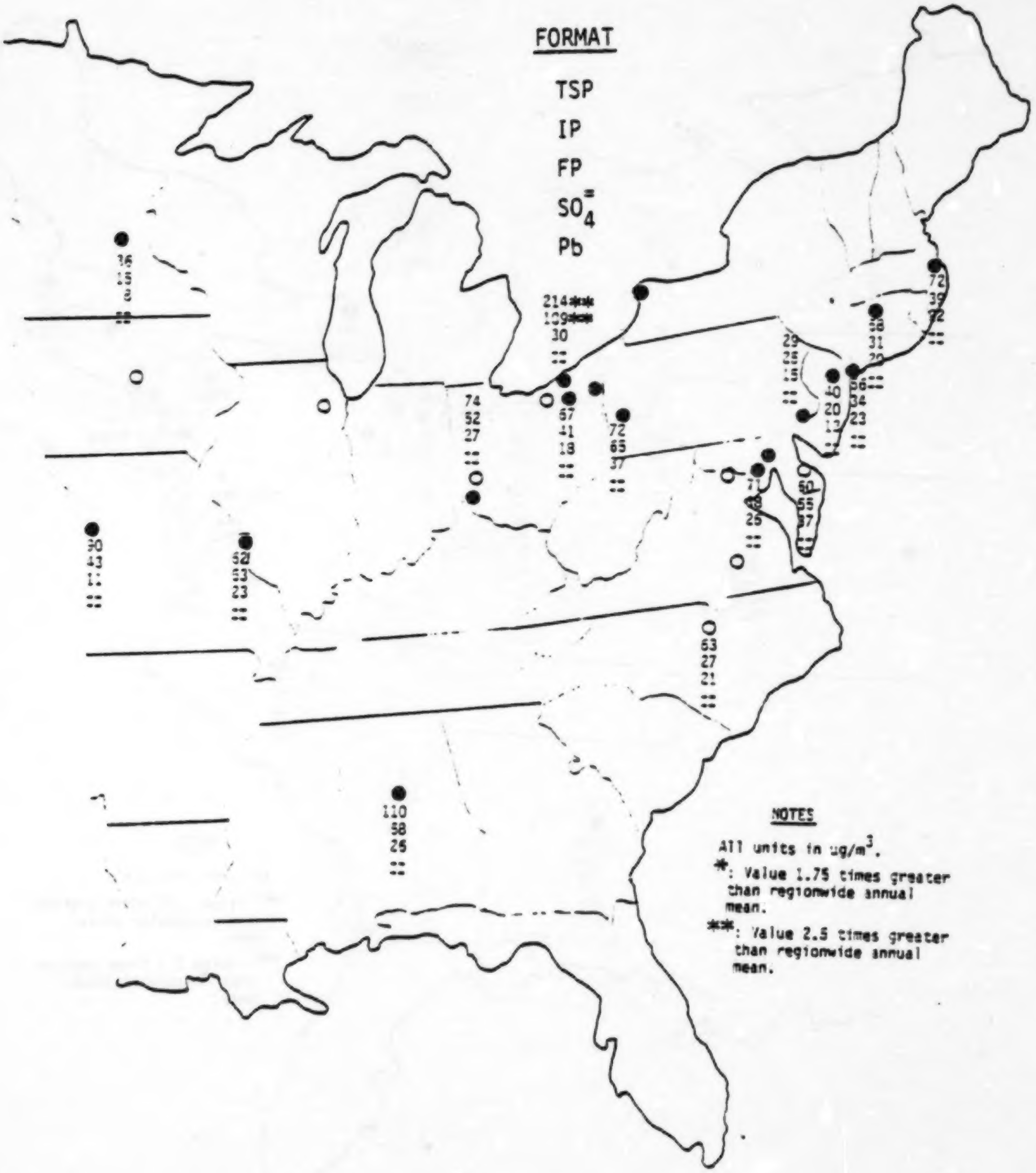
36
15
8
--
--
214**
109**
30
--
--
74
52
27
--
--
67
41
18
--
--
72
65
37
--
--
29
25
15
--
--
38
31
20
--
--
72
39
32
--
--
40
20
13
--
--
56
34
23
--
--
71
48
25
--
--
60
55
37
--
--
90
43
11
--
--
62
53
23
--
--
63
27
21
--
--
110
58
25
--
--

FORMAT

TSP
IP
FP
$SO_4^=$
Pb

NOTES

All units in ug/m^3.

*: Value 1.75 times greater than regionwide annual mean.

**: Value 2.5 times greater than regionwide annual mean.

13 August 1980

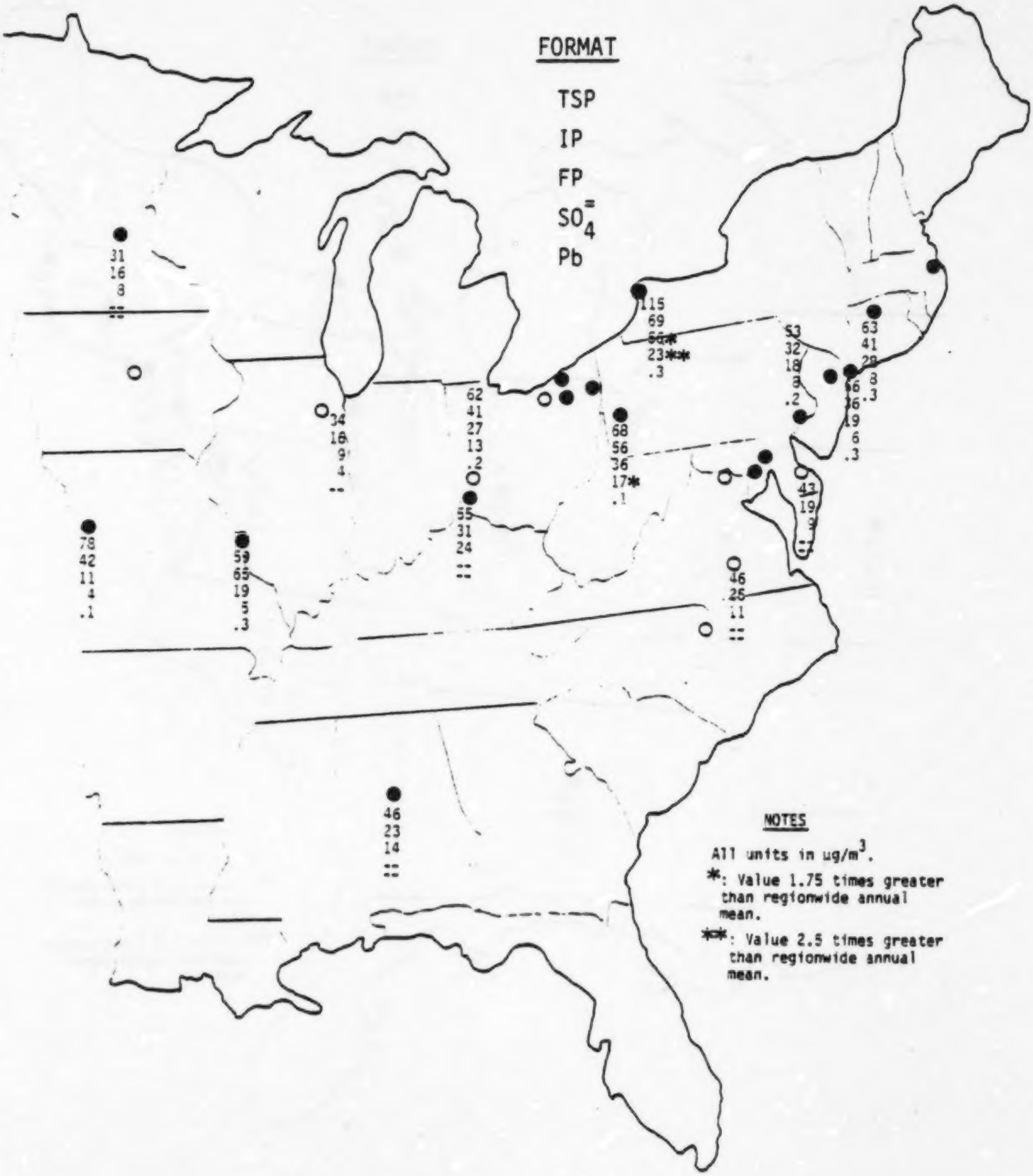
FORMAT
TSP
IP
FP
$SO_4^=$
Pb
31
16
8
--
115
69
60*
23**
.3
53
32
18
8
.2
63
41
29
8
.3
56
36
19
6
.3
34
16
9
4
--
62
41
27
13
.2
68
56
36
17*
.1
43
19
3
--
55
31
24
--
78
42
11
4
.1
59
65
19
5
.3
46
25
11
--
46
23
14
--

NOTES

All units in ug/m^3.

*: Value 1.75 times greater than regionwide annual mean.

**: Value 2.5 times greater than regionwide annual mean.

31 August 1980

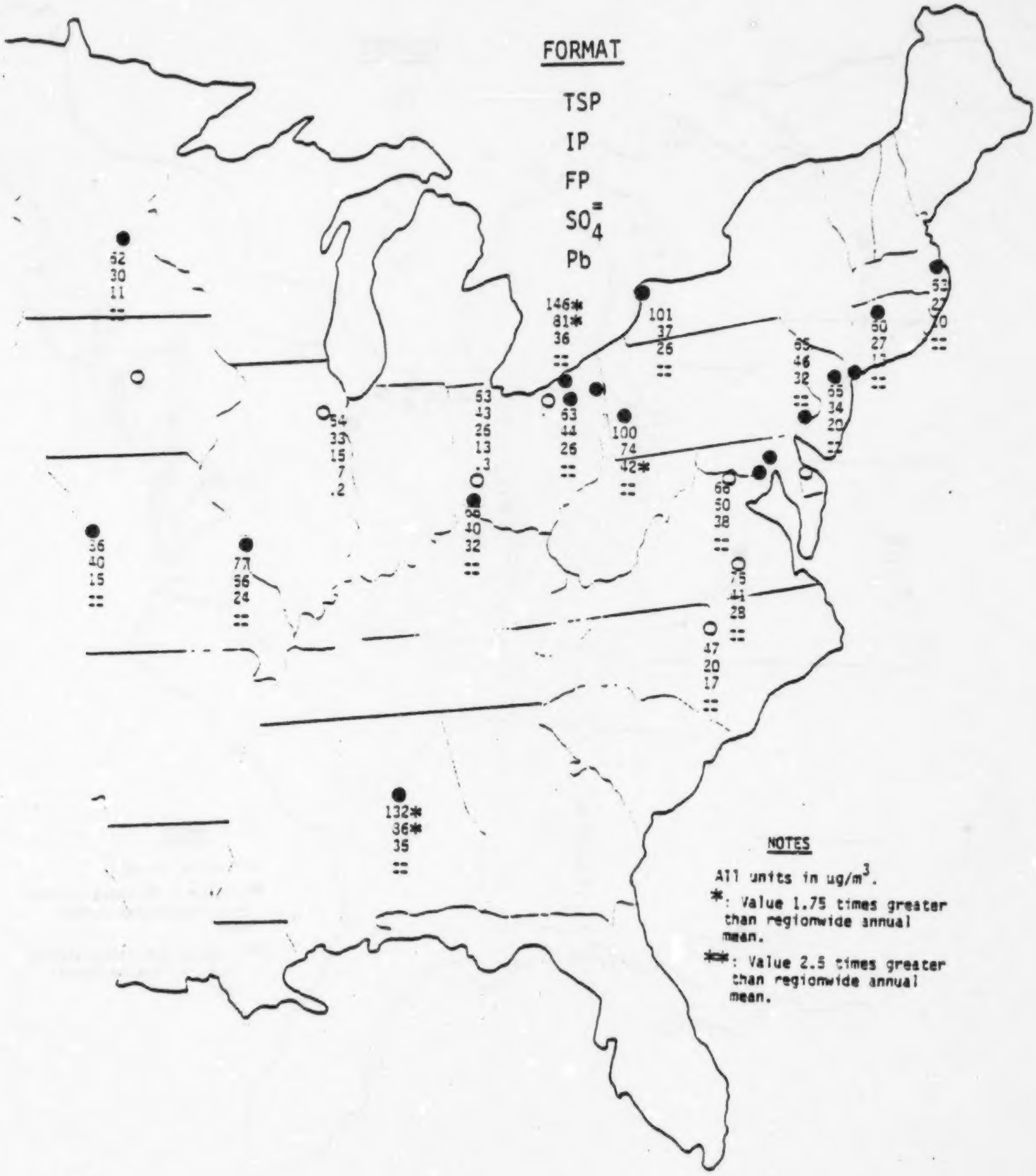
62
30
11
::
146*
81*
36
::
101
37
26
::
65
46
32
::
50
27
13
::
53
27
10
::
54
33
15
7
.2
63
43
26
13
.3
63
44
26
::
100
74
42*
::
55
34
20
::
68
50
38
::
36
40
15
::
77
56
24
::
66
40
32
::
75
41
28
::
47
20
17
::
132*
36*
35
::

FORMAT

TSP
IP
FP
$SO_4^=$
Pb

NOTES

All units in ug/m^3.

*: Value 1.75 times greater than regionwide annual mean.

**: Value 2.5 times greater than regionwide annual mean.

6 September 1980

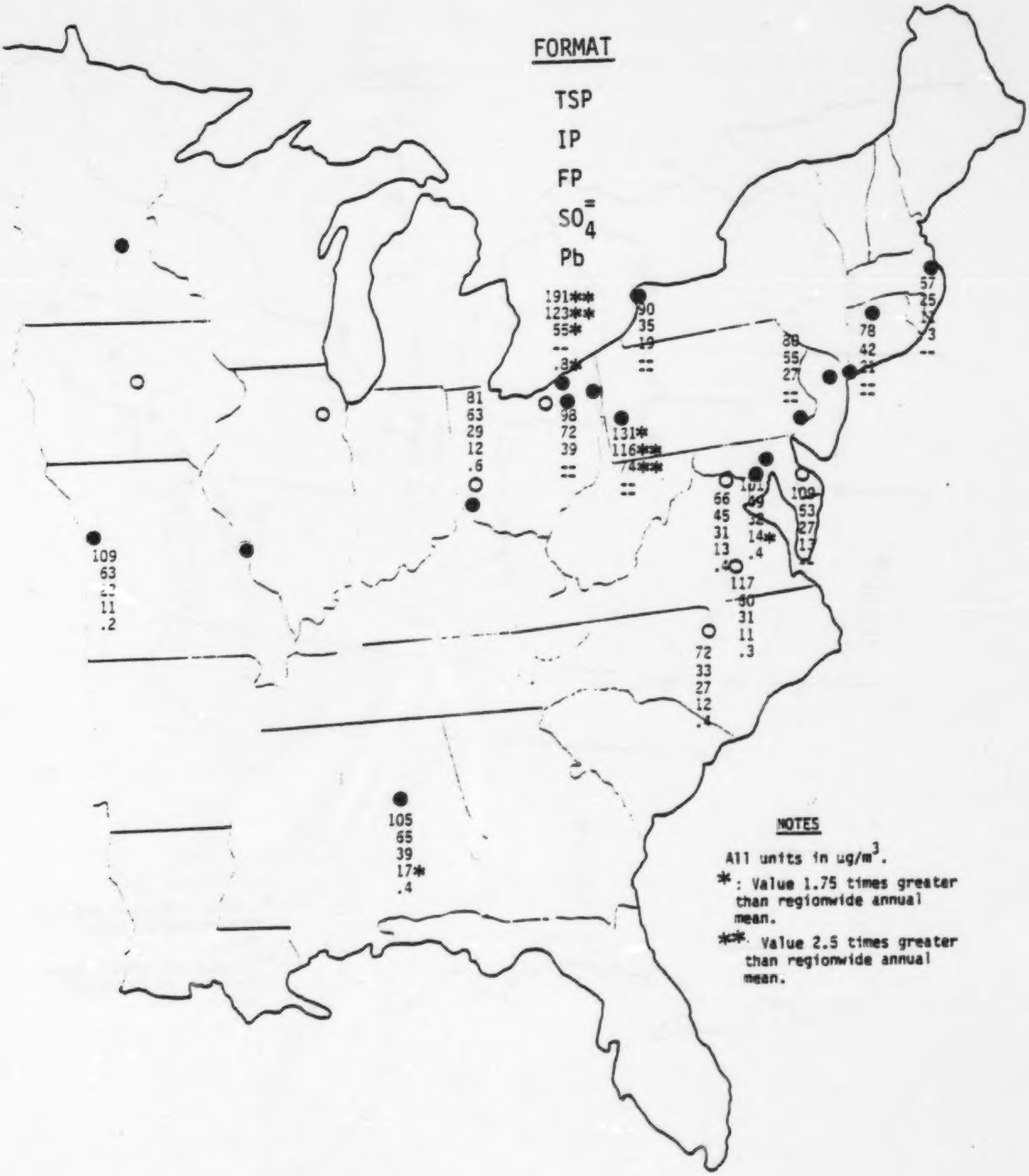
FORMAT
TSP
IP
FP
$SO_4^=$
Pb
191**
123**
55*
--
.8*
90
35
19
--
--
81
63
29
12
.6
98
72
39
--
--
131*
116**
74**
--
--
88
55
27
--
--
78
42
21
--
--
57
25
3
--
66
45
31
13
.4
101
69
38
14*
.4
109
53
27
17
117
90
31
11
.3
72
33
27
12
.4
109
63
23
11
.2
105
65
39
17*
.4

NOTES

All units in ug/m^3.

*: Value 1.75 times greater than regionwide annual mean.

**: Value 2.5 times greater than regionwide annual mean.

12 September 1980

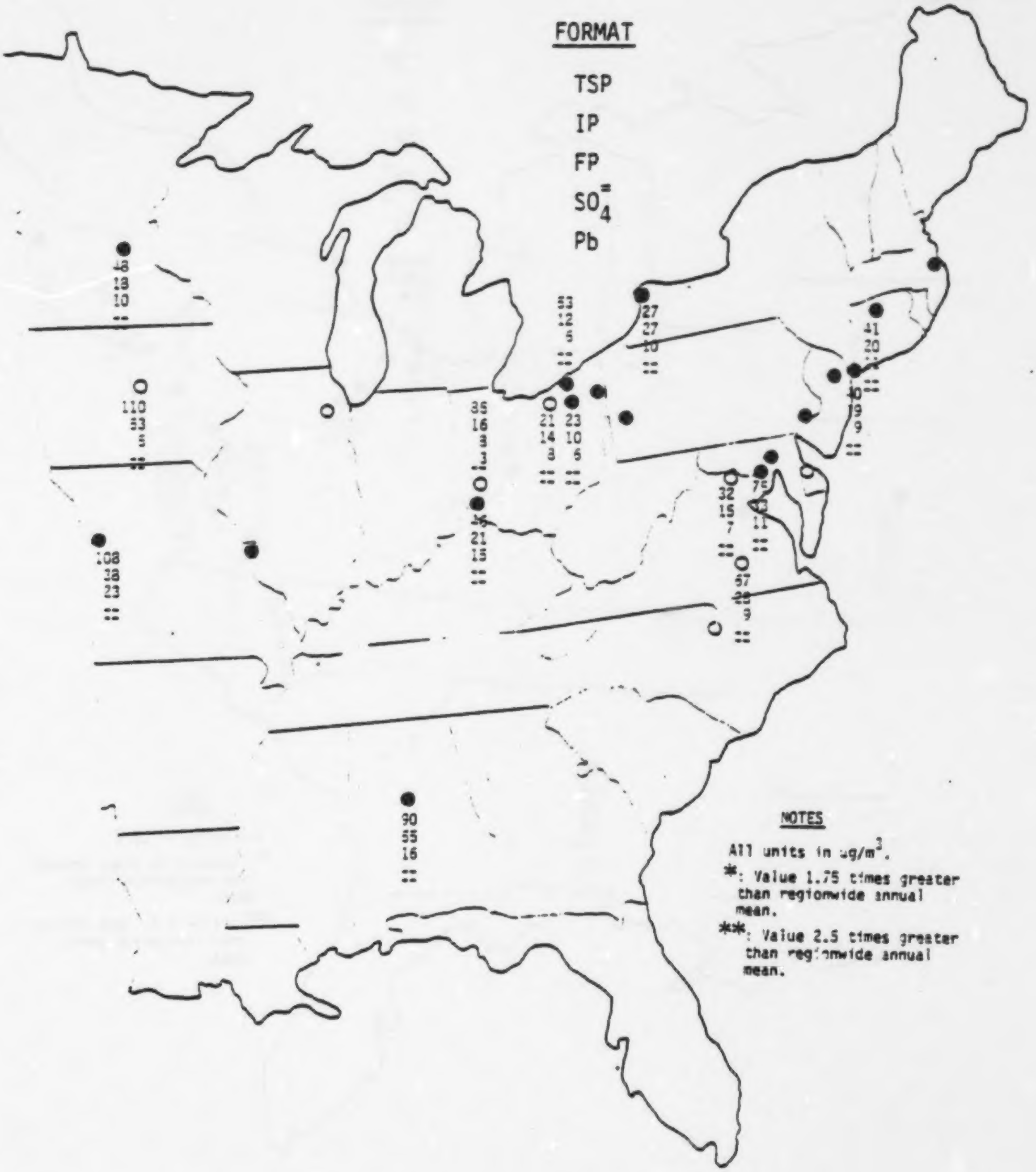
FORMAT
TSP
IP
FP
$SO_4^=$
Pb
48
18
10
::
110
53
5
::
108
38
23
::
35
16
8
3
::
36
21
15
::
53
12
5
::
21
14
8
::
23
10
6
::
27
27
10
::
41
20
::
40
19
9
::
32
15
7
::
75
43
11
::
57
28
9
::
90
55
16
::

NOTES

All units in $\mu g/m^3$.

*: Value 1.75 times greater than regionwide annual mean.

**: Value 2.5 times greater than regionwide annual mean.

12 October 1980

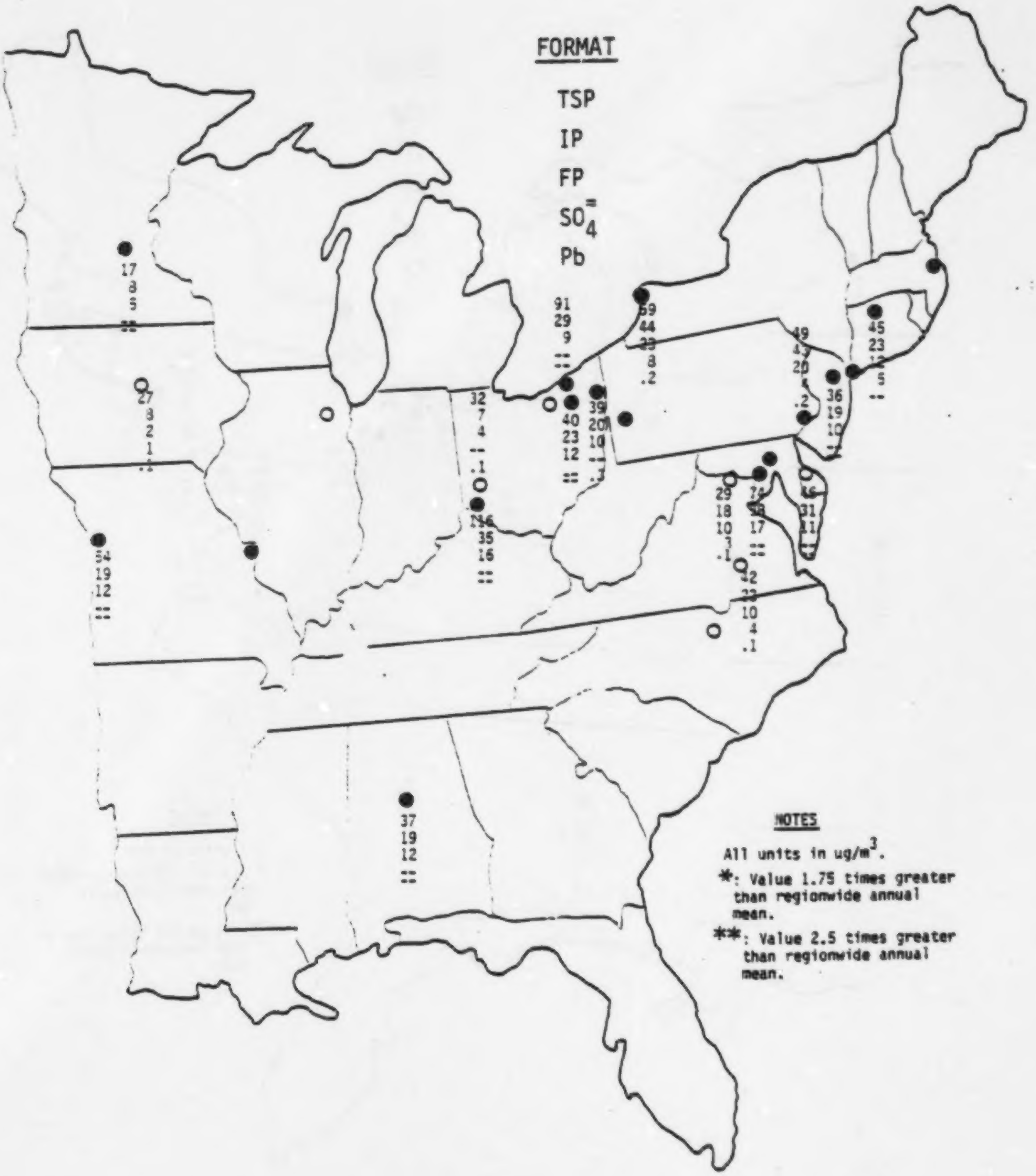
FORMAT
TSP
IP
FP
$SO_4^=$
Pb
17 8 5 ==
27 8 2 1 .1
54 19 12 ==
37 19 12 ==
32 7 4 -- .1
116 35 16 ==
91 29 9 ==
40 23 12 ==
39 20 10 -- .3
59 44 23 8 .2
49 43 20 .2
36 19 10 --
45 23 12 5 --
29 18 10 3 .1
74 58 17 ==
46 31 11 ==
42 22 10 4 .1

NOTES

All units in ug/m^3.

*: Value 1.75 times greater than regionwide annual mean.

**: Value 2.5 times greater than regionwide annual mean.

18 October 1980

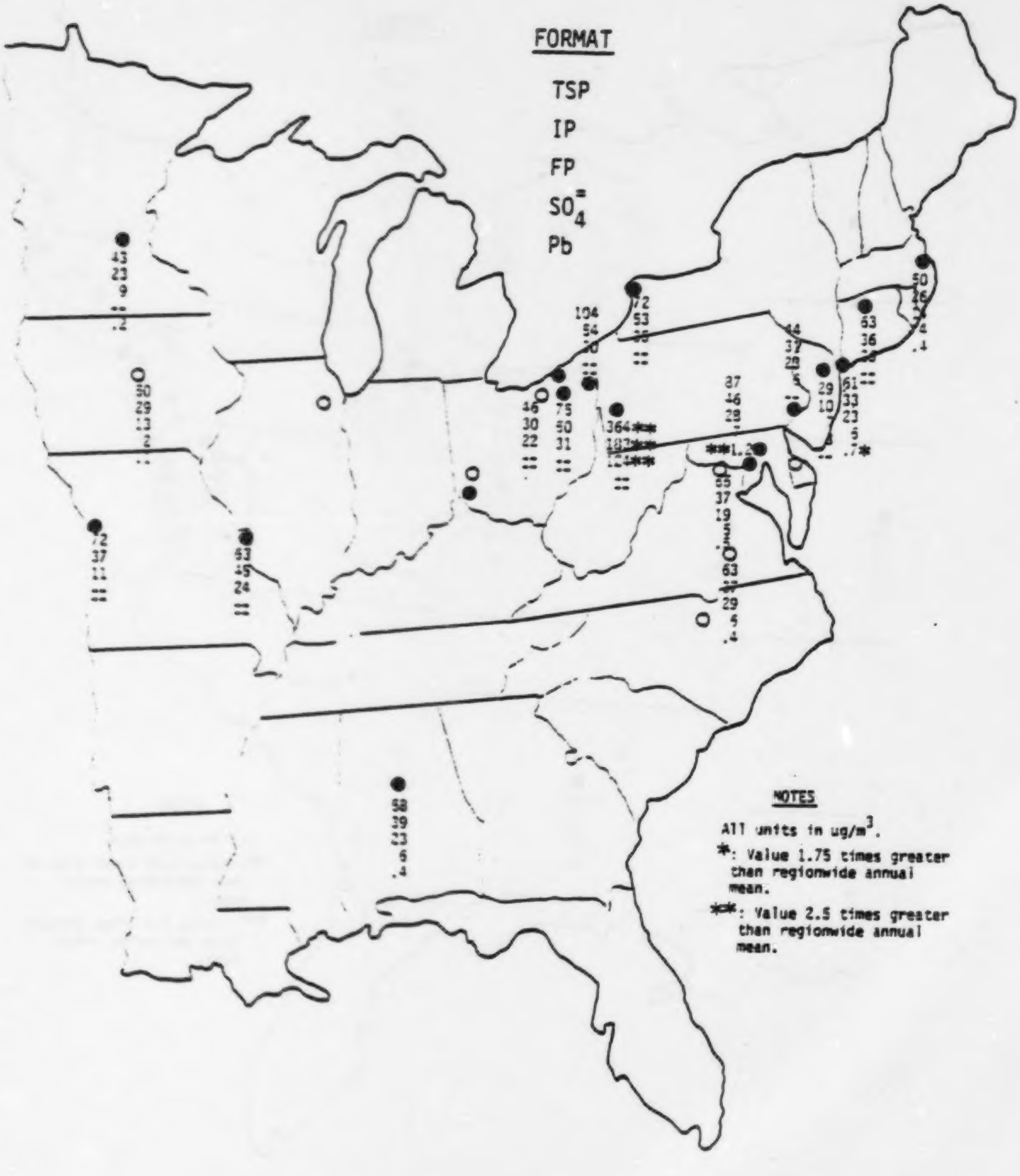
FORMAT
TSP
IP
FP
$SO_4^=$
Pb
43 23 9 -- .2
50 29 13 2 --
72 37 11 --
63 45 24 --
58 39 23 6 .4
46 30 22 --
75 50 31 --
104 54 30 --
72 53 38 --
364** 187** 121** --
87 46 28 -
**1.2
55 37 19
63 29 5 .4
44 37 28 5 --
29 10
61 33 23 5 .7*
63 36 --
50 26 4 .4
NOTES
All units in ug/m³.
*: Value 1.75 times greater than regionwide annual mean.
**: Value 2.5 times greater than regionwide annual mean.

30 October 1980

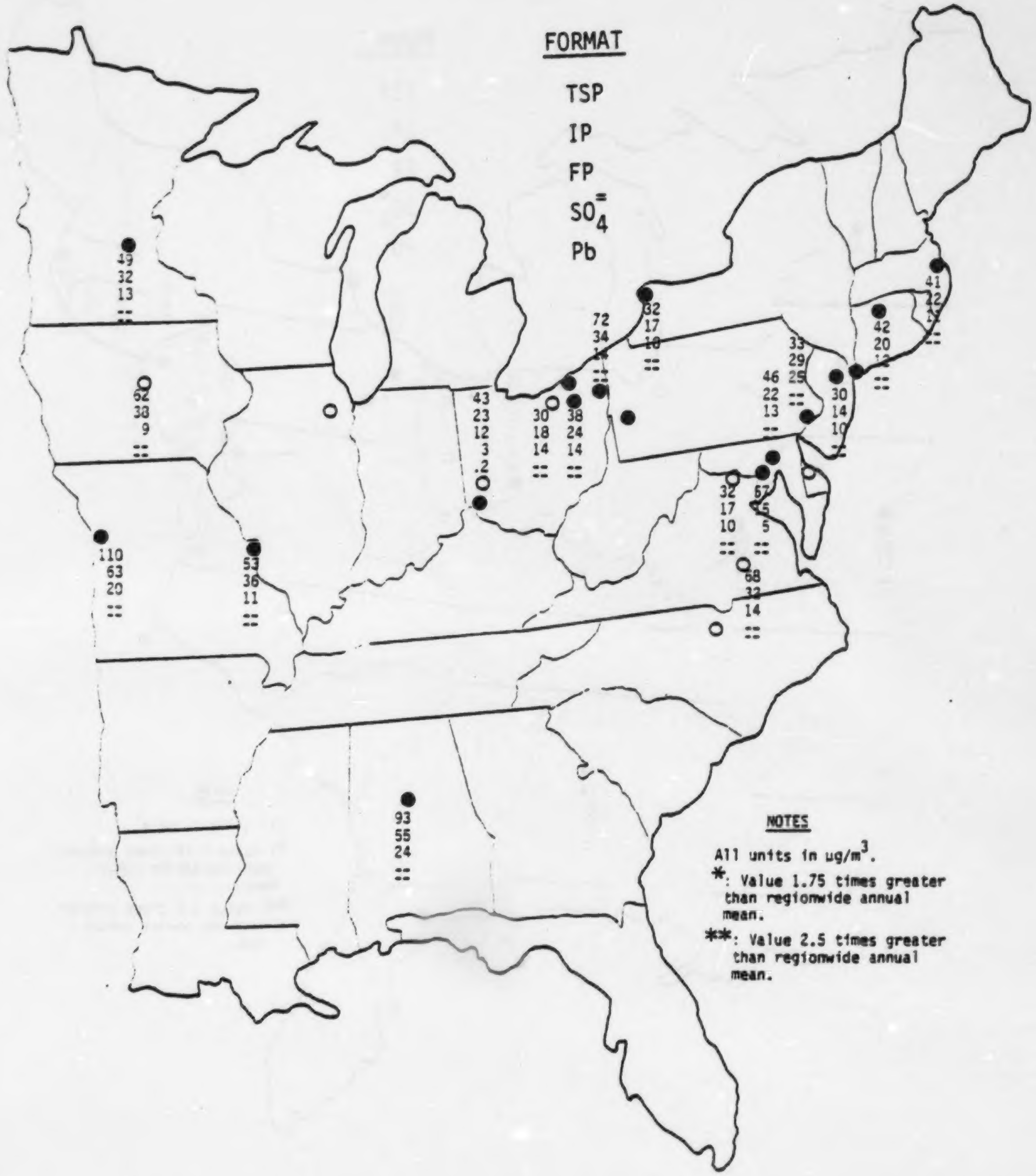
FORMAT
TSP
IP
FP
$SO_4^=$
Pb
49
32
13
--
--
62
38
9
--
--
110
63
20
--
--
53
36
11
--
--
93
55
24
--
--
43
23
12
3
.2
30
18
14
--
--
38
24
14
--
--
72
34
14
--
--
32
17
18
--
--
46
22
13
--
--
33
29
25
--
--
30
14
10
--
--
42
20
12
--
--
41
22
11
--
--
32
17
10
--
--
67
15
5
--
--
68
32
14
--
--

NOTES

All units in $\mu g/m^3$.

*: Value 1.75 times greater than regionwide annual mean.

**: Value 2.5 times greater than regionwide annual mean.

5 November 1980

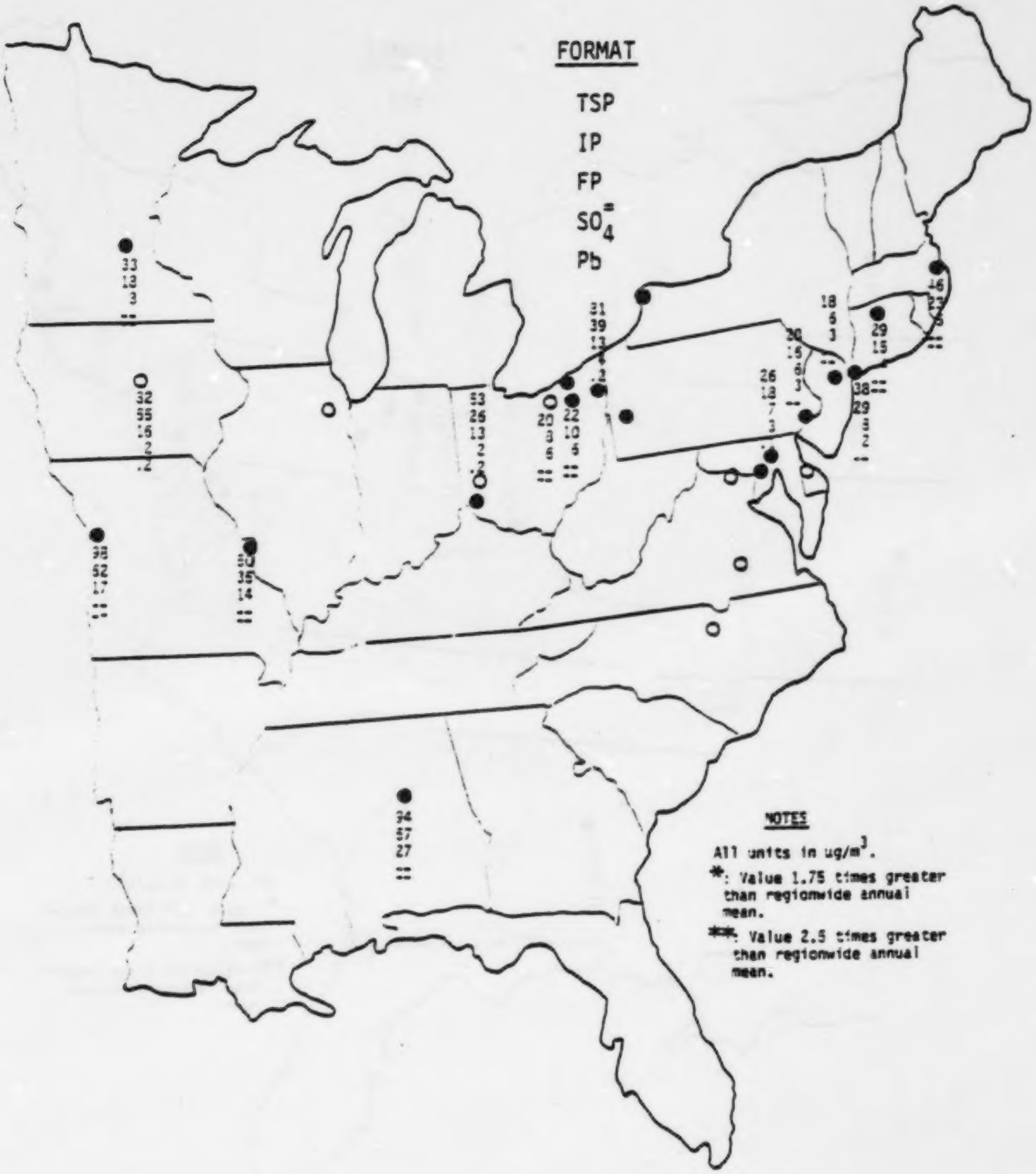

33 13 3 --
32 55 16 2 .2
98 52 17 --
80 35 14 --
53 26 13 2 .2
20 8 6 --
22 10 6 --
31 39 13 6 .2
94 57 27 --
18 6 3 --
30 15 6 3 --
26 18 7 3 --
29 15
46 27 5 --
38 29 8 2 --

FORMAT

TSP
IP
FP
$SO_4^=$
Pb

NOTES

All units in ug/m^3.

*: Value 1.75 times greater than regionwide annual mean.

**: Value 2.5 times greater than regionwide annual mean.

11 November 1980

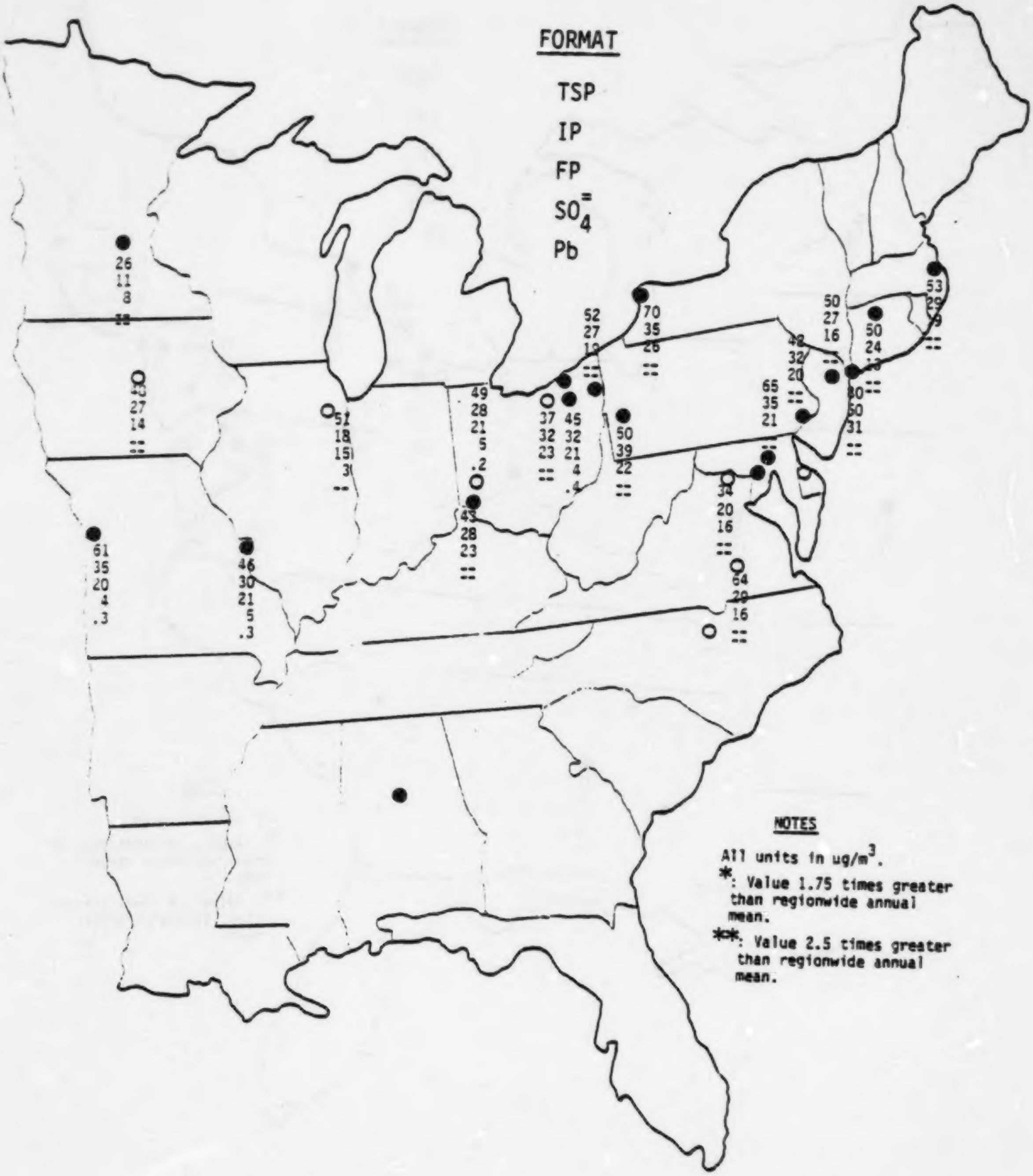
26
11
8
==
40
27
14
==
51
18
15
3
==
49
28
21
5
.2
43
28
23
==
61
35
20
4
.3
46
30
21
5
.3
52
27
19
==
70
35
26
==
37
32
23
==
45
32
21
4
.4
50
39
22
==
42
32
20
==
65
35
21
==
50
27
16
==
50
24
13
==
53
29
19
==
80
50
31
==
34
20
16
==
64
29
16
==

FORMAT

TSP
IP
FP
$SO_4^=$
Pb

NOTES

All units in ug/m^3.

*: Value 1.75 times greater than regionwide annual mean.

**: Value 2.5 times greater than regionwide annual mean.

17 November 1980

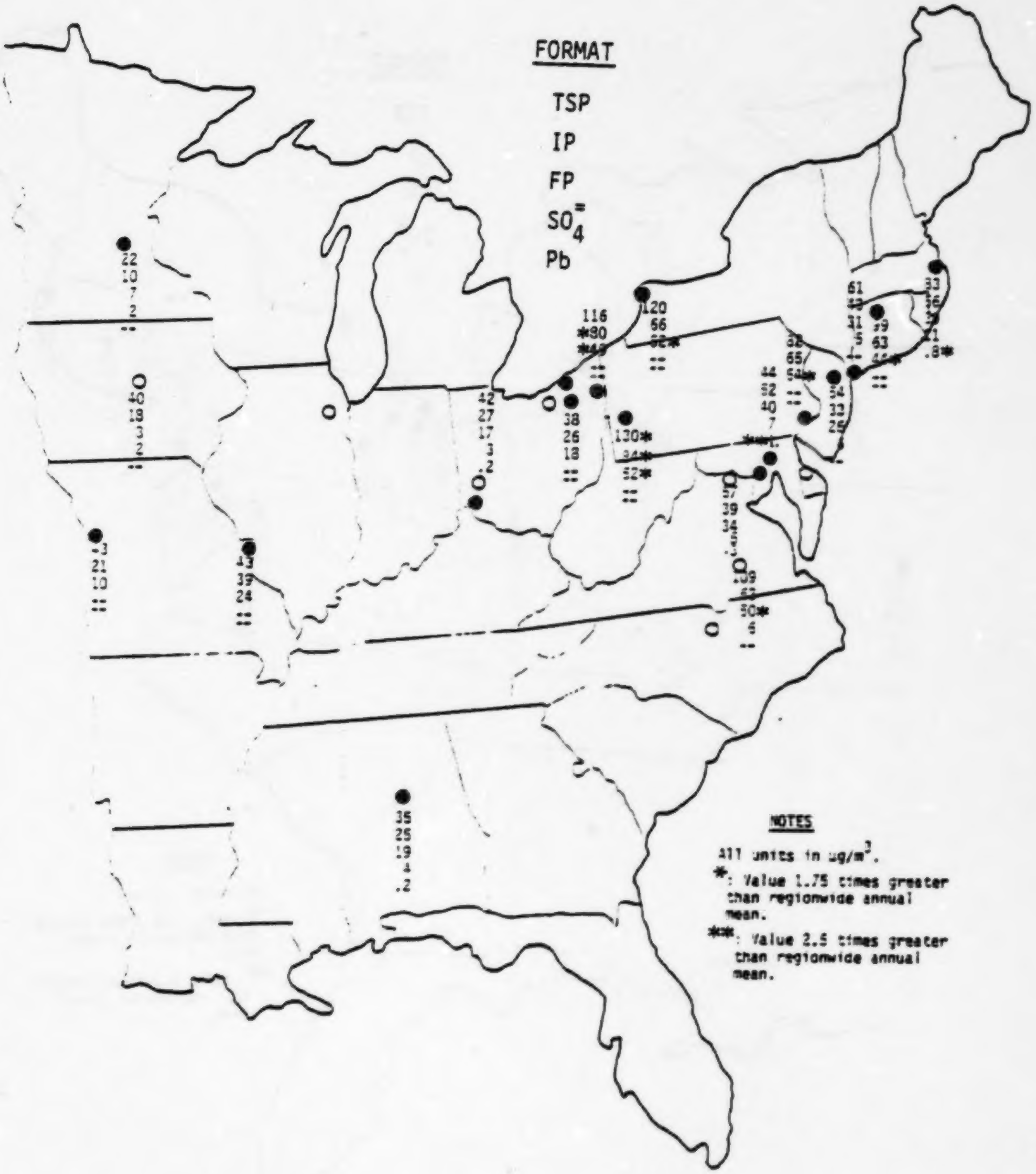
22
10
7
2
--
40
18
3
2
--
43
21
10
--
43
37
24
--
42
27
17
3
.2
38
26
18
--
116
*90
*49
--
120
66
66*
--
120*
34*
52*
--
44
52
40
7
88
65
54**
--
54
33
26
61
43
31
5
--
39
63
44*
--
33
36
31
21
.8*
57
39
34
109
67
50*
6
--
35
25
19
4
.2

FORMAT

TSP
IP
FP
$SO_4^=$
Pb

NOTES

All units in $\mu g/m^3$.

*: Value 1.75 times greater than regionwide annual mean.

**: Value 2.5 times greater than regionwide annual mean.

23 November 1980

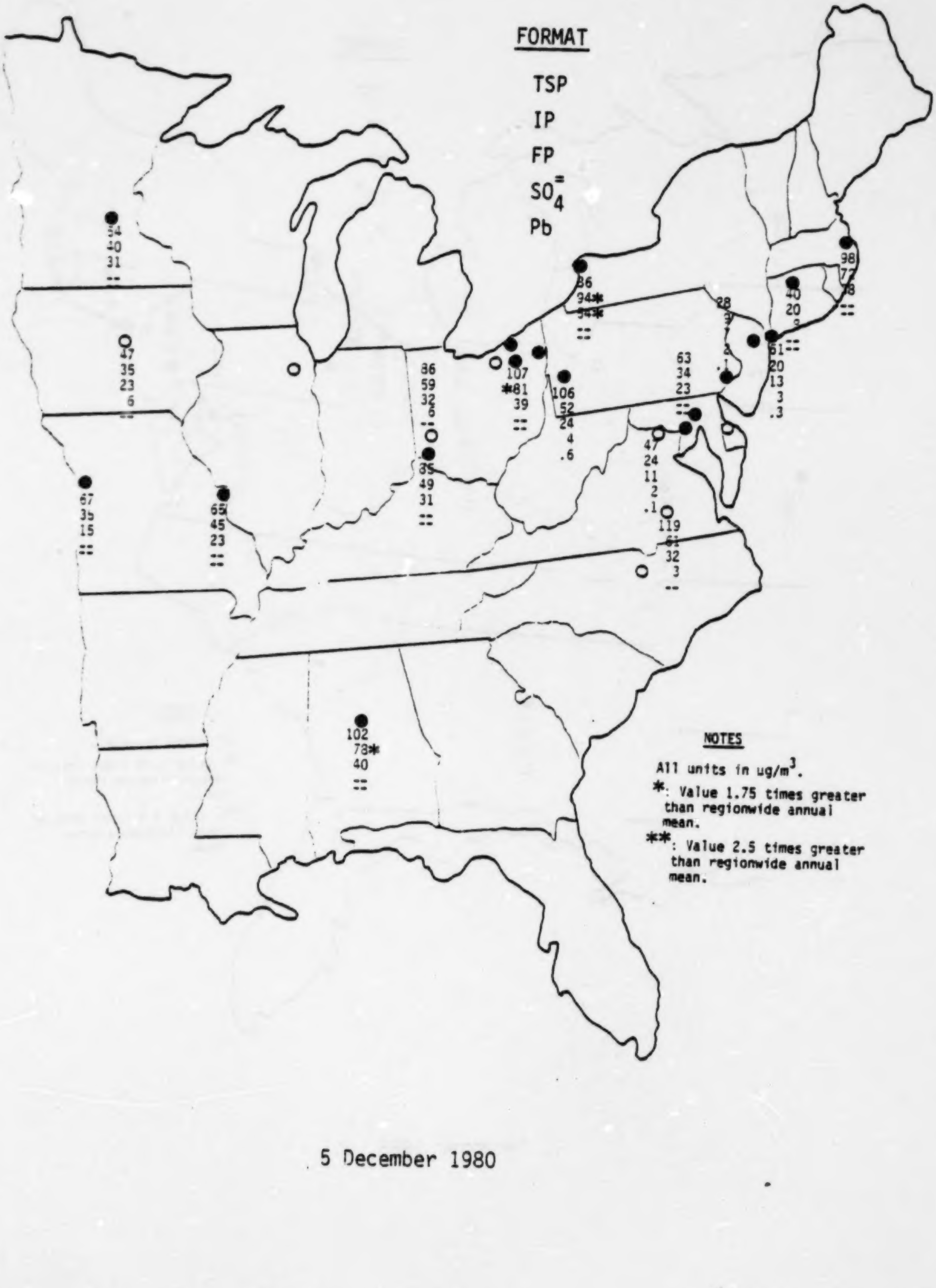
54
40
31
--
47
35
23
6
--
67
35
15
--
65
45
23
--
86
59
32
6
--
85
49
31
--
107
*81
39
--
106
52
24
4
.6
86
94*
54*
--
28
9
7
2
.1
63
34
23
--
47
24
11
2
.1
119
61
32
3
--
40
20
8
--
61
20
13
3
.3
98
72
38
--
102
78*
40
--

FORMAT

TSP
IP
FP
$SO_4^=$
Pb

NOTES

All units in ug/m^3.

*: Value 1.75 times greater than regionwide annual mean.

**: Value 2.5 times greater than regionwide annual mean.

5 December 1980

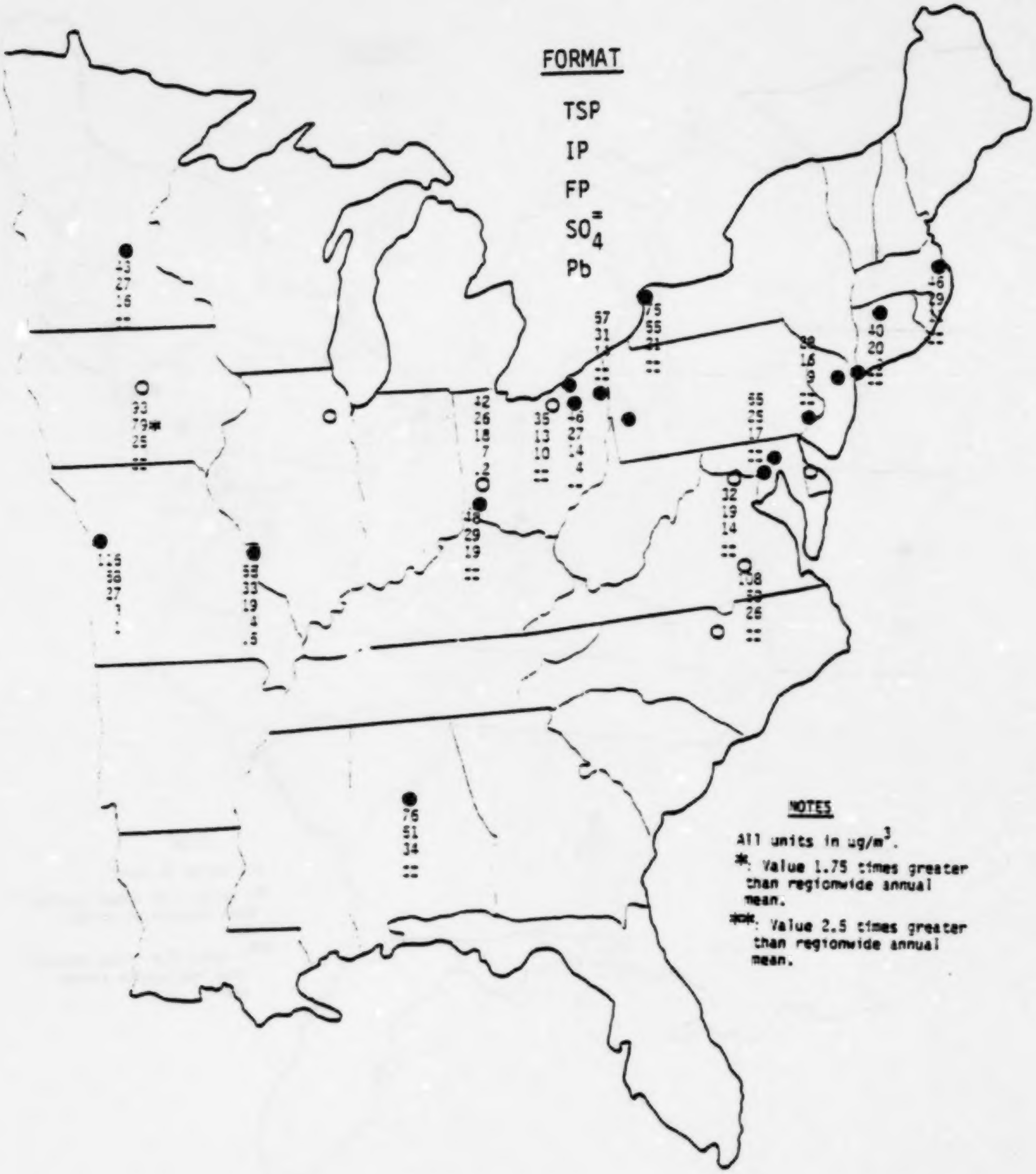
43
27
16
33
79*
25
116
58
27
58
33
19
4
.5
42
26
18
7
.2
48
29
19
35
13
10
46
27
14
4
57
31
75
55
21
55
25
17
28
16
9
40
20
46
29
32
19
14
108
26
76
51
34

FORMAT

TSP
IP
FP
$SO_4^=$
Pb

NOTES

All units in ug/m^3.

*: Value 1.75 times greater than regionwide annual mean.

**: Value 2.5 times greater than regionwide annual mean.

11 December 1980

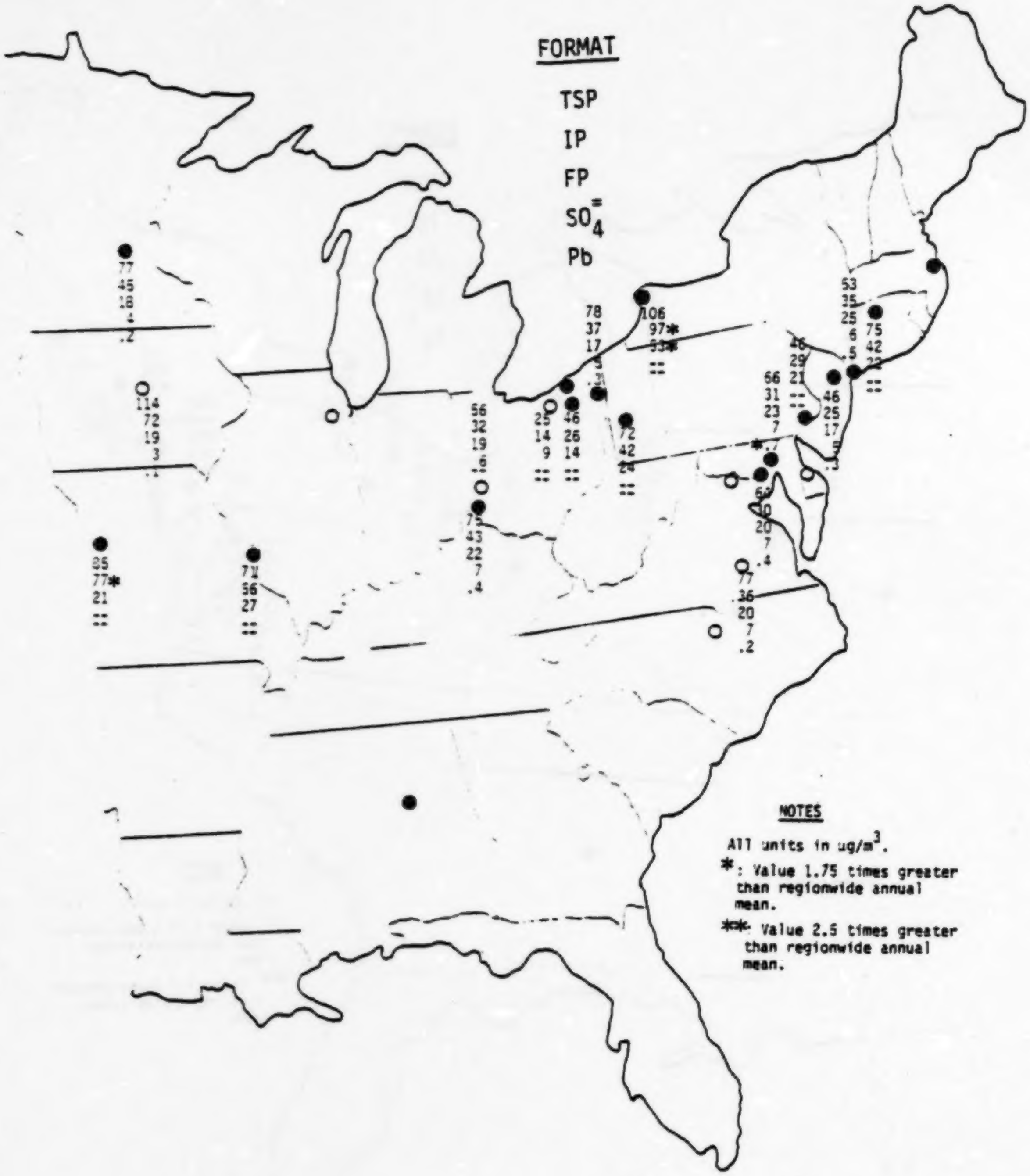
77
45
18
4
.2
114
72
19
3
56
32
19
.6
75
43
22
7
.4
85
77*
21
71
56
27
78
37
17
5
.31
25
14
9
46
26
14
72
42
24
106
97*
53*
46
29
21
66
31
23
7
.7
64
30
20
7
.4
77
36
20
7
.2
53
35
25
6
.5
75
42
22
46
25
17
5
.3

FORMAT

TSP
IP
FP
$SO_4^=$
Pb

NOTES

All units in ug/m^3.

*: Value 1.75 times greater than regionwide annual mean.

**: Value 2.5 times greater than regionwide annual mean.

17 December 1980

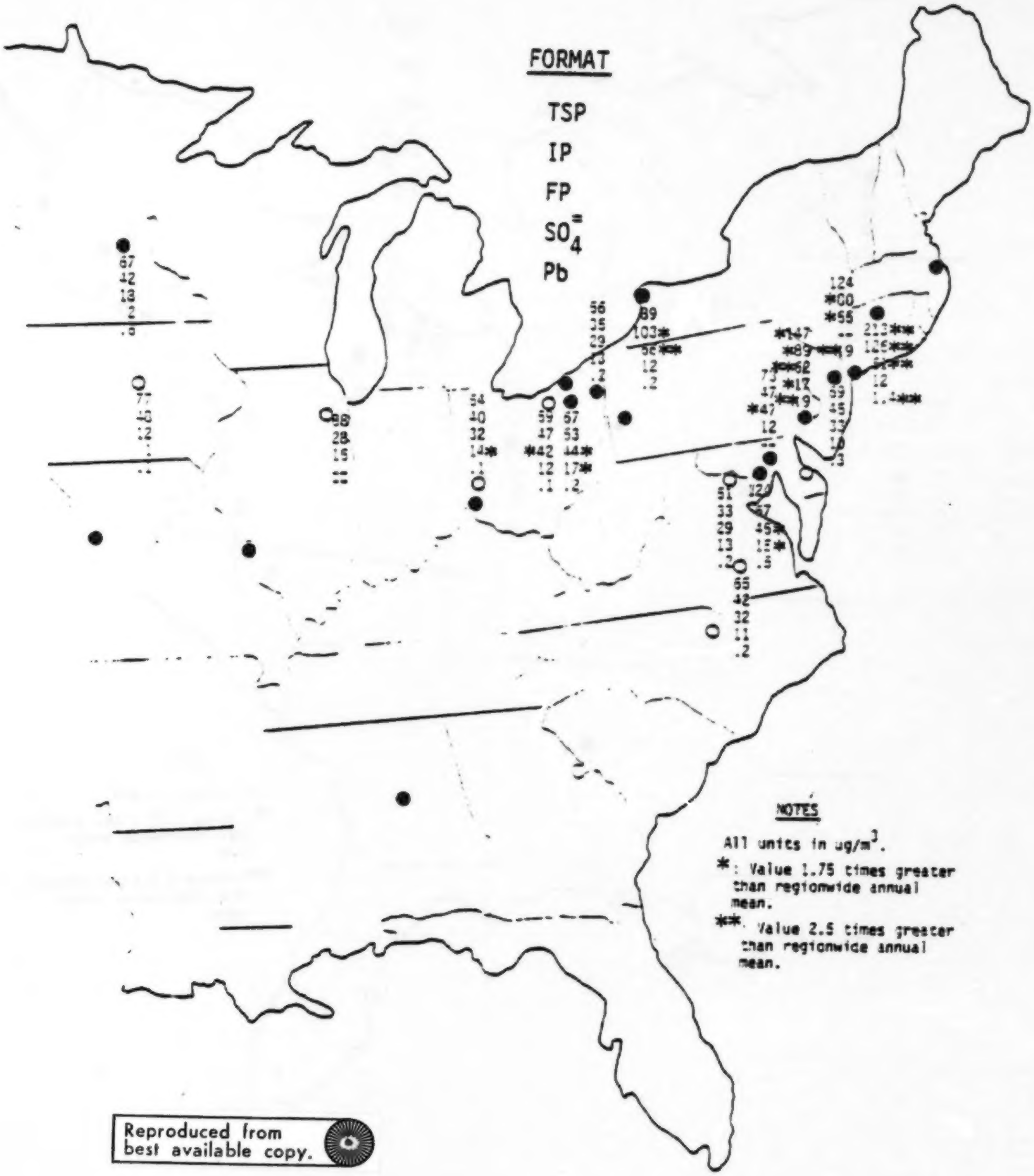
67 12 13 2 .8
77 40 12
98 28 15 --
54 40 32 14* .1
59 47 *42 12 .1
67 53 44* 17* .2
56 35 29 13 .2
89 103* 56** 12 .2
124 *60 *55 -- **9
*147 *89 **62 *17 **9
73 47 *47 12 --
213** 126** 51** 12 1.4**
59 45 33 10 .3
51 33 29 13 .2
124 67 45* 15* .3
65 42 32 11 .2

FORMAT

TSP

IP

FP

$SO_4^=$

Pb

NOTES

All units in ug/m^3.

*: Value 1.75 times greater than regionwide annual mean.

**: Value 2.5 times greater than regionwide annual mean.

Reproduced from best available copy.

22 January 1981

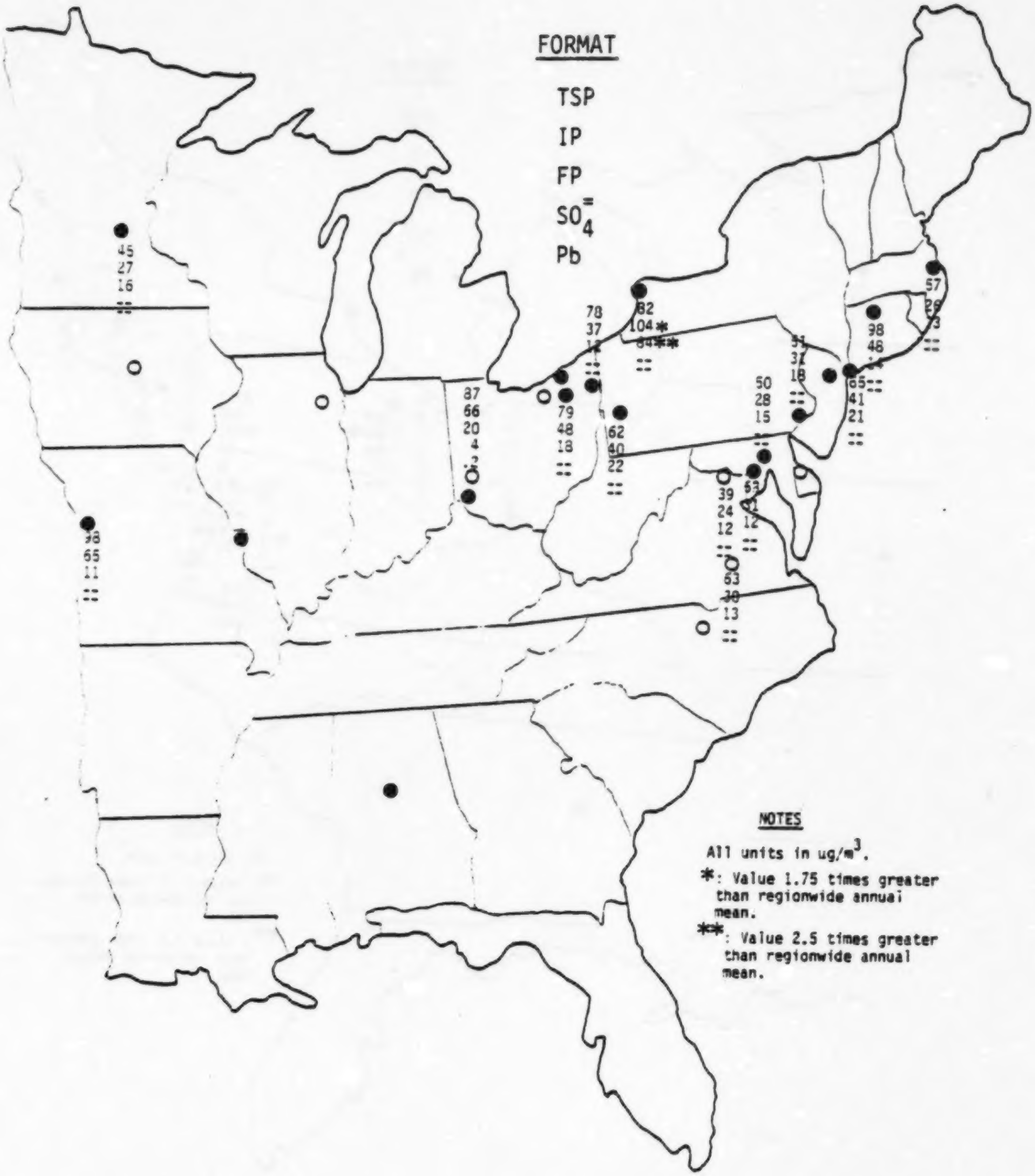
FORMAT
TSP
IP
FP
$SO_4^=$
Pb
45 27 16
98 65 11
87 66 20 4
78 37 12
82 104* 84**
79 48 18
62 40 22
51 31 18
50 28 15
39 24 12
63 31 12
63 38 13
98 48
65 41 21
57 28 13

NOTES

All units in ug/m^3.

*: Value 1.75 times greater than regionwide annual mean.

**: Value 2.5 times greater than regionwide annual mean.

9 February 1981

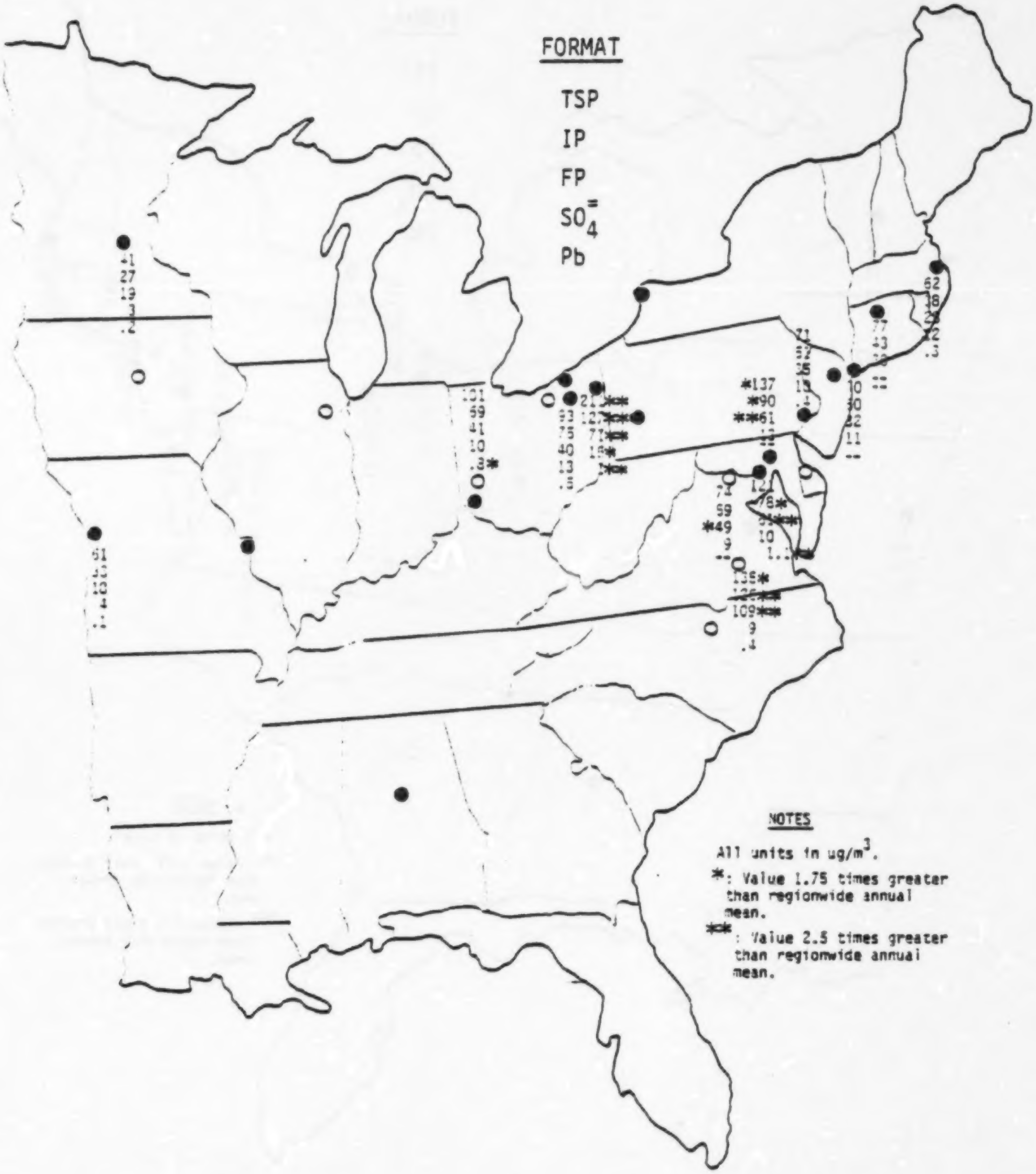

FORMAT
TSP
IP
FP
$SO_4^=$
Pb
41
27
19
3
.2
101
59
41
10
.3*
93
75
40
13
.3
21**
127**
71**
15*
**
*137
*90
**61
71
52
35
15
62
38
12
.3
77
43
10
30
22
11
--
121
78*
**
10
1.1
71
59
*49
9
--
135*
**
109**
9
.4
61
4

NOTES

All units in ug/m^3.

*: Value 1.75 times greater than regionwide annual mean.

**: Value 2.5 times greater than regionwide annual mean.

15 February 1981

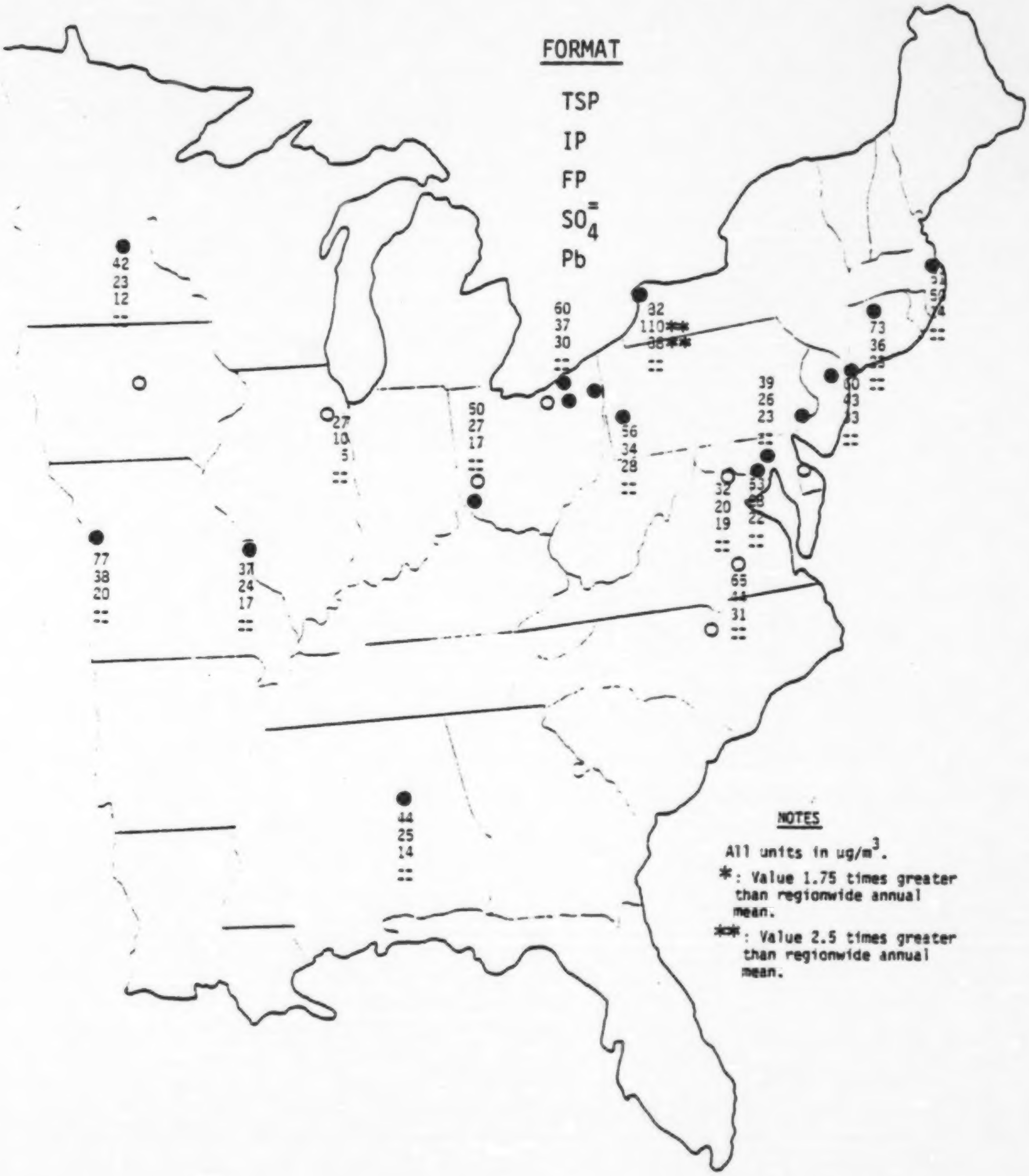
42
23
12
--
60
37
30
--
32
110**
38**
--
73
36
33
--
52
50
14
--
27
10
5
--
50
27
17
--
56
34
28
--
39
26
23
--
60
43
33
--
32
20
19
--
53
28
22
--
77
38
20
--
37
24
17
--
65
44
31
--
44
25
14
--

FORMAT

TSP
IP
FP
$SO_4^=$
Pb

NOTES

All units in ug/m^3.

*: Value 1.75 times greater than regionwide annual mean.

**: Value 2.5 times greater than regionwide annual mean.

5 March 1981